FACULTY OF LIFE SCIENCES
UNIVERSITY OF COPENHAGEN

**Master's thesis**

# Implementation of advanced echocardiographic methods in equine cardiology

- Tissue Doppler imaging and speckle tracking

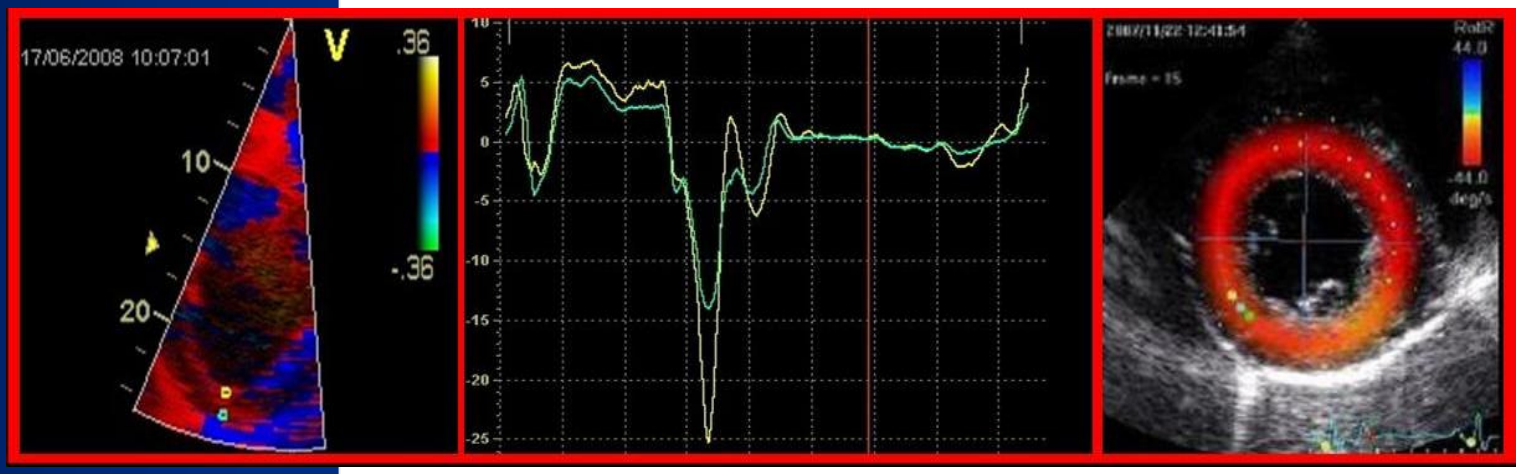


Submitted:
October 2008

Mette Flethøj
V.9518
Stud. Med. Vet.

Academic advisors:
Rikke Buhl
Jørgen Koch

# ABSTRACT

This master's thesis investigates the echocardiographic techniques tissue Doppler imaging (TDI) and speckle tracking, and the possibilities of using them as tools in equine cardiology. The thesis is divided into two sections; Part I comprises the theoretical foundation and Part II is an experimental study.

*Part I* – Tissue Doppler imaging and speckle tracking are two recently developed echocardiographic techniques. Both have the ability to quantify regional myocardial function, although they rely on very different technicalities. The two methods analyze the three-dimensional motion and deformation of the myocardium that happens with each heart beat, by assessing four parameters (velocity, displacement, strain and strain rate) along three cardiac axes (i.e. the longitudinal, radial and circumferential).

Common to the two methods is that only a very limited number of studies have been made on horses. Hence, the goal of this thesis was to investigate the prospects of implementing the two techniques in equine cardiology. However, the echocardiographic examination of the horse involves some restrictions due to the anatomy of this species – thus the implementation of TDI and speckle tracking in equine cardiology involves some technical challenges. Therefore, a pilot trial was designed to evaluate the performance of the two techniques in the horse and their feasibilities for appliance in equine sports medicine.

*Part II* – **Material:** The study population comprised two groups of healthy adult horses (6 athletic and 5 non-athletic). **Method:** Two study protocols were performed. Protocol 1 investigated the method agreement of the two techniques and the correlation on TDI measures taken from different examinations and different offline analyses, respectively. Protocol 2 compared the measures of the two groups of horses to determine if the two techniques would be able to distinguish between athletic and non-athletic horses. **Results:** In general, the results showed a high degree of dispersion, presumably due to some specific errors in the conduction of the study. The level of agreement between TDI and speckle tracking on the size of the measures varied with the individual parameters. The correlation of TDI measures from different examinations was diverse, while the measures obtained from different offline analyses all showed a strong positive correlation. Very few significant differences between the athletic and non-athletic horses were found. However, evaluation of the sample sizes revealed that these were too small to make any valid conclusions. **Conclusion:** Despite the restricted number of solid conclusions in the study, this thesis has provided both knowledge and tools that can be of value in the conduction of future studies.

# RESUME

Dette speciale omhandler de ekkokardiografiske metoder tissue Doppler imaging (TDI) og speckle tracking, samt mulighederne for at bruge dem som redskaber i kardiologi hos hest. Specialet er opdelt i to dele; Part I udgør specialets teoretiske grundlag, mens Part II er et eksperimentelt studie.

*Part I* – Tissue Doppler imaging og speckle tracking er to nyligt udviklede teknikker til ultralydsskanning af hjertet. Begge er i stand til at måle den regionale funktion af myocardiet, selvom de bygger på meget forskellige tekniske principper. De to metoder analyserer den tredimensionelle bevægelse og deformation, der sker af hjertemusklen med hvert hjerteslag, ved at bestemme fire parametre (hastighed, displacement, strain og strain rate) langs hjertets tre akser (dvs. den longitudinelle, radiale og circumferentielle).

Fælles for metoderne er endvidere at kun meget få studier er foretaget på hest. Målet med specialet var derfor at undersøge mulighederne for at implementere de to teknikker i kardiologi hos hest. Den ekkokardiografiske undersøgelse af hestehjertet indebærer dog en række begrænsninger som følge af hestens anatomi – og dette udgør således en tekniske udfordring i implementeringen af TDI og speckle tracking. Et pilotforsøg blev således designet til at evaluere de to teknikkers evner under anvendelse på hest og deres muligheder for anvendelse indenfor equin sportsmedicin.

*Part II* – **Materiale:** Studiepopulationen bestod af to grupper af raske voksne heste (6 trænede og 5 utrænede). **Metode:** To forsøgsprotokoller blev udført. Protokol 1 undersøgte teknikkernes overensstemmelse samt korrelationen mellem TDI målinger taget fra henholdsvis forskellige skanninger og forskellige analyser. Protokol 2 sammenlignede målinger i de to grupper af heste for at fastslå om de to teknikker er i stand til at skelne mellem trænede og utrænede heste. **Resultater:** Der var generelt stor spredning på målingerne, formodentlig pga. nogle specifikke fejl i udførelsen af forsøget. Graden af overensstemmelse mellem TDI og speckle tracking på størrelsen af målingerne varierede afhængigt af den enkelte parameter. Korrelationen mellem TDI målinger fra forskellige skanninger var også varierende, mens målinger fra forskellige efterfølgende analyser var stærkt positiv korrelerede. Der påvistes kun få signifikante forskelle mellem de trænede og utrænede heste. Evaluering af stikprøvestørrelserne viste imidlertid at disse var for små til at kunne danne grundlag for gyldige konklusioner. **Konklusion:** Dette speciale har, til trods for den begrænsede mængde pålidelige konklusioner, foranlediget en større viden og nogle redskaber, der kan bruges i fremtidige studier.

# PREFACE

Present paper is a master's thesis in veterinary medicine of 27 ECTS points composed at the University of Copenhagen – Faculty of Life Sciences – Department of Large Animal Sciences. The thesis is directed at anyone who has an interest in equine cardiology.

I would like to thank all the people who helped me in the process of making this thesis. A special acknowledgement goes out to my advisors; associate professor Rikke Buhl, DVM, PhD, and associate professor Jørgen Koch, DVM, PhD, at the Department of Large Animal Sciences and Department of Small Animal Clinical Sciences, respectively, for their indispensable help and guidance throughout the process. Their commitment and willingness is even more exceptional in this case, as I during the process of writing have lived as an expatriate in both Vietnam and the United States. Thus I have only been in Denmark for the preparation and conduction of the experimental study in this thesis. My living abroad has therefore put some additional demands on them as advisors, but they have taken this challenge in an amazingly positive way, and I am most grateful for that!

Other special thanks are send to Colin Schwarzwald, Dr. med. vet. PhD, Dipl. ACVIM at the University of Zurich, Switzerland, for his great help and willingness to share his experience on the tissue Doppler imaging and speckle tracking techniques as the author of some of the only published studies of these techniques in equine cardiology.

I also want to thank Peter Søgaard, Dr. med., and Rasmus Møgelvang, Ph.D. stud., at Department of Cardiology, Gentofte Hospital, Denmark for their recommendations and guidance in the post-processing of data in the EchoPac software system. Likewise I would also like to thank Professor Hans Houe and associate professor Nils Toft at Department of Large Animal Sciences, University of Copenhagen for their advice on the study statistics. And finally, I would like to thank Axel Jacobsen, the owner of the athletic horses (except one) used in the study, for allowing us to examine his horses on his premises in Farum.

Mette Flethøj

# CONTENTS

# INTRODUCTION

THE HEART IS OF FUNDAMENTAL IMPORTANCE FOR THE MAINTENANCE OF LIFE FOR ANY INDIVIDUAL AND FOR THAT REASON IT IS WELL PROTECTED BY THE SURROUNDING THORAX. WHILE THIS LOCATION PROVIDES PROTECTION IT ALSO MAKES CARDIOLOGIC EXAMINATION VERY DIFFICULT. ULTRA-SONOGRAPHY HAS THE ADVANTAGES OF BEING NON-INVASIVE AND PAINLESS AND THEREFORE ECHOCARDIOGRAPHY HAS BECOME A STANDARD DIAGNOSTIC TOOL IN CARDIOLOGY.

## BACKGROUND

In equine clinical practice echocardiography basically has two applications; detection of pathologic changes and study of physiologic adaptations to training. Accordingly, echocardiography is a very useful tool when making an exact diagnosis on the cause of a cardiac murmur (1), as well as when assessing the cardiac dimensions in an athletic horse (2). Currently, routine imaging methods in equine echocardiography include; B-mode, M-mode and Doppler in the forms of continuous wave (CW), pulsed wave (PW) and colour flow Doppler (3). B-mode, better known as two-dimensional echocardiography, provides real-time greyscale images in which cardiac structures are displayed in two dimensions (2-D) (3). M-mode displays the myocardium in one dimension (1-D) against time, and enables measurements of cardiac movement (4). The Doppler methods are routinely used for measuring velocities of blood flows. CW Doppler measures the complete range of flow velocities, including peak velocities, along a single image line by continuously transmitting and receiving sound waves (4). In contrast, PW Doppler measures flow velocities within a small cell (sample volume) at a specified depth by transmitting and receiving sound waves with certain time intervals (4). Finally, velocities measured by colour flow Doppler are colour coded according to the direction and rapidity of the flow and can be superimposed on both real-time B-mode and M-mode images (4).

However, the conventional echocardiographic techniques do contain certain limitations as far as assessing the regional myocardial function – namely the contraction. Cardiac contraction is essential for generating the blood circulation that the body is so highly dependent upon. This applies both at rest and especially in physical performances of athletes – both human and equine. If myocardial function is abnormal or inadequate the cardiac output becomes insufficient to meet the demands of the body. The ability to measure myocardial function is therefore crucial in cardiology. When assessing cardiac performance both global and regional myocardial functions are important. Global myocardial function refers to the performance of the heart as a unit, while regional myocardial function refers to the local contraction in a given myocardial segment (5). So far ultrasonic quantification of regional myocardial function has been performed using either M-mode imaging or visual assessment on B-mode images (6). Unfortunately, these

two methods possess some obvious drawbacks since data acquired by visual assessment on B-mode images are remarkably subjective, and the use of M-mode is restricted to a few myocardial segments as the insonation angle has to be perpendicular to the wall of interest to estimate myocardial thickening and thinning (6).

## CURRENT DEVELOPMENT AND POSSIBILITIES

With the disadvantages of the currently applied methods for quantifying regional myocardial function improved techniques are required. As the heart contracts the myocardium deforms and this myocardial deformation is designated as “strain”. Recently new methods for objectively quantifying regional myocardial deformation, collectively referred to as tissue deformation imaging or strain echocardiography (6;7), have emerged in human cardiology. At present the acknowledged techniques are; tissue Doppler imaging and speckle tracking. Tissue Doppler imaging (TDI) basically relies on the same principles as traditional Doppler methods for estimation of blood flow velocities, but involves different filter settings so that the high velocities of the blood is filtered out in order to display the relatively low velocities of the myocardium instead (5). On the other hand, speckle tracking, which is the most recently developed of the two techniques, uses conventional 2-D real-time B-mode images for tracking speckle patterns between consecutive frames (6). The use of TDI and speckle tracking yields parameters of myocardial motion and deformation that sum up to an objective quantitative description of the regional myocardial performance. This hallmark of the two techniques have lead to suggestion that they will be of value in the following fields of human cardiology; detection of ischemia (5;8;9), visualization of infarcts (10), stress echocardiography (5;10;11), cardiac hypertrophy (5), heart transplantation (5), assessment of right ventricular function in patients with pulmonary disease (6), and evaluation of patients for cardiac resynchronization therapy (pacemaker device implantation) (6;12). However, in veterinary cardiology the use of TDI and speckle tracking is still very sparse. Published literature on the subject includes reviews and a limited number of research studies mainly performed on dogs and cats. Suggested clinical applications in small animal practice includes; early detection of dilated cardiomyopathy (13;14), hypertrophic cardiomyopathy (15) and evaluation of myocardial synchronicity (16).

The motive for implementing TDI and speckle tracking in equine cardiology is the same as for human and small animal practice – i.e. the need for new diagnostic tools that are able to objectively quantify the regional myocardial function. At the time of writing just a few studies have been performed applying tissue Doppler imaging on horses (17-21) and to the authors knowledge there is only one published abstract (22) of a study that applies speckle tracking in equine echocardiography. With such new unexplored techniques it can be difficult to assess the significance of an examination outcome if the techniques have not been validated. A number of validation studies on both TDI and speckle tracking have

been performed in various settings (see later on). But the amount of validation in equines is still limited and this has brought forth the motive of this thesis.

## THE STUDY OBJECTIVES

The purpose of this thesis is to investigate the prospects of implementing tissue Doppler imaging and speckle tracking in equine cardiology. More specifically, the aims are to evaluate the use of the two techniques in the equine species and to examine if these two techniques are of any value in equine sports medicine. To achieve this, a study was performed in the settings of two groups of healthy adult horses – one athletic and one non-athletic group. It was chosen to focus on parameters in the left ventricle due to the assumption, that this cardiac chamber will exhibit the most pronounced changes in response to physical training. Furthermore, only one "subtype" of tissue Doppler imaging (2-D colour TDI) was used in order to delimit the study.

As it was the premier time that these techniques were tested on horses at the university, the study should be considered as a pilot trial. The objectives of the study can be summarized as; *1)* to evaluate tissue Doppler imaging and speckle tracking when applied to the horse, and *2)* to determine if the two methods are able to demonstrate any significant differences in the regional myocardial performance of athletic versus non-athletic horses.

## READERS GUIDE

Present thesis is composed of two sections. Part I is the theory. As the TDI and speckle tracking techniques are new in and rather unknown to veterinary medicine, the theoretical basis of this thesis is deliberately made very thorough. It begins with an outline on myocardial function in relation to echocardiography and gives definitions on various parameters related to regional myocardial function, e.g. strain and strain rate. This leads on to an account for the characteristics of equine echocardiography. Then follows reviews on TDI and speckle tracking with respect to the principles and limitations of the two techniques as well as descriptions of studies performed on small animals and the few studies performed on horses. Finally, the impact of training on the heart of the equine athlete is considered.

Part II consists of the study in which TDI and speckle tracking are applied to the horse in order to evaluate the two methods in the horse and their feasibilities for appliance in equine sports medicine. This part has the typical structure of a scientific research article (see Figure 1).

A basic comprehension of the conventional imaging methods in equine echocardiography mentioned in the beginning of this introduction is considered indispensable for the understanding of this thesis. For that reason, a brief account on the conventional echocardiographic imaging methods is provided in Appendix 1. Thesaurus and abbreviations are given in Appendix 2. Additionally, as tissue Doppler imaging and speckle tracking each goes under a number of different terms

in the literature, a list of synonymous names of the two techniques is given in Appendix 3. The results of the study are summarized in Appendix 7, and the statistic calculations are shown in Appendix 8 and 9. Lists of references in the text as well as references for figures are given on the last pages of this thesis.

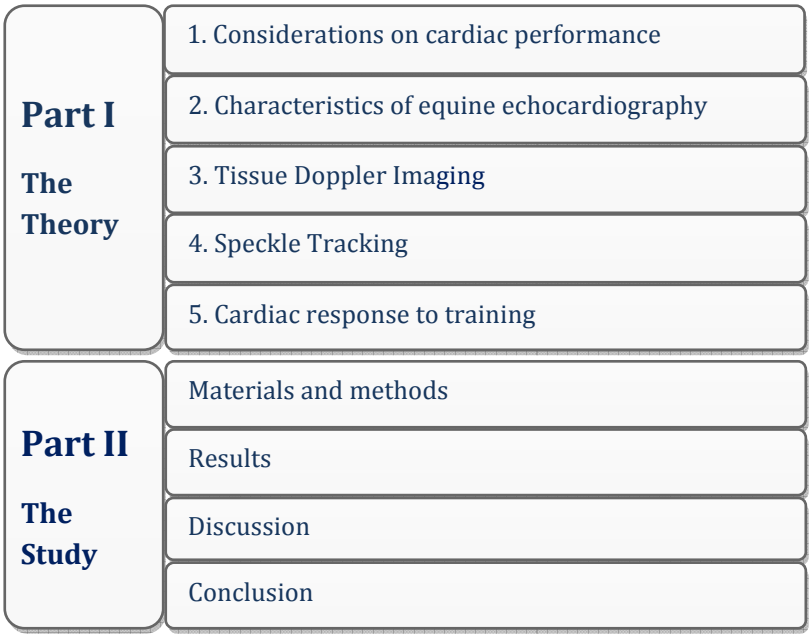


**Figure 1** Structure of the thesis.

# PART I

# THEORY

# 1. Considerations on cardiac performance

In order to comprehend the techniques of tissue Doppler imaging and speckle tracking various concepts need to be described. The following considerations are primarily based on literature from human cardiology as veterinary literature on the subject is limited, however the description tends to be species non-specific.

## Myocardial function and timing

The myocardium consists of cardiomyocytes arranged in a complex meshwork of fibres. These fibres are able to contract upon electrical stimulation to generate a circulation of blood in the body. For that reason a healthy myocardium is essential for the body, and as such the ability to assess myocardial performance becomes an important element in cardiology. Myocardial performance can be divided into global and regional myocardial function (5). Global myocardial function refers to the performance of the heart as a unit to create a circulation of blood, while regional myocardial function refers to the contraction of local myocardial segments (5). Thus the regional function underlies the global function of the heart – and as such the ability to assess regional myocardial function becomes even more important.

When assessing myocardial function it is convenient to be acquainted with different aspects of timing. Each cardiac cycle can be divided into a series of global events that relate to all regions of the (ventricular) myocardium at the same time (5). These global phases include; isovolumetric contraction period, ejection phase, isovolumetric relaxation period, early diastolic filling, diastasis and late diastolic filling (5). It is beneficial to use these points in time as landmarks when looking at echocardiographic recordings, especially if an electrocardiogram (ECG) is recorded

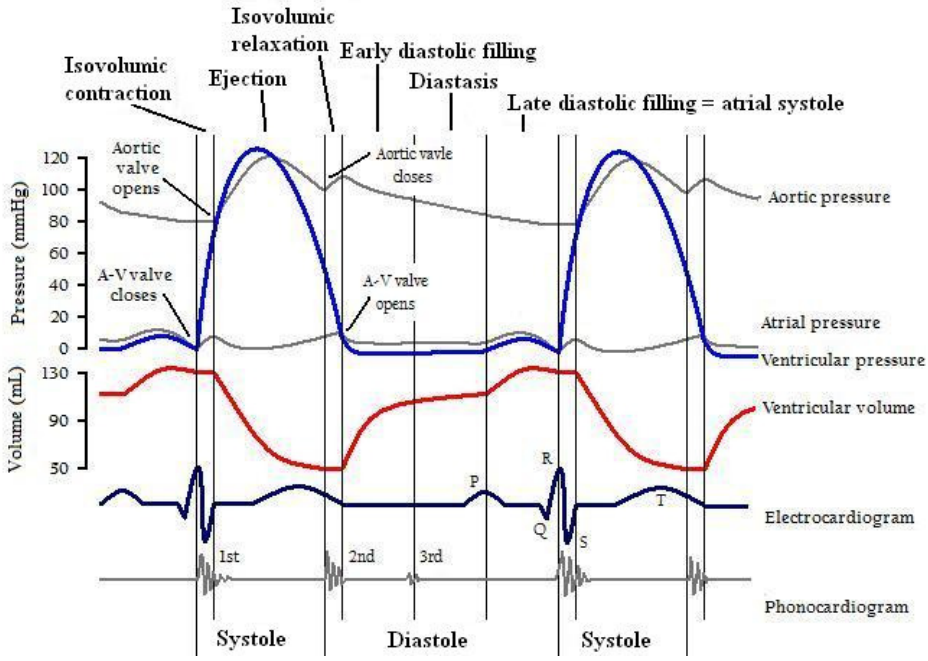


**Figure 2** Timing of the different phases in the cardiac cycle.

simultaneously to depict the onset of systole. The relationship between the global phases and the ECG during the cardiac cycle is shown in Figure 2. The timing of regional events, that is contraction and relaxation, does necessarily coincide with the timing of global events. In fact differing onsets of contraction or relaxation in differing local myocardial segments is normal (5). But further explanation on these matters will not be given in this thesis.

### System of reference

In order to describe and quantify the movements of the heart it is necessary to define a system of reference. As cardiac motion is three-dimensional the reference system also needs to be so. To achieve this, a three-dimensional (3-D) coordinate system is applied to the heart. Such a coordinate system can be mathematically defined and designed in various ways, but one specific coordinate system consisting of a longitudinal, a radial and a circumferential axis has proven itself to be favourable for cardiac purposes (5) (see Figure 3). The longitudinal axis of this system goes from the apex to the base of the heart. The radial axis is perpendicular to the longitudinal axis and is thereby transecting the heart wall. Finally, the circumferential axis is perpendicular to both the longitudinal and the radial axes (5). Because this system is routinely used in connection to the heart, it will make up the system of reference throughout this thesis. It should be noted that this coordinate system cannot be applied to the most apical myocardial segments since it is not possible to preserve the mutual perpendicular orientation of the axes in this area. At the apex the longitudinal and radial axes will coincide and the circumferential axis will be impossible to define (5). Additionally, some authors (23) operate with a transverse ”axis” as the shortest possible distance across the myocardial wall, which not always co-inside with the radial axis – however, that term will not be used further in this thesis.

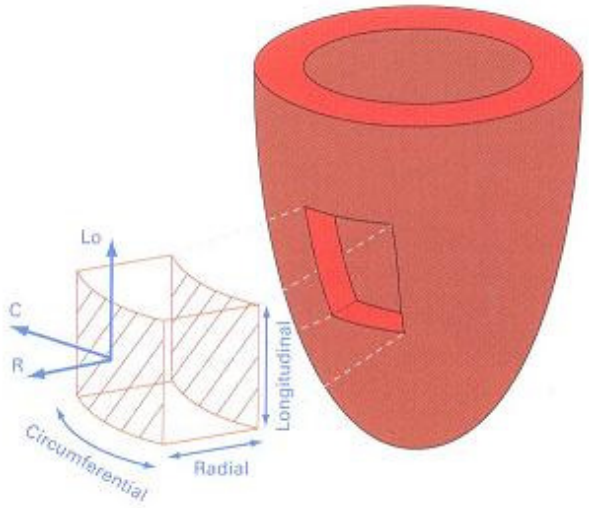


**Figure 3** Coordinate system of the left ventricle.

## CARDIAC MOTION

The overall motion of the heart during contraction is characterized by a compound three-dimensional movement in which the heart shortens lengthwise and across at the same time as it twists around its longitudinal axis (24). Consequently, the longitudinal and circumferential axes of the myocardium shorten while the radial axis of myocardium thickens during systole (6). The motion reverses during diastole and the myocardium retains its original dimensions (24). As the study in part II of this thesis is focused on conditions related to the left ventricle, a more specified description of the motion in this part of the heart is required, though a complete account for the left ventricular movement pattern lies beyond the scope of this thesis. The motion of the left ventricle is also three-dimensional. During systole the left ventricle shortens in the longitudinal axis, but the motion is not symmetric.

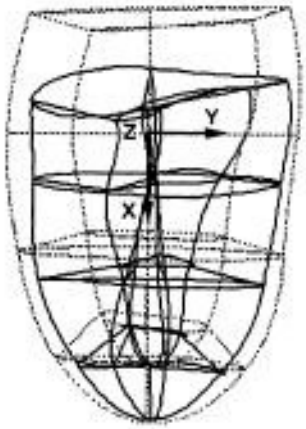


**Figure 4** Left ventricular motion illustrated by end-diastolic dimensions (dotted lines) and end-systolic dimensions (solid lines). Notice the descent of the base towards the apex, and the rotation around the longitudinal axis indicated by the curved vertical lines at end-systole.

While the base moves in apical direction the apex practically stays in position. As a result the base moves up and down during diastole and systole respectively, while the apex is almost static (25;26). The radial motion of the left ventricle consists of movement of the ventricular walls in direction of the ventricular lumen during systole and away from the lumen during diastole (24). The circumferential motion of the left ventricle is complex, but in broad outline the base turns clockwise while the apex turns counter-clockwise when observed from the apex during systole and returns during diastole (25). Figure 4 summarizes the left ventricular motion.

The above description of the left ventricular movement pattern is based on studies of the human heart. However, it is less certain if the same pattern applies to the equine heart or not.

### IMPACTS ON CARDIAC MOTION – TETHERING AND TRANSLATION

The verb “tether” means to bind or attach. Accordingly, *tethering* refers to the fact that all segments of the heart are interconnected, and as such the motion of any myocardial segment is influenced by the movement of neighbouring segments (10). In other words the contraction of one segment “pulls” on another segment. In addition, the attachment of the heart to the rest of the body causes *translation* of the entire heart in response to general thoracic motion, e.g. respiratory

movements (10). These circumstances are natural aspects of cardiac motion, but may interfere with echocardiographic measurements. Hence, echocardiographic recordings should ideally be made at breath hold in order to avoid the cumulative velocity and passive motion; however in veterinary medicine this is very difficult to carry out without anesthetizing the animals.

## PARAMETERS RELATED TO MYOCARDIAL FUNCTION

In addition to the concepts described so far, various parameters need to be defined in order to describe and quantify regional myocardial function. In the following the four parameters of myocardial velocity, displacement, strain and strain rate will be defined.

### TISSUE VELOCITY AND DISPLACEMENT

The motion of any object can be dissolved into the speed at which the motion is made, i.e. the velocity, and the distance travelled during the motion, i.e. the displacement (27). Thus, the first parameter of interest is the *velocity* of the myocardium during cardiac contraction. Myocardial velocity is expressed in cm/s (or m/s) and typically reaches values of 4-15 cm/s (human values)(28). This is in contrast to blood flow velocities which typically are ten times higher (28). Figure 5 shows an example of a longitudinal velocity profile a normal human heart.

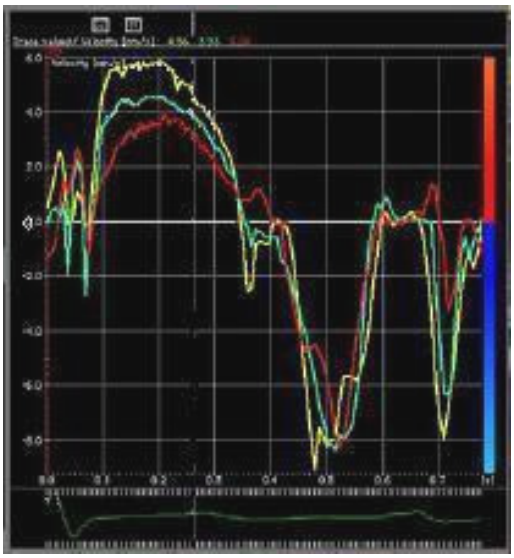

**Figure 5** Velocity profile of the longitudinal motion in the interventricular septum of a normal human heart. The Y-axis represents velocity and the X-axis represents time (one cardiac cycle). A positive systolic wave and two negative diastolic waves are seen consistent with the peak velocities in systole, early diastole and late diastole, respectively. The waves are also named the S, E and A waves, respectively. Note the decrease in the systolic velocities from the base (yellow curve) to the apex (red curve) – indicating a longitudinal velocity gradient.

As mentioned earlier the apex practically stays in position while the base moves up and down during the cardiac cycle. This means that the velocity of the myocardium is increasing from the apex towards the base (11) – because while the velocity measured in the apical myocardium represents mainly local contraction, the velocity measured in basal segments is a combination of both local contraction and velocity resulting from the connection to the apex, i.e. tethering (10). This cumulative velocity results in an base-apex velocity gradient (9;10).

The second parameter is the *displacement* of the myocardium – that is how big a distance the myocardium travels during cardiac contraction. It is typically expressed in mm and has been shown to reach a maximum value of > 12 mm in humans (10). A curve of the longitudinal displacement is plotted in Figure 6. The displacement data can be calculated by time integrating the velocity data, i.e. summing up velocity values over time (27;29). As a result of this time integration and because of the existing base-apex velocity gradient, the distances travelled by the myocardium during cardiac contraction is also increasing from the apex towards the base (10) – consisting with the statement that the apex stays in position while the base moves up and down during the cardiac cycle. Note that both myocardial velocity and displacement is thereby influenced by tethering.

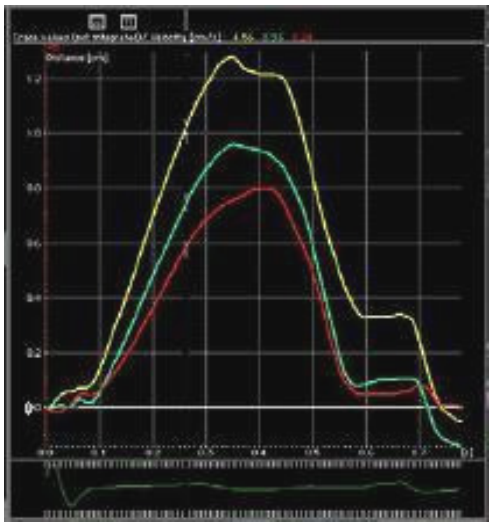

**Figure 6** Displacement of the interventricular septum along the longitudinal axis of a normal human heart. Data are integrated from the velocity profile in Figure 5. The Y-axis represents displacement and the X-axis represents time (one cardiac cycle). Notice that the base (yellow curve) travels longer distances than the apex (red curve).

## STRAIN AND STRAIN RATE

Contraction of the heart causes the myocardium to alter its shape – it deforms (6). The deformation of an object can be characterized by the amount and the rate of which it occurs. Myocardial deformation is a third parameter of interest when quantifying regional myocardial function, and is designated as *strain* (ε). According to Sutherland et al. (5) the overall definition of strain is *"the deformation of an object, normalized to its original shape"*, and two kinds of strain can be calculated; Lagrangian strain and natural strain (see Appendix 4 for further explanation). Though natural strain seems to be the most suitable for cardiac purposes, Lagrangian strain is the most commonly used in practice (5). Further use of the term "strain" in this thesis will therefore refer to Lagrangian strain unless otherwise noted. Lagrangian strain is defined as the change in length (L) relative to the initial length ($L_0$) (Formula 1), and is consequently a dimensionless quantity often expressed in percent (5).

*Formula 1:*

$$\varepsilon = \frac{L - L_0}{L_0}$$

An additional consequence of this definition is that a relative shortening produces a negative strain value, while a relative lengthening produces a positive strain value (5;10). The longitudinal and circumferential shortening of the myocardium during systole (as mentioned earlier) therefore yields negative strain values, while the concurrent radial thickening results in positive strain values (6). Figure 7 shows the longitudinal strain curve of a normal human heart. Note that the strain value will return to zero at the end of a cardiac cycle, since the myocardium retains its original dimensions (5).

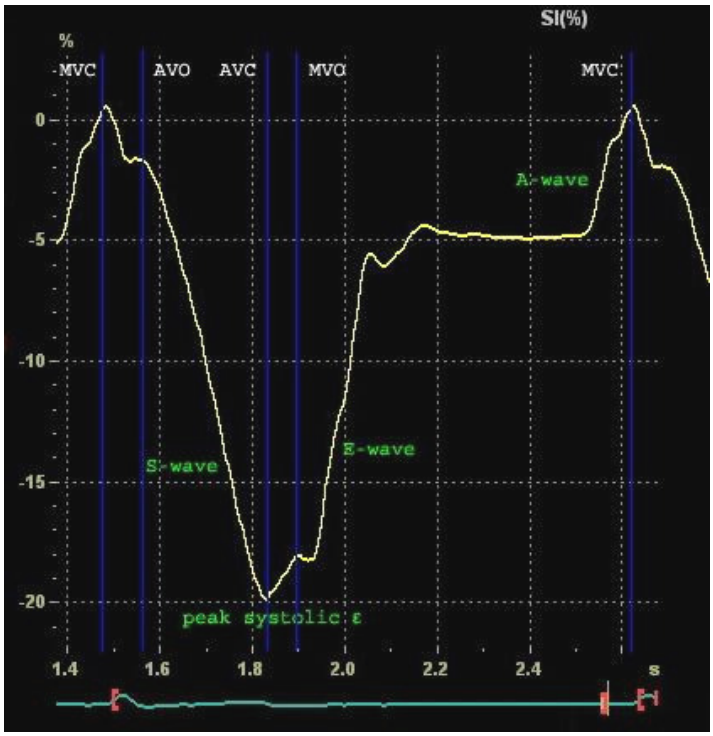


**Figure 7** Strain profile resulting from longitudinal motion in the interventricular septum of a normal human heart. The Y-axis represents strain (%) and the X-axis represents time (one cardiac cycle). The negative S wave indicates systolic shortening and the two E and A waves indicate the return to of the myocardium to its original dimensions during diastole (the strain value returns to 0%). MVC, mitral valve closure, MVO, mitral valve opening, AVC, aortic valve closure, AVO, aortic valve opening.

The forth parameter is the speed of the myocardial deformation – the *strain rate* (ε'). Strain rate is expressed in $s^{-1}$ as it is defined as strain pr unit time and strain is a dimensionless quantity (10). Following this definition the peak systolic strain rate has the same sign as its corresponding strain value. This means that a negative strain value correspond to a negative strain rate and vice versa (6). This means that the longitudinal and circumferential shortening of the myocardium during systole result in negative strain rates, while the concurrent radial thickening generates positive systolic strain rates (6). A longitudinal strain rate curve from a normal human heart is shown in Figure 8. Strain rate can additionally be calculated as the difference in velocities in two different points in the myocardium ($v_1$, $v_2$) divided by the distance between them (Δx) (Formula 2) (6;8;27;30).

*Formula 2:*

$$\varepsilon' = \frac{v_1 - v_2}{\Delta x}$$

As can be seen from Formula 2, the advantage of this method is that the component of tethering and translation of the heart is automatically subtracted as this will be the same in all points of the myocardium (8;27).

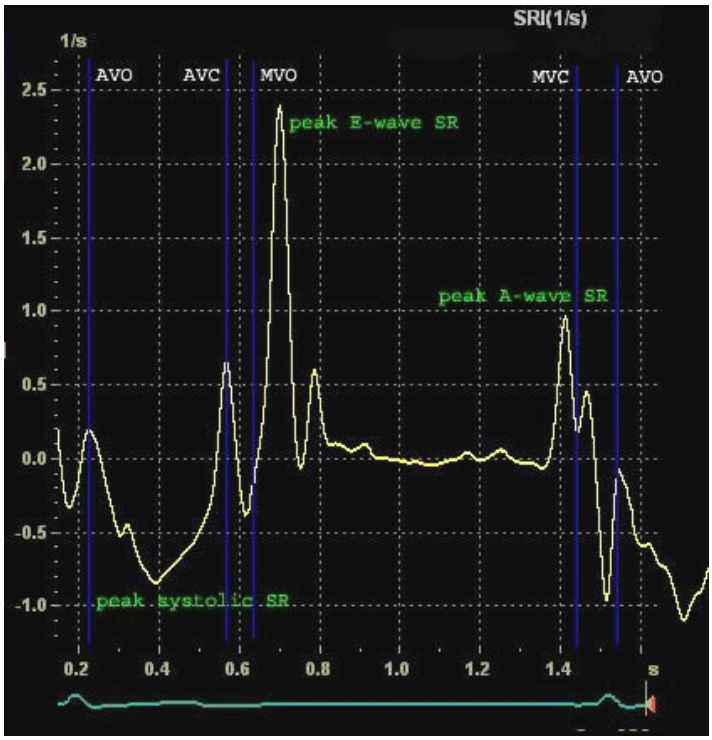


**Figure 8** Strain rate profile of the longitudinal motion in the interventricular septum of a normal human heart (corresponding to the strain profile in Figure 7). The Y-axis represents strain rate ($s^{-1}$) and the X-axis represents time (one cardiac cycle). The peak systolic strain rate (peak systolic SR) is negative in accordance with the negative peak systolic strain in Figure 7. The strain rate is zero when no change in deformation occurs as indicated by the diastasis phase between the early diastole (E wave) and late diastole (A wave). MVC, mitral valve closure, MVO, mitral valve opening, AVC, aortic valve closure, AVO, aortic valve opening.

## ADDITIONAL COMMENTS ON THE PARAMETERS

It is essential to realize that the four parameters defined above are all interconnected. As already stated displacement data is achieved by time integrating the velocity data. The same relationship exists between strain and strain rate (5;6;30). Furthermore, as seen in Formula 2 strain rate is the spatial derivate of velocity (5). This is also the relation between strain and displacement as indicated in Formula 1. These interconnections are summarized in Figure 9.

To put this in other words, the deformation parameters (strain and strain rate) are spatial derivates of the motion parameters (displacement and velocity). And as a result of this spatial derivation strain and strain rate are unaffected by tethering and cardiac translation unlike velocity and displacement (16;27;30). This has two important consequences; first, there is no base-apex gradient in the strain and strain rate values – instead these are approximately equal throughout the left ventricular walls (5) (See Figure 10). And secondly, strain and strain rate are more efficient for detecting dyskinetic areas, e.g. infarcts, as there is no deformation in a

nonviable myocardial segment during cardiac contracting, while the velocity and displacement curves of the same segment might appear normal due to tethering and translation (5). This implies a clinical advantage and has lead to the concept of strain (rate) imaging, in which the strain and strain rate parameters are used to assess myocardial viability and cardiac performance (5). As presented later on in this thesis, strain (rate) imaging can be performed by means of both tissue Doppler imaging and speckle tracking.

Finally, a complete overview of the four parameters along all three cardiac axes is given in Figure 11, summarizing a lot of the information given in this chapter.

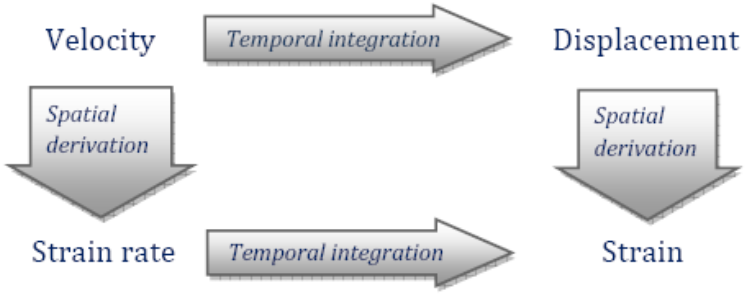


**Figure 9** The interconnection between the four parameters.

## SUMMING UP

This section has outlined myocardial function and defined various concepts. It was stated that myocardial function is divided into global and regional, referring to the work of the heart as a unit and the local cardiac contraction, respectively. Various timing aspects of myocardial function were also defined. In order to describe cardiac motion a reference system in form of a 3-D coordinate system with a longitudinal, a radial and a circumferential axis was applied to the heart. The three-dimensional movements of the heart were described with special attention paid to the motion of the left ventricle – though it is uncertain to which extent the same movement patterns apply to the horse. The concepts of tethering and cardiac translation were defined. And finally four parameters for quantification of regional myocardial function were described – tissue velocity and displacement representing myocardial motion, and strain and strain rate representing myocardial deformation. The next chapter will describe the characteristics of echocardiography in the horse.

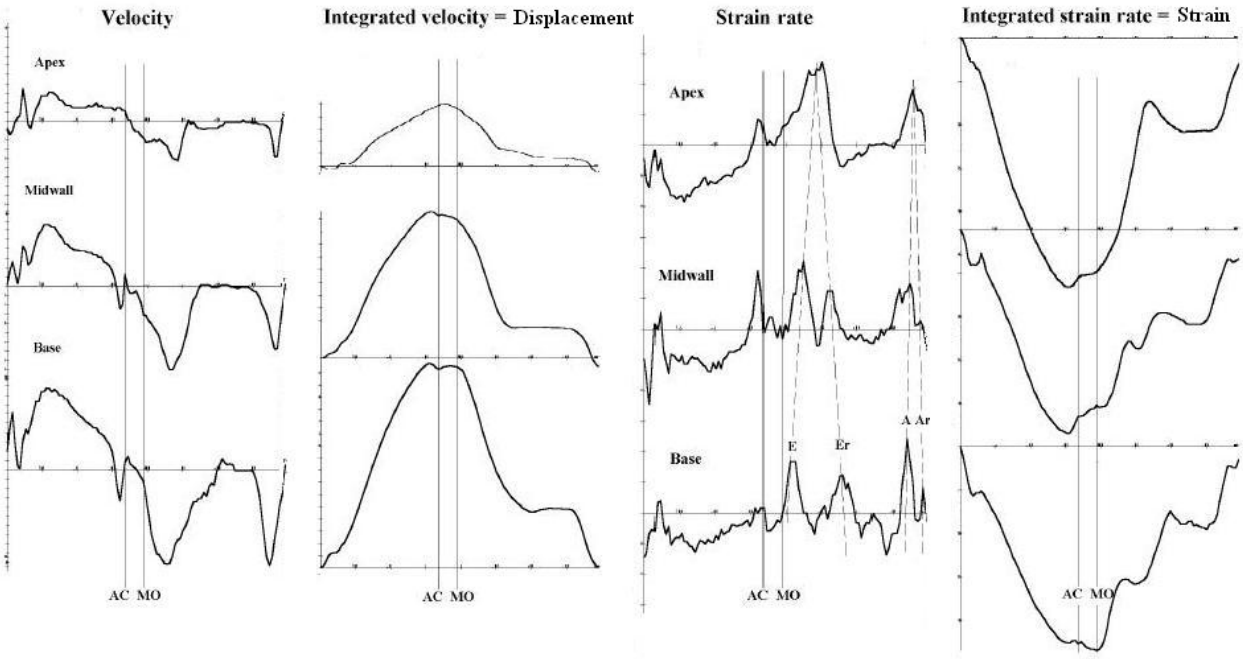


**Figure 10** Display of the longitudinal movement at the apex (top), midwall (middle), and base (bottom) with respect to all four parameters. Notice that the base-apex gradient in the motion parameters (velocity and displacement), is lacking in the deformation parameters (strain and strain rate). AC, aortic valve closure, MO, mitral valve opening.

**Figure 11** (see the next page) Overview of data profiles of all four parameters along all three cardiac axes. Data profiles are obtained from a greyhound in the midsegment of the left ventricular free wall. The Y-axis displays the parameter in question, while the X-axis shows the time (one cardiac cycle). Notice the presence of a positive peak systolic wave (S wave), and two negative diastolic waves (E and A wave) consistent with the early and late diastole, respectively, in all three velocity profiles. Notice also the positive displacement of the myocardium along all three axes during systole, and that the circumferential motion "overshoots" a little when returning during diastole. In accordance with the theory the longitudinal and circumferential systolic strain values are negative due to systolic shortening along these axes, while the radial systolic strain value is positive due to a systolic thickening along this axis. This relationship is also seen in the strain rates where the radial strain rate profile has the opposite polarity of the longitudinal and circumferential strain rate profiles.

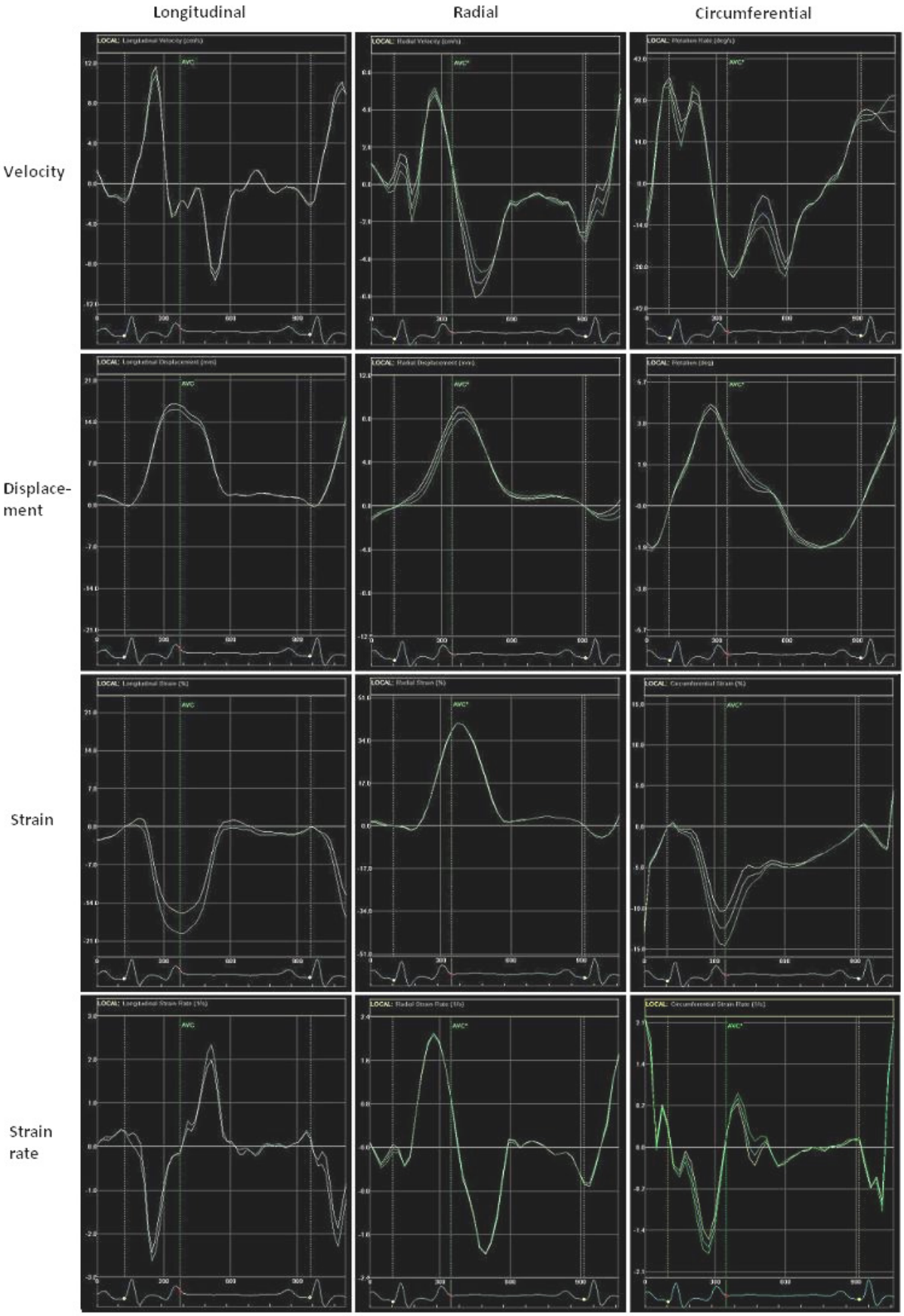
Longitudinal
Radial
Circumferential
Velocity
Displace-
ment
Strain
Strain
rate

# 2. Characteristics of equine echocardiography

The conventional echocardiographic imaging methods in equine cardiology were presented in the Introduction and shortly accounted for in Appendix 1. This chapter will illustrate some of the restrictions that are related to the echocardiographic examination of the horse and explain how these may affect the prospects of implementing tissue Doppler imaging and speckle tracking in this species.

## Limitations from equine anatomy

The initial challenge in equine echocardiography is the size of the heart. Table 1 shows the size of the equine heart compared to the hearts of humans, dogs and cats. It can be difficult to include the entire heart in a 2-D echocardiogram and for a normal adult horse the imaging depth should be 26 to 30 cm (4;31). To generate sound waves with this degree of penetration a low-frequency transducer (2.5 MHz) is the most suitable (4;31).

**Table 1 Estimated heart size based on weight in different species (own making)**

| | Cat | Dog* | Human | Horse |
|---|---|---|---|---|
| Weight/g | 20 | 160 | 250-350 | 3800-5000 |

* Middle sized dog ~ 20kg

The heart of the horse is positioned within the thorax almost vertically on the sternum with its long-axis in a dorso-ventral direction (32). Furthermore, it is positioned with its right chambers most cranially and its left chambers most caudally (31) (see Figure 12) .

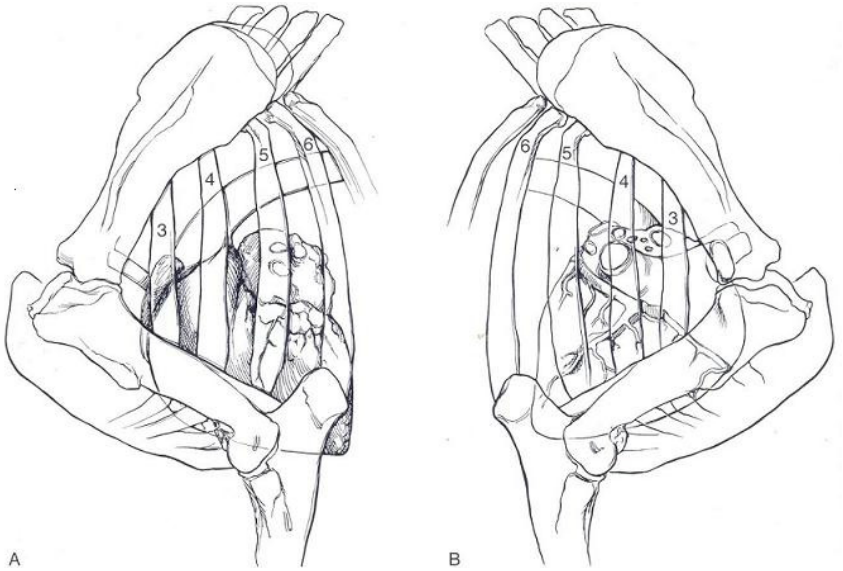


**Figure 12** Position of the heart within the thorax of the horse. The cranial thorax with the third to the sixth costae and the proximal front leg consisting of scapula, humerus and the proximal part of radius and ulna, is shown. Parasternal echocardiographic recordings are made with the transducer positioned in the axilla.

The standard echocardiographic examination of the horse commences from the right side of the thorax where a variety of right parasternal long- and short-axis views of the heart is obtained. Additionally, various M-mode and Doppler (on blood flow) examinations are performed (31). Continuation of the examination from the left side of the thorax is indicated; when left-sided cardiac murmurs are present, if further evaluation is wanted, or if the size the heart exceeds the depth capacities of the equipment when imaged from the right side of the thorax (4;31). When indicated, a range of left parasternal long- and short-axis views as well as M-mode and Doppler (on blood flow) recordings are obtained from the left hemithorax.

**Table 2 Available echocardiographic views - references (4;33)**

| | |
|---|---|
| Images from the right side of the thorax | |
| Parasternal long-axis views | Four-chamber<br>Left ventricular outflow |
| Parasternal short-axis views | Left ventricle at the level of the apex<br>Left ventricle at the level of the papillary muscles<br>Left ventricle at the level of the chordae tendinae<br>Left ventricle at the level of the mitral valve<br>Heart base and aortic valve |
| Images from the left side of the thorax | |
| Parasternal long-axis views | Two- or four-chamber<br>Five-chamber |
| Parasternal short-axis views | Left ventricle<br>Heart base – right ventricle, pulmonary artery |

The most common 2-D echocardiographic views in the horse are listed in Table 2. It is important to notice that true apical images are not available in the horse, as the left parasternal apical views that are used in human and small animal echocardiography are impossible to obtain in this species (4;32). The reason for this circumstance lies in the anatomy of the horse as the apex of the heart rests on the sternum which thereby prevents the recording of true apical images (32). Indeed, some authors (4;33) describe a left parasternal “apical” four- or five-chamber view in the horse, in which the long-axis of the heart is displayed as vertically as possible. However, the display of the left ventricle in this view is highly compromised due to foreshortening (4).

The lack of a true apical image is a disadvantage in the echocardiographic examination of the horse as this echocardiographic projection is of value for Doppler examination of the blood flow through the mitral and aortic valves (4). However, it is even more relevant in connection with this thesis, as a true apical image is necessary to determine the longitudinal parameters in tissue Doppler imaging. As mentioned later in Chapter 3, alignment of the ultrasound beam with the direction of the myocardial motion is critical for the accuracy of the parameters obtained by TDI. When a true apical view is not available it is not possible to determine the longitudinal velocity and accordingly nor the displacement, strain and strain rate by tissue Doppler imaging. In contrast, the lack of true apical views

has no influence on the speckle tracking examination as this technique is angle independent (see Chapter 4).

Another important limitation in equine echocardiography is the great imaging depth that is necessary to visualize the whole heart on the screen (32). The depth capacities of the echocardiographic equipment are developed primarily for the intentional use in human echocardiography (4). And as a direct consequence of the required depth in the horse, the transducer has to wait longer for the sound waves to come back before transmitting a new wave. This causes the frame rate (i.e. the number of recorded frames pr second) to go down (32). This is not normally a problem with conventional echocardiographic imaging because the lower heart rates of the horse (compared to humans) means that the number of frames per cardiac cycle will be almost the same as in humans (32). However, this could become a problem with the TDI and speckle tracking techniques.

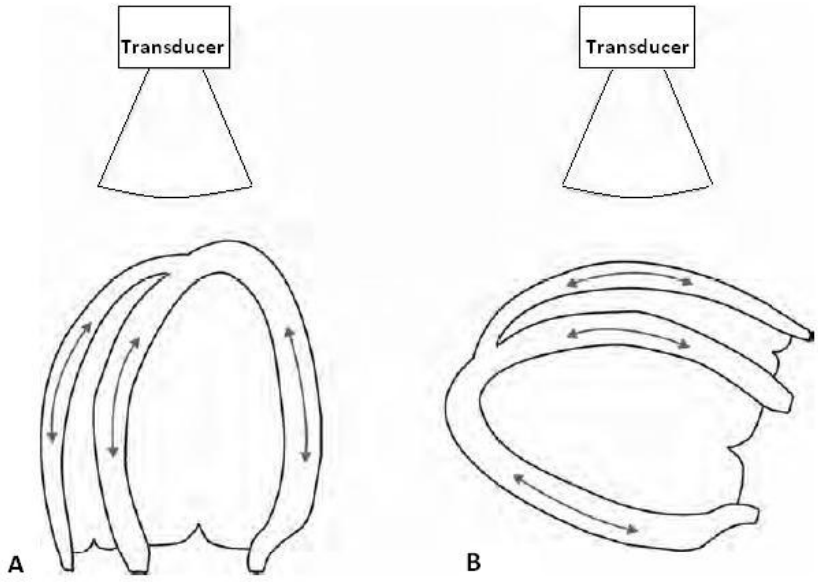


**Figure 13** Schematic drawing of the position of the transducer and direction of the ultrasound beam in an A) true apical projection, and a B) long-axis four-chamber view. The arrows indicate the direction of the longitudinal movement of the left and right ventricle.

## SUMMING UP

The equine echocardiographic examination is to some extent made difficult by the size of the heart and the equine anatomy. True apical echocardiographic projections are not available in the horse. Thus, the longitudinal parameters of myocardial motion and deformation are inaccessible by tissue Doppler imaging, due to the angle dependency of this technique. It is therefore not possible to include longitudinal parameters obtained by TDI in the study in Part II of this thesis, and consequently it was decided not to include longitudinal motion assessed speckle tracking either. The limitations on the frame rate due to the great imaging depth in the horse could become a problem because, as presented next, the tissue Doppler imaging and speckle tracking techniques are dependent on the frame rate.

# 3. Tissue Doppler Imaging

This chapter reviews the method of tissue Doppler imaging with respect to the principles and limitations of the method, and the experiences from studies in healthy humans, dogs and cats. As this is a veterinary thesis, focus will be on validation studies in small animals. And last the available literature of studies applying TDI in the horse will be reviewed.

## Principles

The Doppler principle refers to the shift in frequency that occurs if either the transmitting or receiving object of a sound wave moves relative to each other (see Appendix 1). The traditional use of Doppler echocardiography has been for measuring blood flow velocities, but today the methods of tissue Doppler imaging is becoming generally accepted. While the traditional Doppler estimation of blood flow velocities is performed by recording the frequencies of sound waves reflected by erythrocytes, tissue Doppler estimates tissue velocities by picking up frequencies of sound waves reflected by tissue, i.e. the myocardium (28). Blood flow velocities are normally quite high (40-150 cm/s) but at the same time blood is only weakly reflective (28). In contrast myocardial tissue moves at significantly lower velocities (4-15 cm/s, human values) while being strongly reflective (28). Hence, filter settings that filter out high velocities of weakly reflecting structures are needed in order to display myocardial velocities (5;28). These suitable filter settings are achieved by omitting the so called high-pass filter of the conventional Doppler flow techniques (34).

Three tissue Doppler imaging modes are available; pulsed wave TDI, colour M-mode TDI and 2-D colour TDI (35). *Pulsed wave TDI* analyses peak velocities within a small cell (sample volume) of the myocardium and displays them against time in a way similar to PW Doppler on blood flow (see Figure 14) (5). *Colour M-mode TDI* analyses myocardial velocities along a single scan line. The velocities are colour coded and superimposed on an M-mode image that shows the myocardium in one-dimension against time as seen in Figure 15 (35). *2-D colour TDI* analyses myocardial velocities in two dimensions. The velocity data are colour coded and superimposed on a real-time 2-D echocardiogram as seen in Figure 16 (35).

However, with colour M-mode TDI and 2-D colour TDI the possibilities are not restricted to display of velocity data only. These two imaging modes are also capable of displaying myocardial displacement, strain and strain rate. The data of these three parameters are estimated from the velocity data by the equipment in accordance with the calculation methodologies presented in Chapter 1. The data are then colour coded with a different range of colours for each parameter and superimposed on either M-mode or 2-D real-time images as seen in Figure 16-18 (36). The colour coded display of the myocardial *displacement* has its own specific

term; *Tissue tracking* (10). In this display myocardial segments travelling equal distances during the systole are assigned the same colour (see Figure 19). Each of the resulting colour bands represents an interval of displacement of a specific number of millimetres indicated on the colour scale (10).

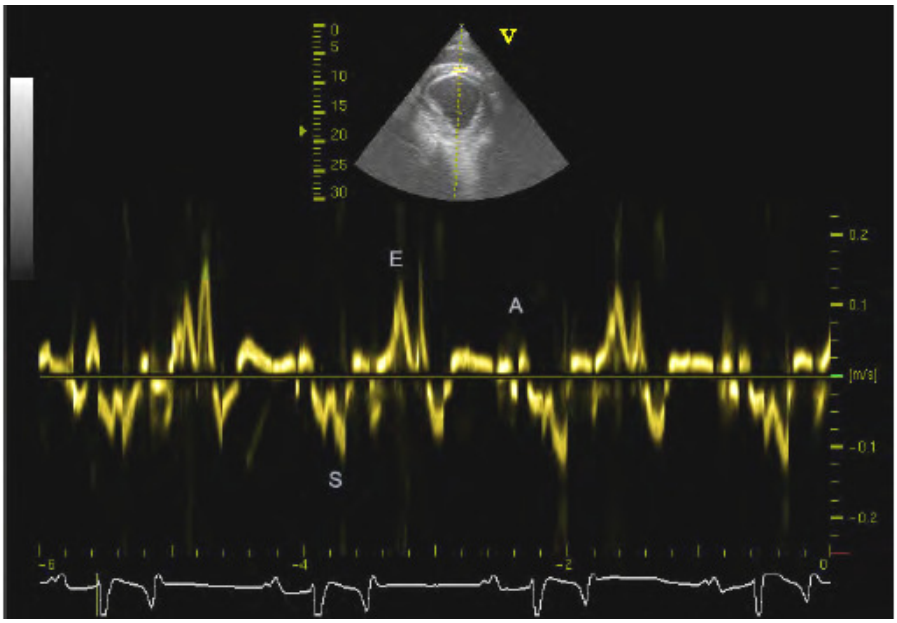


**Figure 14** Example of pulsed wave TDI. The Y-axis represents velocity and the X-axis represents time (four cardiac cycles). A systolic wave (S) and two diastolic waves are seen (E and A), consistent with the peak velocities in systole, early diastole and late diastole, respectively. Notice the opposite polarity of this velocity profile (negative S wave and positive E and A wave) as the sample volume is positioned in the interventricular septum in stead of the free wall. The position of the sample volume is indicated on the two-dimensional image at the top of the screen picture.

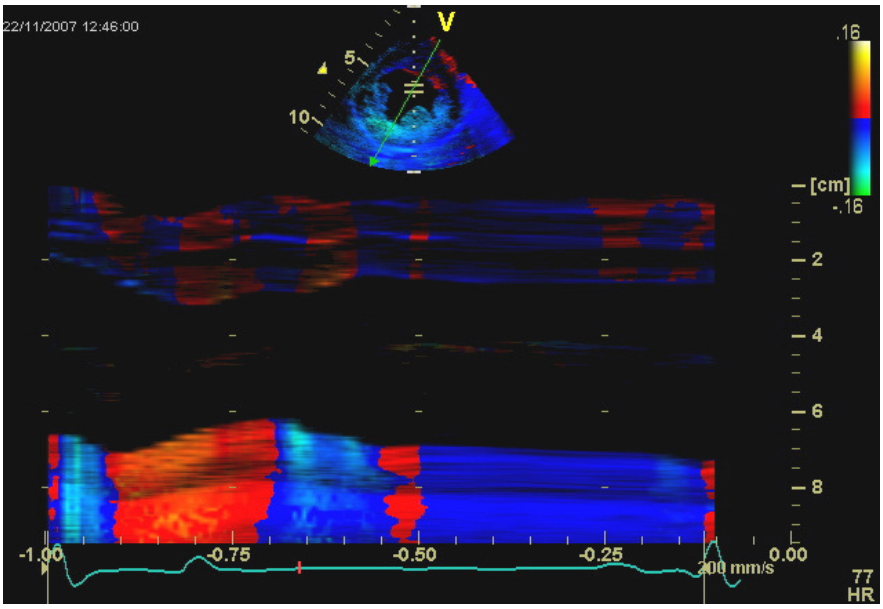


**Figure 15** Example of colour M-mode TDI. The Y-axis represents depth and the X-axis represents time (one cardiac cycle). Myocardial velocities are colour coded. The colour "band" at the bottom is the ventricular free wall, while the black "band" in the middle is the ventricular lumen. The position of the cursor is indicated on the 2-D image at the top.

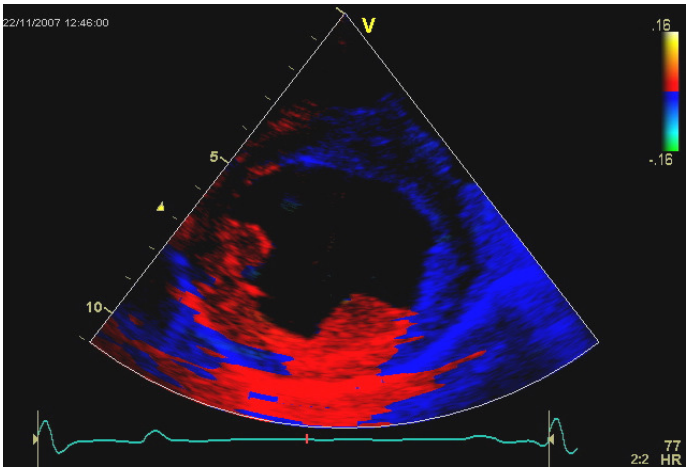


**Figure 16** 2-D colour TDI displaying velocity in a short-axis recording of a greyhound. The velocity data are colour coded, with red indicating motion against the transducer and blue indicating motion away from the transducer.

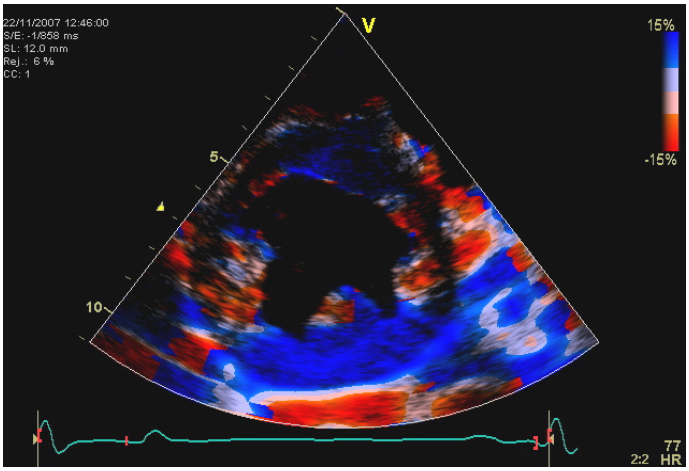


**Figure 17** 2-D colour TDI displaying strain. Same recording as in Figure 16. The strain data are colour coded, with blue indicating positive values and red indicating negative values.

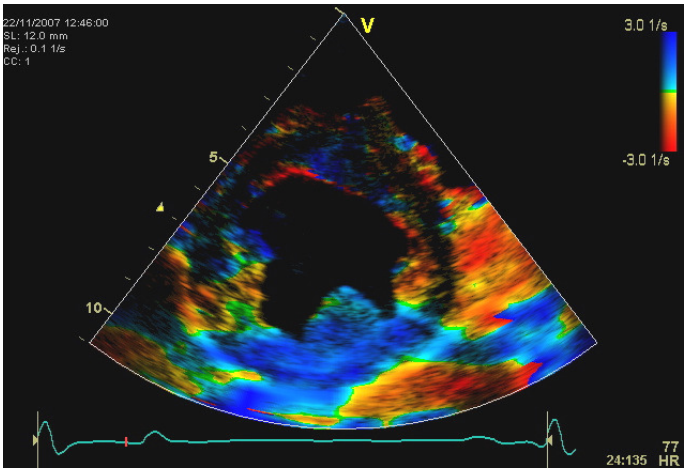


**Figure 18** 2-D colour TDI displaying strain rate. Same recording as in Figure 16. The strain rate data are colour coded, with blue indicating positive values and red indicating negative values. Green colour indicates strain rate values of approximately zero.

Additionally, the display of *strain* and *strain rate* is designated as *strain (rate) imaging* (10;36). This is a general term that applies not only to the strain (rate) estimation in colour M-mode TDI and 2-D colour TDI, but also to strain (rate) estimates derived from speckle tracking as demonstrated in the next chapter.

A further aspect is that the procedure of colour coding in colour M-mode TDI and 2-D colour TDI is synonymous with a semi-quantitative display of the data. But there is limited use of just visually assessing the colour coded TDI data – *"Quantification off line is everything"* (37). For that reason, the 2-D colour TDI

recordings can be post-processed off-line to extract quantitative profiles of velocity, displacement, strain and strain rate in accordance with Chapter 1 (5;35). During the post-processing a specific region of interest (ROI) is selected and the data of the parameter in question is then automatically calculated and presented in a graphic profile. The essence is that one 2-D colour TDI dataset provides information on all four parameters related to myocardial function defined in Chapter 1.

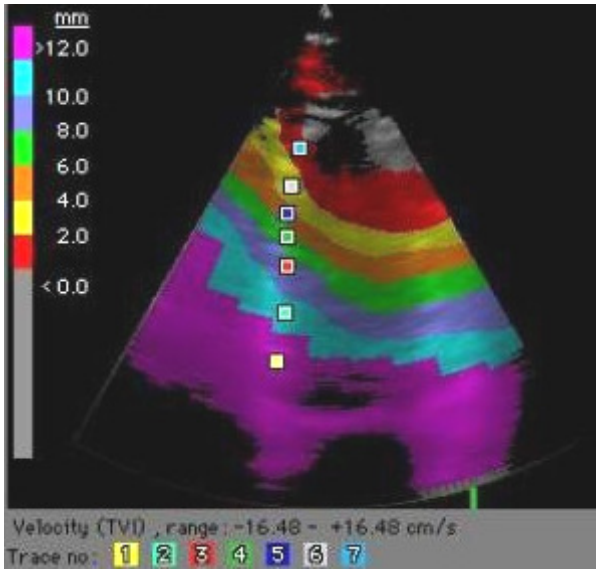


**Figure 19** Tissue tracking in an apical view of a human heart. The myocardial segments are coloured according to the amount of displacement. The resulting colour bands represent areas that travel equal distances during systole. Notice that the basal segments travel longer distances (purple colour) than the apical segments (red colour) – this indicates a base-apex gradient.

## LIMITATIONS

The TDI methods have some inherent limitations. First, just as the conventional Doppler methods for blood flow estimation, TDI estimates velocities relative to the direction of transmitted impulses – thus the measured velocities are only one-dimensional projections of the true velocity vector (38). The accuracy of measured velocities is therefore dependent on alignment of scan lines with the direction of the myocardial motion (35). If proper alignment fails to be achieved the velocities will be underestimated, and as a consequence of this angle dependency a maximum insonation angle of 20º has been suggested (6). Furthermore, as the measured velocities are restricted to be in-line with the scan lines, so are the strain rates calculated from them in TDI derived strain rate imaging (37). However, Storaa et al. (38) investigated the effect of the angle dependency, and found that velocity measurements are more sensitive for angular error than strain and that *"angular correction is of very little importance"* in strain values. Second, as the velocities are measured relative to an external stationary point, i.e. the transducer, the velocity values are influenced by both tethering and translation (10). And third, the filter settings only regard velocity and amplitude of reflected sound waves, and do not necessarily distinguish blood from tissue. This means that blood stasis and thrombi may be misinterpreted as myocardial tissue (28).

In addition to the inherent limitations there are some technical limitations. In ultrasonography the term *temporal resolution* refers to the ability to place structures in time and is determined by the frame rate, i.e. the number of recorded frames pr second (4). Cardiac motion involves movements of short duration (39) and to comprehend these, myocardial imaging should be performed with a sufficient temporal resolution. Lind et al. (39) analysed the optimal frame rate for collection of myocardial velocity data by 2-D colour TDI, and found that it should be at least 100 fps. in order to ensure a sufficient level of details. Teske et al. (6) states that frame rates >180 fps. are required for reliable calculations of strain rate from 2-D colour TDI. And Sutherland et al. (5) states that even higher frame rates are necessary to demonstrate details of diastole (200 fps.) and isovolumetric phases (400 fps.). At frame rates lower than 50 fps. velocities cannot be determined by 2-D colour TDI and data should not be post-processed (5;39). Pulsed wave TDI has a natural high temporal resolution with a typical frame rate of 250 fps. (40). Colour M-mode TDI can be performed with 100-200 fps. (5). However, 2-D colour TDI involves a considerable amount of information because of its two-dimensional character. In order for computer software to be able to handle the amount of data at sufficiently high frame rates, it might be necessary to either reduce the number of scan lines or narrow the sector angle of the recorded image. Sutherland et al. (5) describes a frame rate of 120-140 fps. with a sector angle of 45° in 2-D colour TDI as *"a good clinical compromise"*. However, these settings might not be possible to accomplish in the horse due to the great imaging depth as described in Chapter 2. And a further narrowing of the sector angle will probably be necessary.

Unfortunately, reducing the imaging sector angle also means that less of the myocardium can be displayed in one picture (28). This leads on to the term *spatial resolution*, i.e. the ability to differentiate between different structures in an echocardiographic image (4). Here the opposite hierarchy exists between the three TDI modes. 2-D colour TDI is superior with its ability to display the whole (in plane) left ventricle in an image sector angle of 45°-50° (28). The colour M-mode TDI is able to analyse one myocardial wall at the time, while pulsed wave TDI has the poorest spatial resolution because only a limited part of the myocardium is sampled (30). To analyse more than one myocardial wall at the time by colour M-mode, the *curved colour M-mode* can be used. In this technique a curved M-mode line is drawn freehand in a 2-D colour TDI image as seen in Figure 20. This improves the spatial resolution but unfortunately reduces the temporal resolution to that of 2-D colour TDI (5;37). Notice that the temporal and spatial resolution is interdependent in practice and this might become a challenge when applying the 2-D colour TDI technique on the horse.

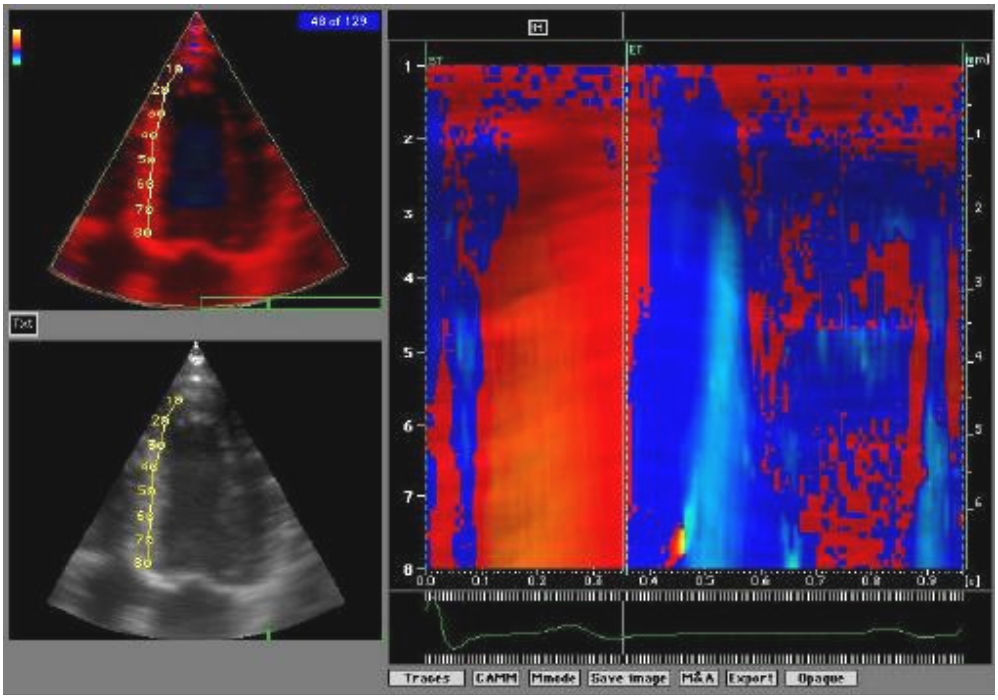


**Figure 20** Curved colour M-mode. Notice the curved line defined by the observer during post-processing of the echocardiographic recordings. The velocity of the myocardium at this line is analyzed and shown in the M-mode display.

## STUDIES ON HUMANS AND SMALL ANIMALS

The use of pulsed wave TDI (41;42), colour M-mode TDI (34) and 2-D colour TDI (34;43) has been validated for measuring myocardial velocities in **humans**. Kukulski et al. (40) compared the pulsed wave TDI and 2-D colour TDI techniques and found good correlation between velocity profiles but poor agreement on peak velocities, and concluded that the techniques should not be used interchangeably for recording of peak velocities. Kukulski et al. (40) partly explains this by the use of differing calculation methodologies in the two methods, but these will not be further elaborated in this thesis. Moreover, TDI derived strain (rate) imaging has been validated *in vitro* (44) and in humans (36).

Tissue Doppler imaging has also recently been introduced in veterinary cardiology (35). The use of 2-D colour TDI for measuring radial and longitudinal velocities in the left ventricle of **dogs** has been validated (45). This study (45) proved the existence of a radial and a longitudinal intrinsic motion in the heart of the dog, and all radial and longitudinal velocity profiles comprised a positive systolic wave (S wave) and two negative diastolic waves (E and A wave). The E wave was significantly greater than the A wave indicating higher velocities in the early diastole. A radial velocity gradient was established as the velocity in endocardial layers was greater than in epicardial layers. Likewise, a longitudinal velocity gradient was proven as basal segments moved more rapidly than the midsegments of the myocardium. The within-day coefficient of variation (CV) for the radial velocities in the endocardium were 16.4%, 15.1%, and 26.6% for the peak systolic S wave, the early diastolic E wave and the late diastolic A wave, respectively. And the

corresponding values for the radial velocities in the epicardium were 2%, 17.6%, and 36%, respectively.

Another study (46) confirmed the findings in the study above (45) and calculated the radial myocardial velocity gradient to be 2.5 ± 0.8 m/s, 3.8 ± 1.5 m/s and 2.3 ± 0.9 m/s in systole, early diastole and late diastole, respectively. Likewise, the longitudinal myocardial velocity gradient was 5.9 ± 2.2 m/s, 6.9 ± 2.5 m/s and 4.9 ± 1.7 m/s in the systole, early diastole and late diastole, respectively. Notice that the use of a myocardial velocity gradient eliminates the effect of cardiac translation, but not the potential error of tethering.

The use of 2-D colour TDI for strain and strain rate imaging in the dog has also been validated (47). This study (47) evaluated the radial and longitudinal deformation parameters in both the right and left canine ventricles. The radial strain profiles were positive consistent with a myocardial thickening in systole. The corresponding radial strain rate profile included a positive peak in systole and two negative peaks in diastole indicating the early and late diastolic filling. In contrast, the longitudinal strain profiles were negative consisting with myocardial systolic shortening, while the longitudinal strain rate profiles comprised one negative peak during systole and two positive peaks in the early and late diastole, respectively. Thus, the longitudinal strain rate profile had the opposite polarity of the radial strain rate profiles. These findings are in agreement with the theory in Chapter 1 (see Figure 11). Additionally, the mean radial strain value (62.9%) was found to be approximately twice the size of the mean longitudinal strain values at both the base (25.5%) and apex (23.2%). The within-day CV for radial peak systolic strain was 4.3% while the within-day CV for the radial peak systolic strain rate was 6.3%. The within-day CV's for the longitudinal peak systolic strain and strain rate values ranged from 3.8% - 8.5% (these variabilities are all considered low).

Assessment of longitudinal velocities in the right canine ventricle by 2-D colour TDI has been studied too (48). In general, the right ventricular velocities were found to be greater than the velocities of the left ventricle. The longitudinal velocity gradient of the left ventricle in this study was calculated to be 5.7 ± 2.0 m/s, 6.7 ± 2.5 m/s and 4.9 ± 1.6 m/s in systole, early diastole and late diastole, respectively, with the highest velocities at the base of the heart. This is very similar to the results (46) mentioned earlier.

The use of 2-D colour TDI has also been validated for measuring radial and longitudinal velocity in the left ventricle of the **cat** (49). The existence of radial and longitudinal myocardial velocity gradients was proven, and both the radial and longitudinal velocity profiles included a positive systolic wave (S wave) and two negative diastolic waves (E and A wave). The E wave was significantly greater than both the S and A wave indicating higher velocities in the early diastole. As a unique feature in cats, a fusion of the E and A wave was seen in 47% to 64% of the examinations due to the high level of normal heart rates in this species (120-240

b.p.m. (50)). The fusion was seen at heart rates exceeding 220 b.p.m. and represents a disadvantage of TDI in this species as it makes evaluation of diastolic velocities difficult. Fusion of the E and A wave was not seen in the above study on dogs (46) as the heart rate of the animals in that study did not exceed 177 b.p.m. (normal heart rate 70-160 b.p.m. (50)). A similar fusion is not to be expected in the horse either, as the normal heart rate of this species is 28-40 b.p.m. (51). The within-day CV for the radial velocities in the endocardium was 8.2% and 6.5% for the peak systolic S wave and the early diastolic E wave, respectively. The corresponding values in the epicardium were 20.0% and 28.9%, respectively.

Another study (52) confirmed these results in the cat. The radial velocity gradient was calculated to be 2.2 ± 0.7 m/s, 3.3 ± 1.3 m/s and 1.8 ± 0.7 cm/s for the systole, early diastole and late diastole, respectively. The corresponding values of the longitudinal velocity gradient were 2.7 ± 0.8 m/s, 3.1 ± 1.4 m/s and 2.1 ± 0.9 cm/s, respectively. Fusion of the E and A wave was seen at heart rates above 210 b.p.m. in the 8% of the radial and 10% of the longitudinal velocity profiles.

In a similar study (53) in a different group of cats with consistent findings, the radial velocity gradients were 2.5 ± 0.8 cm/s, 3.3 ± 1.3 cm/s and 1.7 ± 0.9 cm/s in systole, early diastole, and late diastole, respectively, and the longitudinal gradients were 2.9 ± 0.9 cm/s, 3.4 ± 1.5 cm/s and 2.3 ± 0.9 cm/s.

A common feature of the small animal studies reviewed above is that the longitudinal parameters were obtained from the left parasternal apical view. This view is not accessible in the horse (see Chapter 2), and consequently the limited number of published studies on TDI in horses are all made on short-axis images and do not include longitudinal parameters. The equine studies are evaluated next.

### Studies of tissue Doppler imaging in horses

The use of pulsed wave TDI and 2-D colour TDI for measuring radial velocity in the left atrium of the **horse** was validated by Schwarzwald et al. (19). Based on the reproducibility results of this study the same group of authors later used pulsed wave TDI in an evaluation of left atrial mechanical dysfunction subsequent to atrial fibrillation (17).

Schwarzwald et al. (18) also validated the use of pulsed wave TDI and 2-D colour TDI for measuring of radial velocities in the left ventricle. They found that the variability of 2-D colour TDI was high compared to pulsed wave TDI. The intraobserver measurement variability for PW TDI was generally low with a coefficient of variation of 0.5-12%. The corresponding variabilities for 2-D colour TDI were not given in the published abstract. Furthermore, Schwarzwald et al. (18) states that calculations of the radial myocardial velocity gradient and radial strain rate from 2-D colour TDI recordings were unreliable.

Sepulveda et al. (20) validated the use of pulsed wave TDI and 2-D colour TDI for measuring myocardial velocities of both the left and right equine ventricles. They

found three major movements in all myocardial regions examined consisting with an S, E and A wave in the systole, early diastole and late diastole, respectively. The pattern of these waves was similar in both pulsed wave TDI and 2-D colour TDI but not completely alike in all myocardial regions. In the right ventricular wall and the left region of the left ventricle (alias the left ventricular free wall) the systolic movement (S wave) was in the opposite direction to the diastolic movements (E and A wave) as illustrated in Figure 11. In contrast the direction of the movement in late diastole (A wave) was not consistent in the right and caudal region of the left ventricle, and the movement of the interventricular septum showed great complexity. It is important to notice, that Sepulveda et al. (20) do not define the measured velocities specifically as radial though obtained in a short-axis image. In stead they state that the study *"is most likely to reflect lateral rather than longitudinal movement".* If this lack of definition has lead to less attention to the insonation angle it might be a contributing factor to the observed inconsistency of the A wave patterns.

In general, Sepulveda et al. (20) obtained the highest velocities in early diastole in most myocardial regions, and the right and caudal regions of the left ventricle moved faster than all other myocardial regions throughout the cardiac cycle. The peak mean velocities measured in the left ventricular free wall by 2-D colour TDI gave the following results: -5.4 ± 3.5 cm/s, 15.0 ± 5.2 cm/s and 5.2 ± 1.9 cm/s in systole, early diastole, and late diastole, respectively. Notice the opposite signs of these values with the S wave being negative and the E and A wave being positive. The reason for this is that Sepulveda et al. (20) made the recording from the left parasternal view in stead of from the right side of the horse.

The two techniques did not agree on the size of the velocities. As 2-D colour TDI measures mean velocities, while pulsed wave TDI also measures maximum velocities – Sepulveda et al. (20) concluded that the two modes should not be used interchangeably for measuring velocities, consisting with the statement of Kukulski et al. (40). Compared to pulsed wave TDI, 2-D colour TDI showed less repeatability. For the left ventricular free wall the coefficient of variation in systole, early diastole, and late diastole, respectively, was 24.19%, 11.85% and 13.18% for PW TDI, and 33.71%, 16.48% and 26.88% for 2-D colour TDI.

Finally, Spieker (21) evaluated the use of PW TDI and 2-D colour TDI for diagnosing cardiac diseases in horses. She examined a healthy control group together with 5 other groups of horses with different pathologic cardiac conditions. Examination of the control group proved the existence of a velocity profile similar to those found in humans – with a positive peak systolic wave and two negative diastolic waves indicating the early and the late diastole, respectively. Most of the velocity profiles even included an extra positive wave consistent with the isovolumetric contraction period in the early systole. The mean radial velocities in the left ventricular free wall obtained by 2-D colour TDI in the healthy control group were 5.9 ± 1.6 cm/s,

−10.3 ± 2.0 cm/s, and −7.5 ± 1.9 cm/s in the systole, early diastole, and late diastole, respectively (these data are based on calculations from Spieker's results – see Appendix 5). The velocity profiles were uniform when obtained with the PW TDI and the 2-D colour TDI method, but again the velocities measured by PW TDI obtained the highest values.

Though this thesis is focused on healthy animals, a supplementary comment should be made on the findings in the horses with cardiac disease made by Spieker (21). Interestingly, a significant increase in the peak systolic velocity (S wave) of the interventricular septum was seen in horses with aortic valve insufficiency, and the velocity wave of the late diastolic filling (A wave) was absent in horses with atrial fibrillation. These findings indicate that the TDI method may indeed be of value for diagnostic purposes in equine cardiology.

### SUMMING UP

Three tissue Doppler imaging modes are available; pulsed wave TDI, colour M-mode TDI and 2-D colour TDI. Pulsed wave TDI provides information on myocardial velocity only, while the colour M-mode and 2-D colour TDI produce information on all four parameters – velocity, displacement, strain and strain rate. In veterinary cardiology most studies have been made on 2-D colour TDI. The existence of one positive systolic and two negative diastolic waves in the myocardial velocity profiles has been proven. Radial and longitudinal velocity gradients have been shown in small animals. Furthermore, a limited number of studies on horses have been published. In relation to TDI and horses, it is important to notice that longitudinal parameters are not available with TDI in the horse because this technique is angle-dependent and true apical views are not available in this species.

A comparison of 2-D colour TDI and speckle tracking with special attention paid to limitations and off-line features is given at the end of the review on speckle tracking in the next chapter.

# 4. SPECKLE TRACKING

THIS CHAPTER ANALYSES THE SPECKLE TRACKING METHOD WITH RESPECT TO THE PRINCIPLES AND LIMITATIONS OF THE METHOD, AND THE EXPERIENCES FROM STUDIES IN HEALTHY HUMANS, DOGS AND CATS. TO EMPHASIZE THE VETERINARY ASPECT OF THIS THESIS SPECIAL ATTENTION IS PAID TO AVAILABLE STUDIES IN SMALL ANIMALS. ACCESSIBLE LITERATURE ON STUDIES OF SPECKLE TRACKING IN HORSES WILL ALSO BE EVALUATED. FINALLY, A COMPARISON OF 2-D COLOUR TDI AND SPECKLE TRACKING IS GIVEN IN THE CHAPTER SUMMARY.

## PRINCIPLES

A "speckle" means a little spot or mark. Speckles are seen in greyscale echocardiographic images and arise from heterogeneity of the myocardium. Small irregularities of the tissue make the ultrasound waves scatter and these scattered sound waves interfere and some are reflected at the transducer (5). There is a close relationship between the positions of these scatters in the tissue and the resulting speckles in the echocardiographic images (5). Thus speckles can also be designated as *"natural acoustic markers"* (54). It is important to realize that speckles are not constant. If the relative positions of scatters in the tissue change, the interference pattern and thereby the speckle pattern change too (5). This can happen for various reasons, for instance; as cardiac fibres move during cardiac contraction, if scatters move out of the imaging plan, or if the angle of the incoming sound waves change, e.g. the transducer is moved (5). The result is that speckles change shape, brightness and position over time (5). However, if echocardiographic images are obtained with a sufficient temporal resolution, i.e. at high frame rates, the change in speckle pattern will be relatively small from frame to frame and tracking of the speckles becomes possible (5).

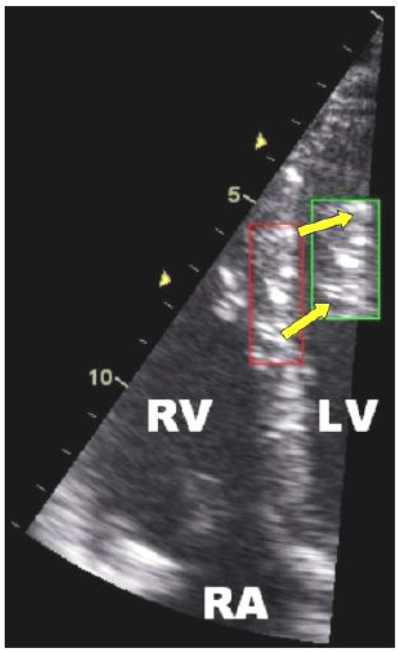


**Figure 21** A greyscale 2-D echocardiogram of the interventricular septum illustrating the principle of speckle tracking. The red square represents the position of a unique speckle pattern at the start of the systole, and the green square represents the new location at the end-systole. This shift can be estimated by the software by tracking the speckle pattern on a frame-to-frame basis. Notice the changed dimensions of the speckle pattern at end-systole (green square) indicating a longitudinal shortening and a radial thickening of the myocardium. RV, right ventricle, RA, right atrium, LV, left ventricle.

Speckle tracking is performed off-line in the post-processing of conventional 2-D greyscale (B-mode) echocardiographic recordings. The endocardial border is initially demarcated and the software will subsequently mark the rest of the myocardium (54). The software will then track the speckles of the myocardium from frame to frame by a software algorithm – this is known as *feature tracking* in computer technical language (55). As mentioned above, speckles are dynamic and change over time. The change in position of the speckles between frames represents the displacement of the tissue, and as the time interval between two frames is known the velocity can be calculated (56). At the same time speckles change their shape – some is becoming longer and others becoming wider. Consequently, the dimensions of the speckle pattern are changed, and from this, strain can be calculated as the change in length relative to the initial length (see Formula 1 and Figure 21) (6;56). Strain rates are then automatically calculated by the computer as well. Thus, speckle tracking is also able to provide all four

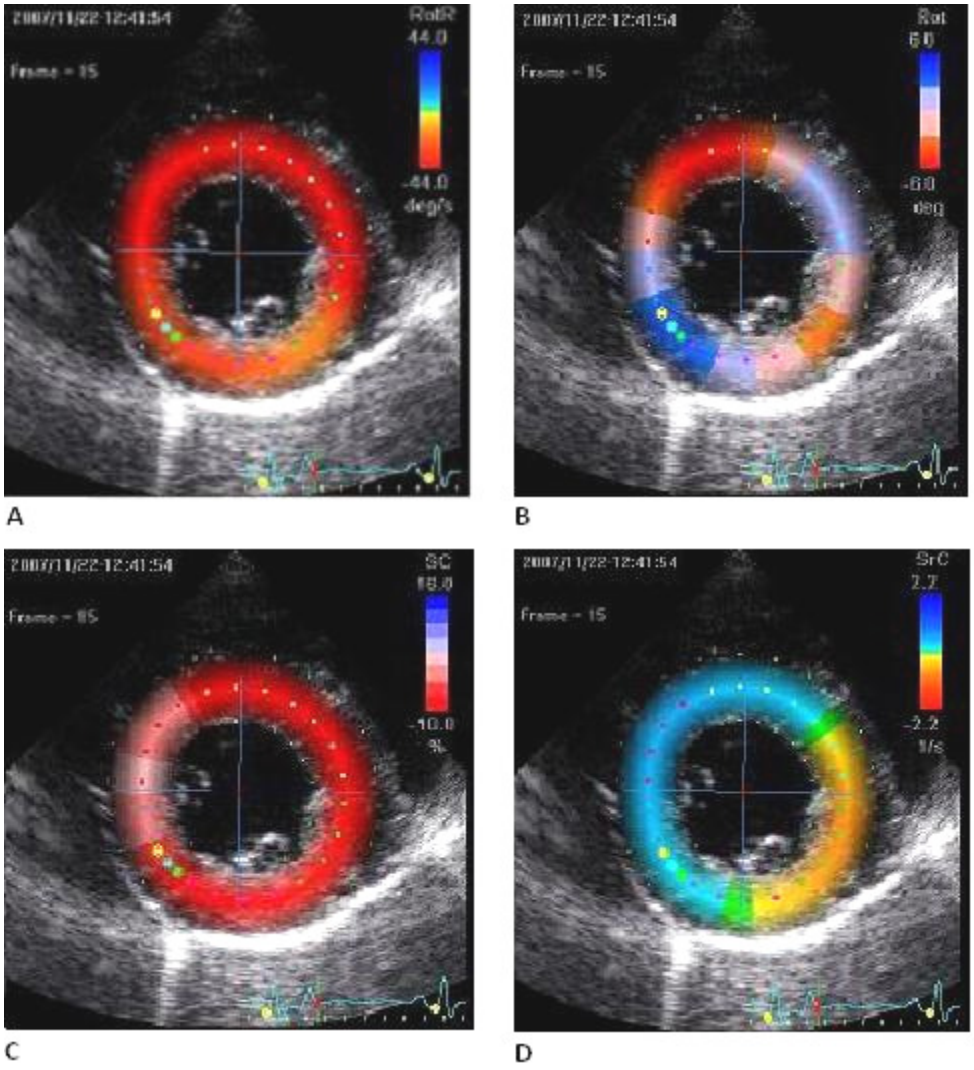


**Figure 22** Speckle tracking analysis on a short axis recording of the circumferential motion in the heart of a greyhound. A) Velocity, B) Displacement, C) Strain, and D) Strain rate. Notice the different colour codes for the different parameters. Except for the displacement data, these colour codes are the same as for 2-D colour TDI in Figures 15-17.

parameters from one data set. The resulting data on the four parameters can be displayed in a number of ways; as semi-quantitative colour coded with a specific range of colours for each parameter superimposed on the 2-D greyscale image (just as the colour coded TDI modes) (see Figure 22), as a semi-quantitative curved colour M-mode, and finally as quantitative data profiles. Accordingly, as mentioned in Chapter 1 *stain (rate) imaging* can be based on speckle tracking as well as tissue Doppler imaging. In fact speckle tracking is also known as *two-dimensional strain imaging* (6;57). A list of synonymous names for TDI and speckle tracking is given in Appendix 3.

### LIMITATIONS

The *temporal resolution* is of great importance in speckle tracking. Software systems track speckles from frame to frame, but if the change in speckle patterns becomes too large between consecutive frames, speckle tracking is no longer possible (6). To keep the change in speckle pattern between frames small, the time interval between frames must be kept low – thus the frame rate must be high. On the other hand, increasing the frame rate too much will reduce the *spatial resolution* – either by reducing the number, and thereby the density, of scan lines, or by narrowing the image sector angle. Consequently, the speckle patterns either become to poorly resolved to track, or speckles might move out of the image during tracking (6). Hence, choosing frame rates for speckle tracking is a balancing act between the temporal and spatial resolution and the optimal frame rate is still under discussion. Rappaport et al. (58) state that frame rates should be between 40-100 fps.. Suffoletto et al. (56) found frame rates of 30-90 fps. were suitable. And Teske et al. (6) suggest 50-80 fps.. These relatively low frame rates involve a risk of undersampling, especially at high heart rates. However, this might be a minor problem in the horse as the normal heart rate in this species is 28-40 b.p.m. (51). An additional limitation is that speckle tracking provides a two-dimensional estimate of the tissue velocity, and thereby still not the true three-dimensional velocity vector but a projection of it.

### STUDIES ON HUMANS AND SMALL ANIMALS

The use of speckle tracking for assessment of myocardial longitudinal velocity, strain and strain rate in healthy **humans** has been validated (59). Estimation of longitudinal velocity, displacement and strain by speckle tracking in the right ventricle of normal children has also been validated (60). Additionally, speckle tracking has been validated for measuring left ventricular rotational movements and torsion (measured in degrees) in humans (61).

As speckle tracking is a very recently developed technology, only a limited number of validation studies have been performed in relation to veterinary echocardiography. To the author's knowledge there are no published studies of speckle tracking in the **cat**. However, the technique has been validated for measuring radial strain and strain rate in the left ventricle of healthy **dogs** (62). The

radial strain profiles were positive, consisting with a radial thickening of the myocardium during systole. The corresponding radial strain rate profiles included a positive peak in systole and two negative diastolic peaks indicating the early and late diastolic filling. These results were compared to 2-D colour TDI derived strain and strain rate profiles which demonstrated similar characteristics and were positively correlated with the speckle tracking results. Furthermore, these speckle tracking results are in agreement with the theory in Chapter 1 and the results given in the study of strain imaging by 2-D colour TDI in dogs presented earlier (47). The within-day CV for radial peak systolic strain was 5.16% while the within-day CV for the radial peak systolic strain rate was 7.76% (62).

Another study examined the use of speckle tracking for quantification of left ventricular rotational movements and torsion in the dog (63). The results showed that the base rotated in a clockwise direction, while apex turned in a counter-clockwise direction during systole when viewed from the apex. This observation is in agreement with the theory in Chapter 1, and indicates that the canine heart actually does twist. The peak end-systolic rotation was 5.4 ± 3.2° at the apex and −3.1 ± 1.3° at the base – indicating that the apex rotated more than the base. Moreover, the peak end-systolic rotation occurred sooner at the apex. The within-day CV for rotation was 9.04% for basal measures and 11.82% for apical measures. Additionally, an initial counter-clockwise rotation of the base and clockwise rotation of the apex was seen in the early systole (isovolumetric contraction phase). A similar observation has been made in human studies (61).

### STUDIES OF SPECKLE TRACKING IN HORSES

At the time of writing the only published literature known to the author that investigate the application of speckle tracking in the **horse** is an abstract by Schwarzwald et al. (22). They studied the feasibilities of speckle tracking for assessment of radial and circumferential strain and strain rate in the left ventricle of the horse. The radial and circumferential strain rates were obtained in systole, early diastole and late diastole, however the automated tracking appeared inadequate during diastole and Schwarzwald et al. (22) point out that the diastolic measurements might not be valid. In addition the radial strain and strain rates were in general more reliable than the corresponding circumferential parameters.

The intra-observer measurement variability (in coefficients of variation) for the radial peak systolic strain and the radial strain rates in systole, early diastole and late diastole were 6.3%, 4.9%, 12.5% and 8.7%, respectively – while the same variability for the circumferential peak systolic strain and the circumferential strain rates in systole, early diastole and late diastole were 9.2%, 17.0%, 5.0% and 5.7%, respectively (22;64).

The results for the radial peak systolic strain and the radial strain rates in systole, early diastole and late diastole were 48.61 ± 10.71%, 1.38 ± 0.17$s^{-1}$, −1.21 ± 0.32 $s^{-1}$ and −1.23 ± 0.43 $s^{-1}$, respectively, while the circumferential peak systolic strain and

the circumferential strain rates in systole, early diastole and late diastole were −14.25 ± 2.49%, −0.83 ± 0.06 $s^{-1}$, 1.59 ± 0.21 $s^{-1}$ and 0.69 ± 0.14 $s^{-1}$, respectively (64).

### SUMMING UP - TISSUE DOPPLER IMAGING VERSUS SPECKLE TRACKING

Speckle tracking is basically a method for post-processing of 2-D greyscale (B-mode) echocardiographic images in which speckles are tracked on a frame-to-frame basis to determine myocardial velocity, displacement, strain and strain rate. Here follows a comparison on speckle tracking and 2-D colour TDI.

In general, the two techniques appear to be equally difficult to master and equally time consuming (65). Both provide information on all four parameters – velocity, displacement, strain and strain rate from just one dataset. However, both techniques also possess different advantages and disadvantages.

The angle dependency of tissue Doppler imaging has two major consequences. First, it limits the number of myocardial segments that can be examined with this technique, as alignment between the sound beam axis and the direction of the myocardial movement is not always possible (5). This circumstance has an important impact on the applicability of TDI in the horse as true apical echocardiographic projections are not available in this species and hence the longitudinal parameters are inaccessible by TDI. Secondly, the measured velocities are only one-dimensional projections on the scan line axis of the true (three-dimensional) velocity vector (38). In contrast, speckle tracking measures velocities as a two-dimensional vector within the two dimensions of the 2-D echocardiogram (6). This not only allows examination in more myocardial segments, it also improves the chances of a more accurate estimate of the true velocity.

The region of interest (ROI) in 2-D colour TDI is fixed in space and as such it does not follow the myocardium during the cardiac cycle (65). In contrast, the ROI in speckle tracking follows the speckles and thereby the myocardium throughout the cardiac cycle (65). Thus, in 2-D colour TDI the myocardium present in the ROI might not be constant throughout the cardiac cycle, and needs to be traced manually to check that it does not move outside the endocardial and epicardial borders during the cardiac cycle (65). Furthermore, as it will be presented in the Materials and Methods section in Part II of this thesis, the ROIs are defined in very different ways in TDI and speckle tracking. This makes a comparison on the results rather complicated.

**Table 3 Summarized advantages and disadvantages (extract from Ingul et al. (65))**

| | 2-D colour TDI | Speckle tracking |
|---|---|---|
| Advantages | B-mode independent | Angle independent<br>ROI follows the myocardium |
| Disadvantages | Angle dependency<br>ROI fixed in space, not in myocardium | Dependent on the frame rate and the quality of B-mode images |

The relatively low frame rates used in speckle tracking in comparison with TDI has been suggested to involve a risk of undersampling at high heart rates (6;65). However, considering the level of normal heart rates in horses this is not expected to pose a problem in the study in Part II of this thesis.

In conclusion, the 2-D colour TDI and speckle tracking both involve different advantages and limitations. However, both techniques provide the same parameters and appear to perform well. Consequently, both techniques can be considered relevant for quantification of regional myocardial function as long as the user is aware that some differences in the calculated parameters should be expected due to technical factors (6). For further comparison on TDI and speckle tracking readers are referred to Ingul et al. (65) and Leitman et al. (59).

The next chapter, which is also the last chapter in Part I, considers the response of the heart to physical training in both human and equine athletes, and reflects on the perspectives of implementing tissue Doppler imaging and speckle tracking in equine echocardiography.

# 5. CARDIAC RESPONSE TO TRAINING

THE HEART IS OF FUNDAMENTAL IMPORTANCE IN ATHLETIC PERFORMANCES OF BOTH HUMAN AND EQUINE ATHLETES. THIS CHAPTER WILL OUTLINE HOW THE HEART ADAPTS TO ENCOMPASS THESE PHYSICAL CHALLENGES, AND CONSIDER THE FEASIBILITIES OF THE TDI AND SPECKLE TRACKING TECHNIQUES IN EQUINE SPORTS MEDICINE.

## THE "ATHLETE'S HEART"

The term "*athlete's heart*" refers to the cardiac remodelling that occurs in response to long-term intensive training (66). The left ventricle undergoes physiological hypertrophy and the morphological changes include increases in left ventricular internal diameter, left ventricular wall thickness and LV mass (66). This physiological hypertrophy of the myocardium has been postulated to exist in two different morphological forms depending on the character of training; an *endurance-trained heart* and a *strength-trained heart* (66). Endurance training and strength training involves different hemodynamic changes. The heart adapts to these changes by normalizing the stress on the cardiac walls through growth of the cardiomyocytes in accordance with the Law of La Place (67) (see Appendix 6).

Endurance training such as long distance running is characterized by dynamic exercise for long periods of time, and is involving a large increase in cardiac output but only a modest increase in blood pressure (11;66). This increases the preload of the left ventricle resulting in volume overload and increased diastolic stress (66). To normalize this stress the cardiomyocytes will grow longer by adding myofibrils in series, thereby increasing the end-diastolic left ventricular internal diameter (32;67). This is known as *eccentric hypertrophy* (67). However, there is a simultaneously proportional wall thickening and this leaves the ratio of wall thickness to internal diameter unchanged in endurance athletes (66;67).

On the other hand, strength training such as weightlifting is characterized by static exercise involving a large increase in blood pressure but only a small increase in cardiac output (66). The elevated systemic blood pressure causes the afterload to increase (66). To overcome this pressure overload the left ventricular cardiomyocytes grows stronger by adding myofibrils in a parallel manner, whereby the ventricular wall thickness is increased (67). This is known as *concentric hypertrophy* (67). The increase in wall thickness is not accompanied by an increase in chamber size so the ratio of wall thickness to internal diameter is increased in strength athletes (66;67).

The existence of two divergent forms of the "athlete's heart" related to the character of training, has been confirmed by a large meta-analysis including 59 echocardiographic studies and 1451 athletes performed by Pluim et al. (68). However, they state that the classification is not absolute and should be regarded more as a *"relative concept"* (68). According to Pluim et al. (68) endurance training

purely involving volume overload and strength training purely involving pressure overload do not exist. Endurance training will always involve an element of pressure load and hence an increase in wall thickness, as strength training will always involve a small increase in cardiac output and hence an increase in left ventricular diameter. Consequently, most, if not all sports, will to some extent represent a combination of endurance and strength training. Spirito et al. (69) investigated the influence of 27 sports on cardiac morphological changes, and ranked them according to their impact on left ventricular diastolic internal diameter and wall thickness. They found that about 80% of the sports had an effect on both chamber size and wall thickness. Athletes performing endurance cycling and rowing exhibited the largest measures of both left ventricular internal diameter (LVID) and wall thickness, while cross-country skiing primarily influenced the LVID and weightlifting primarily lead to increased wall thickness (69).

In addition to morphology, Pluim et al. (68) also investigated the functionality of the "athlete's heart" in their meta-analysis. They found that the left ventricular systolic function in athletes based on evaluation of fractional shortening (FS%) and ejection fraction (EF) was similar to non-athletes. However, Pluim et al. (68) draw attention to the fact that fractional shortening and ejection fraction are measures of the overall ventricular chamber function and not the regional myocardial function, i.e. contraction and relaxation. This brings us back to the TDI and speckle tracking techniques.

### STUDIES OF TDI AND SPECKLE TRACKING IN HUMAN ATHLETES

Recently the tissue Doppler imaging and speckle tracking techniques have been engaged in studies of human athletes. The purposes of these studies mainly fall into two categories; to evaluate the myocardial function of the "athlete's heart", and to assess the ability of the techniques to distinguish between pathologic cardiac hypertrophy and the presumably benign physiologic hypertrophy of the "athlete's heart".

Poulsen et al. (70) examined the myocardial function of endurance athletes, strength athletes and an untrained control group by using 2-D colour TDI. In this study, the peak E myocardial velocity in early diastole was significantly higher in both groups of athletes compared to the control group – indicating an enhanced early diastolic filling. Additionally, the longitudinal myocardial velocities in basal and mid segments of the left ventricle were significantly higher in the strength athletes than in the endurance athletes and the control subjects. However, evaluation of myocardial function by quantifying only myocardial velocities might be misleading as the velocity measurements are influenced by tethering and hence are incapable of distinguishing between active local contraction and the passive motion from neighbouring segments (36). For that reason Poulsen et al. (70) also investigated the longitudinal strain rates, and found that the systolic strain rates in both the basal, mid and apical segments of the left ventricle were significantly

increased in the strength trained athletes compared to the endurance athletes and the control group.

Saghir et al. (71) studied the longitudinal strain and strain rate derived from 2D colour TDI in the interventricular septum of strength athletes. They found a significant increase in longitudinal strain in the basal segment of the athletes, but otherwise there were no significant differences compared to the control group.

Speckle tracking has also been applied to evaluate the "athlete's heart". Stefani et al. (55) studied the consistency of TDI and speckle tracking in assessment of strain values in athletes, and found a substantial agreement between the two methods when measuring longitudinal strain in the basal segments of the right and left ventricles – indicating that the two methods might be used interchangeably for stain imaging in athletes.

Another study by Stefani et al. (72) found equivalent longitudinal strain values at rest in athletes and controls by use of the speckle tracking technology. In contrast, Richand et al. (73) also used speckle tracking for strain imaging in athletes, but observed decreased longitudinal strain in all examined myocardial segments when comparing with control subjects. Additionally, Richand et al. observed higher radial strain in the athletes but no significant difference in the circumferential strain values.

In general, studies (71;73) have shown a tendency of decreased strain and strain rate values in patients with pathologic cardiac hypertrophy compared with athletes and healthy controls – suggesting that TDI and speckle tracking derived strain (rate) imaging may indeed have a clinical relevance in distinguishing between physiologic and pathologic cardiac hypertrophy.

Notice that the reported studies of myocardial function in athletes in comparison with control subjects are mostly concerned with longitudinal parameters obtained from apical views. However, in the horse the longitudinal parameters are not accessible with TDI and only might be so with speckle tracking (have not been studied so far). Additionally, the results are somewhat divergent and a uniform description of myocardial velocity, displacement, strain and strain rate data in the "athlete's heart" is lacking. This makes the speculations on what to expect from the study of athletic versus non-athletic horses in Part II rather difficult.

### PROSPECTS FOR TDI AND SPECKLE TRACKING IN EQUINE ATHLETES

The human exploitation of the horse as an athlete makes this species unique compared to other domestic animals. This also influences the field of equine cardiology as this is primarily concerned with "minor" heart diseases and their effect on the performance capability of the horse (32). Equine sports include a variety disciplines that make different demands and impacts on the body of the equine athlete. For instance, breeding for speed in Thoroughbred racehorses has left this breed with a proportionately larger heart but unfortunately also a

proneness to valvular regurgitation, atrial fibrillation and exercise-induced pulmonary haemorrhage (74). Increased cardiac dimensions have for a long time been associated with success in the horseracing industry and there has been a strong urge to find methods that can predict the performance potential of a horse – thereby saving the costs of maintaining horses without athletic potential (67;74). A number of different echocardiographic studies have been performed to evaluate the relationship between equine athletic performance and cardiac parameters.

Young (75) examined 2-year-old Thoroughbreds before commencement and after 18 weeks of commercial flat-race training. Young found that all the horses experienced increases in the left ventricular internal diameter, wall thickness and relative wall thickness during the 18 weeks study period – and this lead her to the suggestion that commercial flat-race training in horses leads to a combined cardiac response that falls between the two extreme categories of an endurance-trained and a strength-trained heart. Buhl et al. (76) followed a group of 2-year-old trotters for 1½ year and found comparable results with increases in LVID, wall thickness and LV mass, except that the relative wall thickness was unchanged. However, both Young (75) and Buhl et al. (76) point to the fact that hypertrophy due to normal growth plays a substantial role when dealing with young animals, and it is not possible to estimate this influence without including an untrained control group.

Regarding the functionality of the heart in equine athletes, Young (75) found significant reductions in ejection fraction and fractional shortening during the 18 weeks study period. Buhl et al. (76) also found a decrease in FS% during their 1½ year study period. A lower fractional shortening in athletic compared to non-athletic horses was found by Gehlen et al. (77), who also found a greater stroke volume in the athletic horses. This is also stated by Patteson (32) who writes that: *"The maximum heart rate appears to be similar in trained and untrained animals; however, trained horses appear to be able to maintain stroke volume at high heart rates better than untrained animals, resulting in increased performance capability".* And a study by Ohmura et al. (78) demonstrated significant increases in stroke volume and cardiac output in Thoroughbreds during their first year of training. However, just as with the evaluation of the functionality in the heart of human athletes by Pluim et al. (68), these measures are indicators of the overall function of the left ventricle and not the regional myocardial function.

The question now arises: Are the TDI and speckle tracking techniques of any use in equine sports medicine? One very relevant application would be if the two methods could be used to predict the performance potential of a horse. However, this application implies that the two methods are able to differentiate an athletic from a non-athletic horse – presuming that there is indeed a disparity in the parameters related to the regional myocardial function. This presumption is somewhat uncertain as the results of TDI and speckle tracking examinations in human athletes are diverse. Nevertheless, the study in Part II will apart from

evaluating the two methods of TDI and speckle tracking also investigate if the two methods can differentiate a group of athletic horses from a group of non-athletic horses with respect to some of the parameters defined in Chapter 1.

### SUMMING UP

The cardiac response to physical training is a physiologic hypertrophy, which exists in two forms according to the character of training; an endurance trained heart and a strength trained heart – although this classification should be regarded more as a relative concept. Tissue Doppler imaging and speckle tracking have been used to evaluate the functionality of the heart in human athletes. However, the results are conflicting. The heart of equine athletes has so far only been evaluated by conventional echocardiographic methods. The study in Part II will investigate the feasibilities of TDI and speckle tracking in equine sports medicine.

# PART II

# STUDY

# MATERIALS AND METHODS

## STUDY POPULATION AND PRELIMINARY EXAMINATIONS

The study population consisted of 11 standardbred trotters (7 mares, 3 geldings and 1 stallion) of age between 3 and 9 years and bodyweight 485 ± 65 kg. The bodyweight was estimated indirectly from the chest girth circumference measure by use of a weight band. All horses were considered healthy with no history of cardiovascular disease. The preliminary examinations included physical examination, auscultation and routine echocardiographic examination. An inclusion criterion was that no auscultative cardiac murmurs ≥ degree III/VI were present. The routine echocardiographic examination involved 2-D and M-mode examination of the heart, as well as colour flow Doppler of the cardiac valves to rule out any structural abnormalities as well as any substantial valvular regurgitation (79).

Six of the horses were considered to be in an athletic condition as they were regularly trained and raced (although one had been out of training for 3 months preceding the study due to lameness). The individual best 1 km trotting time (kilometre time) was registered as an indication of their athletic performances. The remaining 5 horses were considered non-athletic as they had not been in training for at least 1 year preceding the study and only went to the field or into the paddock. Hence the study population was subdivided into two groups. The 6 athletic horses were examined at the client-owner's facilities, while the 5 non-athletic horses belonged to the University of Copenhagen - Faculty of Life Sciences, The Department of Large Animal Science and were examined at the university hospital. Thus all horses were accustomed to the surroundings in which they were examined and none of them received tranquilizers or sedatives during the examination.

## EXPERIMENTAL DESIGN

Two separate protocols were performed in accordance with the two objectives of the study outlined in the Introduction. The study was focused on the left ventricle as it was assumed that this cardiac chamber exhibits the most pronounced change in response to physical training, and for delimitation purposes only the 2-D colour TDI mode of the three TDI modes was included (see Chapter 3).

***Protocol 1.*** The 2-D colour TDI and speckle tracking techniques were evaluated according to their agreement, and the correlations between different examinations and offline analyses. For that reason all 11 horses were examined once with each technique to assess the method agreement. And furthermore, the athletic horses had an additional examination by 2-D colour TDI after an interval of approximately 15 minutes, while an extra offline analysis was performed on the 2-D colour TDI data of the non-athletic horses.

***Protocol 2.*** The ability of 2-D colour TDI and speckle tracking to detect any potential physiological adaptations to training in the equine heart was evaluated by comparing measurements obtained in the two groups of athletic and non-athletic horses. All 11 horses were therefore examined once with each technique.

## ECHOCARDIOGRAPHY

All echocardiographic examinations were performed by the same experienced echocardiographer using a Vingmed Vivid 7 ultrasound system[1] with a phased array transducer[2]. Recordings were made with harmonic imaging at frequencies of 1.7/3.4 MHz and an imaging depth of >24cm. Three consecutive cardiac cycles were recorded in each echocardiographic projection and stored digitally for subsequent offline analysis. Recordings were exclusively made at heart rates below 55 b.p.m. and cardiac cycles following second degree atrioventricular-blocks were omitted. An ECG was recorded simultaneously and superimposed on the echocardiographic recordings for timing purposes. The off-line analysis was performed by a single experienced observer using EchoPac[3] software system to extract measures of myocardial velocity, strain and strain rate from the 2-D colour TDI and speckle tracking recordings.

### THE PRELIMINARY ECHOCARDIOGRAPHIC EXAMINATION

The routine echocardiographic examination was performed prior to the study with the conventional echocardiographic modes. 2-D imaging was used to asses the diameter of the aorta (AO) from the right parasternal long-axis view. M-mode imaging was used to asses left ventricular dimensions by measuring the left ventricular internal diameter (LVID) and the thickness of both the interventricular septum (IVS) and the left ventricular free wall (LVFW) in both diastole and systole. This was done at the level of the papillary muscles from the right parasternal short-axis view. Additionally, the fractional shortening was obtained and the heart rate calculated in this view. Colour flow Doppler was used to evaluate all four of the cardiac valves from the right parasternal long-axis view with different angleling of the transducer to enable maximum visualization of the individual valves.

### THE 2-D COLOUR TDI EXAMINATION

For the 2-D colour TDI examination, real-time colour coded Doppler recordings were obtained from the right parasternal short-axis view at the level of the papillary muscles. The velocity range was set as low as possible to avoid aliasing – in practice the range was set to ±0.36 m/s. The sector angle was narrowed to achieve a frame rate above 140 fps. while at the same time encompassing the relevant cardiac structures. Three consecutive cardiac cycles were recorded and store digitally.

[1] Vingmed Vivid 7, GE Medical Systems, Glostrup, Denmark
[2] Phased array 4S transducer, GE Medical Systems, Glostrup, Denmark
[3] EchoPac, version 6.0, GE Medical Systems, Glostrup, Denmark

In the following off-line analysis recordings of good quality were selected for Q-analysis in the EchoPac software system. Wherever possible, each of the following measurements were taken three times (one time for each cardiac cycle) and averaged. For measuring the radial velocities, two ROIs of 6x6 mm were placed manually by the observer in the endocardium and epicardium of the left ventricular free wall (see Figure 23). The peak systolic, early diastolic and late diastolic velocities (S, E and A waves) were hereby obtained in both the endocardium and epicardium in a short-axis view at the level of the papillary muscles. The radial peak systolic strain and the S, E and A waves of the radial strain rate were obtained by manually placing one ROI of 20x6 mm in the ventricular free wall. Whenever possible the ROIs were traced to ensure that they stayed within the borders of the myocardium throughout the cycle.


**Figure 23** Screen picture in the TDI analysis of radial velocities. Notice the two ROIs placed in the endocardium (yellow) and epicardium (green) of the left ventricular free wall, and their corresponding velocity profiles.

## THE SPECKLE TRACKING EXAMINATION

For the speckle tracking examination conventional 2-D greyscale images were obtained from the right parasternal short-axis views at the levels of the apex, the papillary muscles and the mitral valve. The sector angle was adjusted to optimize the frame rate to the preferred between 40 and 90 fps.. Three consecutive cardiac cycles were recorded and store digitally.

The greyscale images were then processed in the EchoPac software system. Only one cardiac cycle in each projection was selected to ensure the best image quality. Consequently, measurements were only obtained once, and not averaged as in the TDI examination. It is important to realize that the post-processing of data using speckle tracking is fundamentally different compared to the 2-D colour TDI

technique because the region of interest is defined in a completely different way. With speckle tracking the observer marks the endocardial border and then adjusts the width of the circular ROI suggested by the computer so it fits the myocardium (see Figure 24). The computer then automatically divides the myocardium into 6 segments, and subsequently provides six curves (one for each segment) for the requested parameter. An averaged value for each segment as well as a global value for the six segments all together is also available on demand.

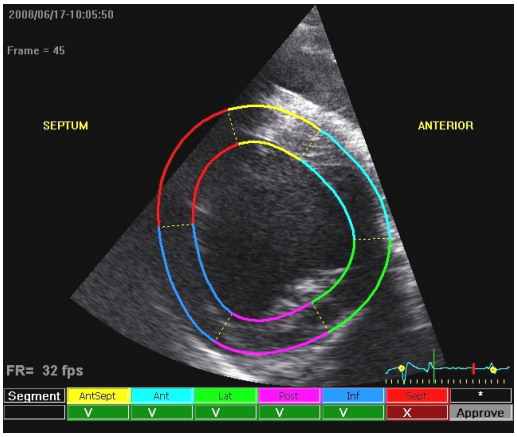


**Figure 24** Region of interest on a short-axis image in speckle tracking. Notice that the red segment is not automatically approved for speckle tracking by the computer (indicated by by an X in a red field in the bottom bar) as a part of this segment lies outside the imaging sector. Notice also that the frame rate is lower that desired (32 fps).

The radial velocity of the left ventricular free wall was obtained in systole, early diastole and late diastole (S, E and A waves) at the level of the papillary muscles. The radial peak systolic strain (see Figure 25) and the S, E and A waves of the radial strain rate were also obtained. Finally, the global rotation and rotation rate (alias circumferential displacement and velocity, respectively) were measured in the short-axis views at the level of the apex and the mitral valve, representing the apical and basal parts of the left ventricle, respectively.

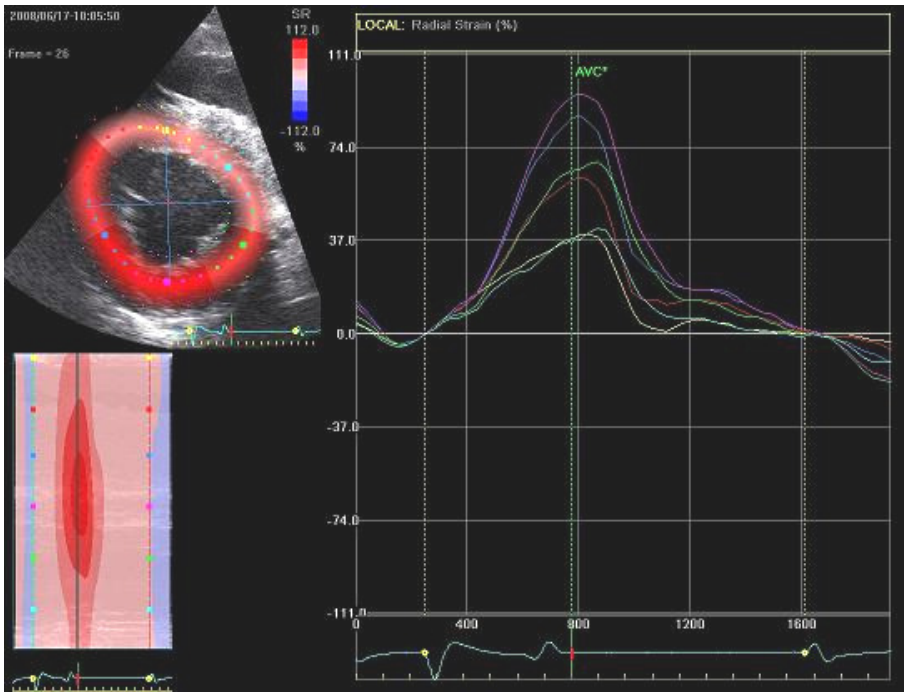


**Figure 25** Screen picture in the speckle tracking analysis of radial strain. Notice the six automatically defined segments (depicted with coloured dots) and the six corresponding strain profiles.

## STATISTICAL ANALYSES

Data are expressed as mean ± SD. The statistical analyses were performed by use of Excel[4]. A p-value ≤ 0.05 was considered statistically significant.

***Protocol 1.*** The agreement between the 2-D colour TDI and speckle tracking measures of radial velocity, strain and strain rate was analysed and presented in Bland-Altman plots. Examinations 1 and 2 of the radial velocities by 2-D colour TDI were tested for any significant differences with Students paired t-test (two-sided), and the Pearson correlation coefficient was used to assess the correlation between the first and second examination. The exact same procedure was then used on the two offline analyses of radial velocities obtained by 2-D colour TDI.

***Protocol 2.*** The presence of a radial velocity gradient was determined by subjecting the endocardial and epicardial radial velocities obtained by 2-D colour TDI to a paired Students t-test (one-sided). Then a comparison of the two groups of horses regarding the radial velocities, strain and strain rates obtained by both techniques was performed using two-sided Students t-tests. And finally, the theoretically required sample sizes, i.e. the number of horses required in each group to detect a significant difference in means, and the minimum detectable differences with the sample size available, were calculated.

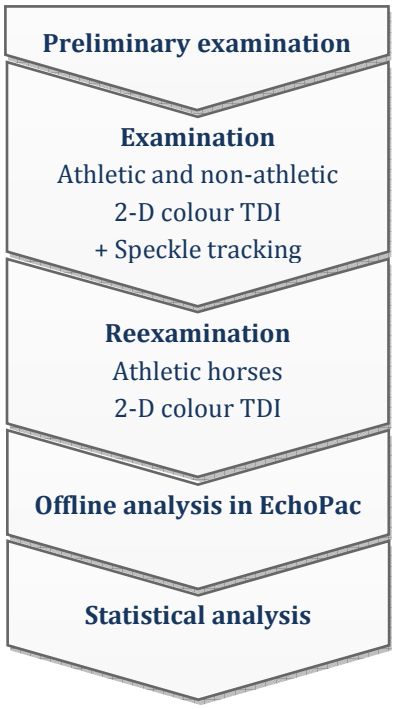


**Figure 26** Overview of the study.

[4] Microsoft Office Excel 2007, Microsoft Corporation, Redmond, USA

# RESULTS

## GENERAL DESCRIPTION OF THE LEFT VENTRICULAR MOTION

All radial velocity profiles obtained by both 2-D colour TDI and speckle tracking contained one positive peak systolic wave (S) and two negative diastolic waves (E and A) in the early and late diastole, respectively. The TDI examinations suggested a good synchronicity between the endocardial and epicardial radial motion. Radial strain profiles obtained by both TDI and speckle tracking showed positive peak systolic values consistent with radial thickening of the myocardium during systole. Additionally, all radial strain rate profiles obtained by both techniques contained one positive peak systolic wave (S) and two negative diastolic waves (E and A).

Analysis of the circumferential motion assessed by speckle tracking showed varying results. In the majority of the horses both the apex and the base turned counter-clockwise when viewed from the apex (positive rotation) - and the apex generally rotated more that the base. Only two horses showed a twisting motion like the one described in Chapter 1 with the apex turning counter-clockwise (positive rotation) and the base turning clockwise (negative rotation) when viewed from the apex. And finally, two horses actually showed an opposite twisting motion with the apex turning clockwise and the base turning counter-clockwise. Besides that, the rotation rates generally appeared more uniform than the rotation values.

## PROTOCOL 1: EVALUATION OF THE TECHNIQUES

A summary of the descriptive statistics for the 11 horses as a common group are shown in Table 4 (see Appendix 7 for results). Regarding the coefficient of variation, this statistical measure makes no sense if it is negative. The CVs in this study were therefore calculated from the absolute values of the means, which can be justified since the negative sign in the diastolic measures are related to the direction of the myocardial motion and not the magnitude of the measure per se.

**Table 4 Descriptive statistics of radial parameters for all the horses as a common group (N=11)**

| | | | 2-D colour TDI | | Speckle tracking | |
|---|---|---|---|---|---|---|
| | | | Mean ± SD | CV | Mean ± SD | CV |
| Velocity (cm/s) | S wave | Endo* | 8.3 ± 1.4 | 17.0 | 5.2 ± 1.1 | 21.8 |
| | | Epi* | 5.9 ± 1.0 | 16.6 | | |
| | E wave | Endo* | -22.3 ± 6.4 | 28.7 | -5.1 ± 2.2 | 43.3 |
| | | Epi* | -14.3 ± 2.9 | 20.1 | | |
| | A wave | Endo* | -6.8 ± 3.2 | 47.5 | -2.6 ± 1.2 | 44.3 |
| | | Epi* | -5.2 ± 3.4 | 64.4 | | |
| Strain (%) | | | ¤51.7 ± 31.4 | ¤60.8 | 71.2 ± 19.8 | 27.8 |
| Strain rate ($s^{-1}$) | S wave | | 1.6 ± 0.4 | 22.4 | 1.6 ± 0.3 | 22.3 |
| | E wave | | -5.0 ± 1.3 | 25.6 | -1.5 ± 0.6 | 43.3 |
| | A wave | | -1.6 ± 0.8 | 48.7 | -0.7 ± 0.5 | 65.8 |

* Concerns the TDI measurements only, Endo, endocardium, Epi, epicardium, CV, coefficient of variation (%), ¤ strain measures obtained by TDI incl. two suspected outliers – excl. outliers mean ± SD was 49.6 ± 16.8 , CV was 33.9%

The agreement of the 2-D colour TDI and speckle tracking techniques on the radial velocities, strain and strain rate were assessed by constructing a Bland-Altman plot for each of the parameters. See Appendix 8. To reduce the number of plots an average of the endocardial and epicardial velocities was used for the TDI measures. The general tendency was that the diastolic velocities and strain rates attained considerably higher values when measured with TDI, while strain values were higher when measured with speckle tracking. There was a reasonable level of agreement between the TDI and speckle tracking derived measures on the S wave strain rate (see Figure 27). A more questionable agreement between the two methods was seen on the S and A wave velocities as well as on strain and A wave strain rate measures. And finally, a decidedly poor agreement was observed between the two techniques for measurement of both velocities and strain rates in the early diastole (E waves).

No significant differences between the radial velocities obtained in *examination* 1 and 2 of the athletic horses were found using the Students paired t-test. The Pearson correlation coefficient indicated a strong positive correlation between the two examinations on the A wave velocities in both the endocardium and epicardium, and a less strong but still significant correlation on the endocardial S wave. For the rest of the radial velocities, the correlation between examination 1 and 2 was either non-significant or not existing. See Figure 28 and Appendix 8.

The results of *offline analysis* 1 and 2 of the radial velocities obtained by 2-D colour TDI in the non-athletic horses were more uniform. No significant differences were found between the two offline analyses, and there was a strong positive correlation between them on all radial velocities. See Figure 29 and Appendix 8.

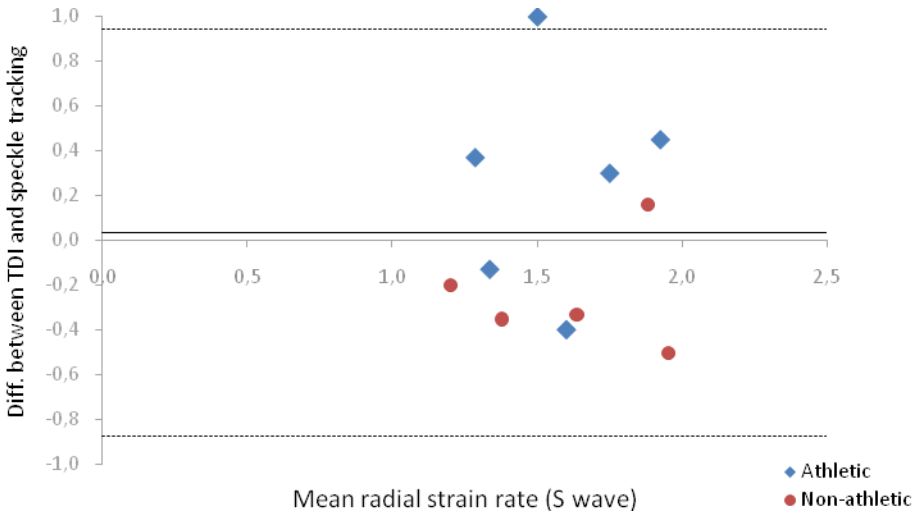


**Figure 27** Bland-Altman plot for the radial systolic strain rate. The best method agreement between 2-D colour TDI and speckle tracking was found on this particular parameter. The mean difference (bias) was ~ 0.0 $s^{-1}$ and the 95% limits of agreement ranged from -0.9 $s^{-1}$ to 0.9 $s^{-1}$. The solid line is the mean difference and the dashed lines are the upper and lower limits of agreement.

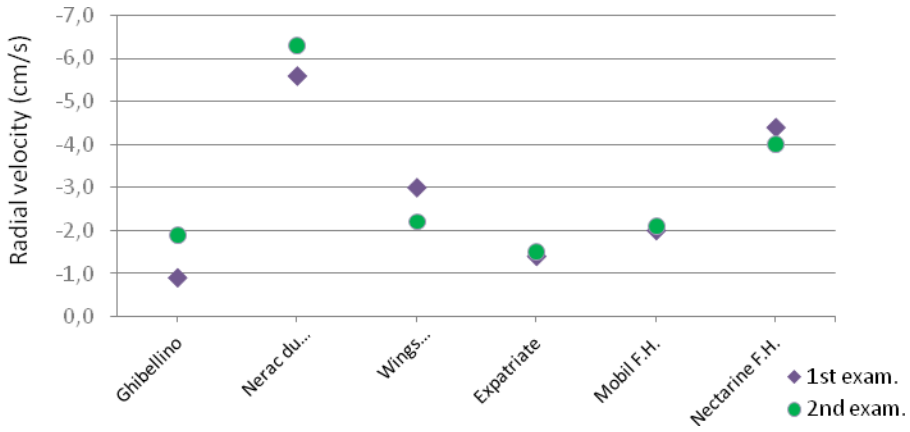


**Figure 28** Chart of the endocardial A wave radial velocity measures obtained from two different examinations. The best correlation between 2-D colour TDI measures from two different examinations was found on this particular parameter. The Pearson correlation coefficient was 0.9333 indicating a strong positive correlation.

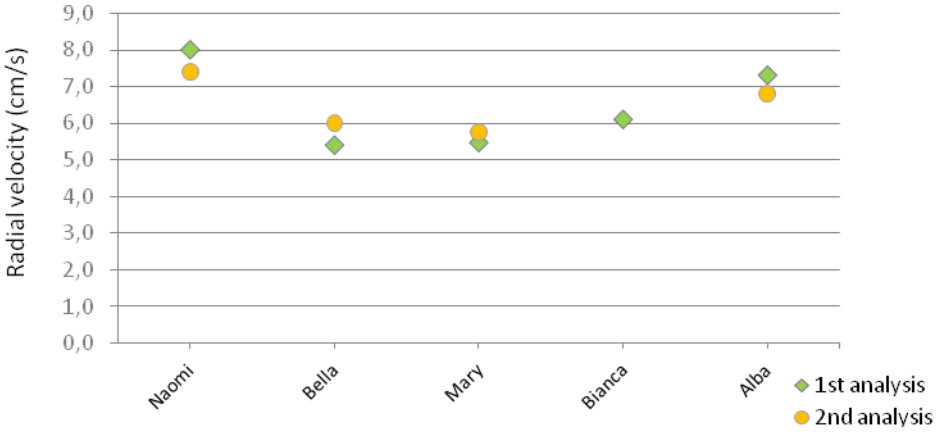


**Figure 29** Chart of the epicardial S wave radial velocity measures obtained from two different offline analyses. The best correlation between 2-D colour TDI measures from two different offline analyses was found on this particular parameter. The Pearson correlation coefficient was 0.9810 indicating a strong positive correlation. Notice that data is missing for the second offline analyses of one horse.

## Protocol 2: Athletic versus non-athletic

A one-sided t-test of the TDI measurements of the 11 horses as a common group confirmed the presence of a radial velocity gradient. During the cardiac cycle the radial velocities were significantly greater in the endocardium than in the epicardium of the left ventricular free wall. The radial velocity gradients calculated as the absolute difference of the endocardial velocity minus the epicardial velocity were (mean ± SD) 2.4 ± 1.1 cm/s, 8.1 ± 4.7 cm/s, and 1.6 ± 1.5 cm/s in systole, early diastole and late diastole, respectively (p-values = 0.00001, 0.0001 and 0.003). See Appendix 9 for calculations.

Then comparisons of the athletic and non-athletic horses as two separate groups were made on the radial velocities, velocity gradients, strain and strain rates obtained by 2-D colour TDI (see Appendix 9 for calculations). The sample means ± SD for the individual parameters are seen in Table 5. The radial peak systolic strain was 65.3 ± 32.7 % for the athletic horses and 35.3 ± 22.8 % for the non-athletic horses. However, one measure in each group was suspected to be a possible outlier, and therefore these two measures were excluded and the means and standard deviations were recalculated. The mean strain was now 54.0 ± 19.2 % for the athletic horses and 44.0 ± 13.7 % for the non-athletic horses.

Overall no significant differences were found between the two groups of horses, except for the late diastolic (A wave) radial velocities. These were significantly greater in the endocardium and epicardium of the non-athletic horses (p-values = 0.02 and 0.003). Additionally, the null-hypothesis for the E wave velocity gradient was close to being rejected with a p-value = 0.056. However, the sample sizes of the two groups of horse were limited with n = 6 for the athletic and n = 5 for the non-athletic group. And therefore the trustworthiness of the conclusions on the two-sided t-tests was evaluated by calculating the *required sample sizes* based on the observed standard deviation of the individual parameter and the observed difference in sample means between the two groups (Table 5). For each and every one of the parameters, the required sample size turned out to be larger than the ones used in this study. The *minimum detectable differences* with the sample sizes available and the observed standard deviation of the individual parameter were then also calculated (Table 5). These were consequently larger than the differences observed. See Appendix 9 for calculations.

**Table 5 Results of 2-D colour TDI in the two groups of horses**

| | | | Athletic | Non-athletic | $H_0$ | Required sample size | Min. detect. difference |
|---|---|---|---|---|---|---|---|
| **Velocity (cm/s)** | **S wave** | Endo | 8.3 ± 1.5 | 8.3 ± 1.5 | A | - | - |
| | | Epi | 5.4 ± 0.5 | 6.5 ± 1.1 | A | 13 | 1.8 |
| | **E wave** | Endo | -24.2 ± 7.1 | -20.1 ± 5.3 | A | 39 | 11.3 |
| | | Epi | -13.7 ± 3.0 | -14.9 ± 2.9 | A | 92 | 5.1 |
| | **A wave** | Endo | -4.9 ± 2.1 | -9.2 ± 2.8 | **R** | 9 | 5.7 |
| | | Epi | -2.9 ± 1.8 | -8.1 ± 2.5 | **R** | 7 | 6.0 |
| **Gradient (cm/s)** | **S wave** | | 2.9 ± 1.2 | 1.8 ± 0.5 | A | 16 | 1.9 |
| | **E wave** | | 10.5 ± 4.9 | 5.2 ± 2.4 | A | 13 | 8.3 |
| | **A wave** | | 2.0 ± 1.9 | 1.1 ± 0.7 | A | 44 | 2.7 |
| **Strain (%)** | | | ¤65.3 ± 32.7 | ¤35.3 ± 22.8 | A | 18 | 55.6 |
| **Strain rate ($s^{-1}$)** | **S wave** | | 1.7 ± 0.4 | 1.5 ± 0.4 | A | 63 | 0.7 |
| | **E wave** | | -5.5 ± 1.6 | -4.5 ± 0.7 | A | 27 | 2.3 |
| | **A wave** | | -1.7 ± 0.7 | -1.4 ± 0.8 | A | 112 | 1.4 |

$H_0$, null-hypothesis, A, accepted, R, rejected, Endo, endocardium, Epi, epicardium,
¤ strain measures incl. two suspected outliers – excl. outliers Athletic = 54.0 ± 19.2%, Non-athletic = 44.0 ± 13.7%

**Table 6 Results of speckle tracking for the two groups of horses.**

| | | Athletic | Non-athletic | $H_0$ | Required sample size | Min. detect. difference |
|---|---|---|---|---|---|---|
| **Velocity (cm/s)** | **S wave** | 4.7 ± 1.0 | 5.9 ± 0.9 | A | 13 | 1.9 |
| | **E wave** | -5.3 ± 1.8 | -4.9 ± 2.9 | A | 475 | 3.9 |
| | **A wave** | -2.7 ± 0.5 | -2.5 ± 1.7 | A | 566 | 2.1 |
| **Strain (%)** | | 68.0 ± 16.8 | 74.9 ± 24.3 | A | 130 | 35.1 |
| **Strain rate ($s^{-1}$)** | **S wave** | 1.4 ± 0.3 | 1.7 ± 0.3 | A | 16 | 0.5 |
| | **E wave** | -1.4 ± 0.4 | -1.6 ± 0.9 | A | 142 | 1.1 |
| | **A wave** | -0.5 ± 0.1 | -1.0 ± 0.7 | A | 16 | 0.9 |

$H_0$, null-hypothesis, A, accepted, R, rejected

The radial parameters obtained by speckle tracking were also compared in order to find differences between the athletic and non-athletic groups of horses. The sample means ± SD for the individual parameters are shown in Table 6.

In all cases the null-hypothesis was accepted and no significant differences between the two groups of horses could be found. As with the 2-D colour TDI, the trustworthiness of the conclusions on these two-sided t-tests was then assessed by calculating the *required sample size* and the *minimum detectable difference* for each parameter based on the observed standard deviation and difference in sample means (Table 6). The general picture was the same as for the TDI examination; the required sample sizes were larger than the ones used in this study and the minimum detectable differences with the sample sizes available were larger than the observed differences. See Appendix 9 for calculations

# DISCUSSION

This study was a pilot trial on the use of tissue Doppler imaging and speckle tracking for analysis of myocardial parameters in the heart of the horse. As outlined in the introduction of this thesis the goals were to evaluate if the two methods can be applied in equine cardiology and to assess their feasibilities in equine sports medicine.

The results of the study indicate that the equine heart has two intrinsic myocardial motions – a radial and a circumferential. The radial motion was similar to that described in the theory, but the circumferential motion did not show the same characteristics as seen in humans and dogs (see Part I). However, the results on the circumferential motion showed a high level of variation and were estimated to be unsuitable for a statistical analysis. The fact that the heart did not twist in the majority of the horses, should therefore probably be interpreted as a result of unreliable measures. And in addition, Schwarzwald et al. (64) have shown contradictory results in which the base of the equine heart turned in the opposite direction of what was observed for the majority of the horses in this study.

All radial velocity profiles obtained by both techniques comprised one positive systolic (S) wave and two negative diastolic (E and A) waves, indicating that the left ventricular free wall moved towards the transducer (and the right thoracic wall) in systole and away from the transducer (and the right thoracic wall) during diastole. The S waves coincided with the systolic contraction. The E and A waves were consistently placed before and after the diastasis, respectively, indicating that the early diastolic (E) wave would represent the early diastolic filling, and the late diastolic (A) wave would represent the late diastolic filling of the left ventricle (see Chapter 1). This pattern would therefore indicate that the E wave comprehends the active (energy consuming) process of the ventricular relaxation that occurs in the early diastole, while the A wave represents a passive motion of the left ventricle as a product of the atrial contraction (46). This might also be the explanation of why the E wave velocity (with some exceptions in the speckle tracking measures) was generally greater than the S and A waves. Because, while the systolic motion of the left ventricle has to work against the aortic valve and the systemic pressure (afterload), and the late diastolic motion is a passive product of the atrial contraction, the E wave comprises an active (energy consuming) motion with no substantial opposing forces to work against (46).

Besides the uniform pattern, the radial velocities also exhibited a transmural gradient like the one seen in small animals (45;46;49;52). The 2-D colour TDI examination of the radial velocities revealed that the endocardium in the left ventricular free wall of the equine heart moved more rapidly along the radial axis than the epicardium. The gradient was calculated as the difference between radial velocities in the endocardium minus the radial velocities in the epicardium as done

by Chetboul et al. (46). This calculation method of the velocity gradients entails that these get the advantage of being independent of cardiac translation – a factor which can interfere with isolated velocity measures (see Chapter 1 and 3).

The peak systolic radial strain measures were positive, consistent with a myocardial thickening during systole. And the radial strain rates showed the same pattern as seen in the velocity measures and described in Chapter 1. In general, the size of these measures were comparable with the ones found by Schwarzwald et al. (64).

### PROTOCOL 1: EVALUATION OF THE TECHNIQUES

A diagnostic technique can be evaluated on its accuracy, repeatability, reproducibility, specificity and sensitivity (49). These properties tell us how well a technique performs and how much we should depend on it in a clinical setting. Ideally the primary goal of this study had been to validate the use of tissue Doppler imaging and speckle tracking in horses. Validation of the techniques would enable us to determine the significance of the measures obtained in an examination (49). However, to conduct a comprehensive validation study requires a large set of data including multiple examinations on multiple occasions (days), with multiple off-line analyses and preferably more than one observer. By conducting such a study one can break down the total variance of the results into its individual components – like the variation attributable to measures being taken from different examinations, on different days, by different observers etc. The repeatability of a technique would then be the ability of an observer to repeat his or her measures on the same horse (intra-observer variation), while the reproducibility would be the ability of another observer to reproduce the results obtained by observer number one (inter-observer variation) – and this can be done on both a within-day and between-day basis.

Knowing the magnitudes of these factors in this particular study would have enabled us to interpret the examination results on a more trustworthy foundation. Unfortunately, the time frame available to this study was not sufficient for conducting a comprehensive validation study. In order to compensate for that, the sources of errors that are likely to have contributed to the dispersion of measurements, the agreement between the two techniques, and the correlation between two examinations and two offline analyses, respectively, will be discussed in the following.

The results of this study showed great dispersion. The coefficients of variation for the radial parameters ranged from 12.4% to 96.2% when obtained by 2-D colour TDI and from 21.8% to 65.8% when obtained by speckle tracking – and were consequently considerably higher than those calculated for conventional echocardiographic parameters (79). The reason why we experienced such a high level of variability is likely to be multifactorial. However, some of more evident errors in the conduction of the study should be mentioned here; First, the study population was chosen primarily out of availability. Ideally, the horses should have

been chosen at random and have been matched according to age and gender. Another aspect concerning the study population was that the body condition of the non-athletic horses was found to be well over normal at the physical examination (bodyweight: athletic group 435 ± 22 kg, non-athletic group 544 ± 44 kg). This could have affected the image quality of the echocardiographic recordings of the non-athletic horses, and hereby become a contributory cause of the great variation that was observed among the measurements. Secondly, we experienced some difficulties accomplishing satisfying frame rates on the recordings – especially with the speckle tracking examination for which the majority of the recordings were made on frame rates below the recommended 40 fps. (see Chapter 4). If future studies are conducted the frame rate must be optimized to >140 fps. for the 2-D colour TDI analysis and 40-90 fps. for the speckle tracking analysis. Third, as some of the recordings were of less ideal quality only the best were selected for post-processing. This meant that in stead of presenting the data as the average of three cardiac cycles, some of the measurements were taken from one cardiac cycle only. For future studies at least three cardiac cycles of sufficient quality must be obtained in order to get an averaged value for each parameter.

The agreement between the TDI and speckle tracking techniques for measuring radial velocities, strain and strain rates was assessed from Bland-Altman plots. When interpreting the results of agreement it is important to realize, that the two methods uses different ROIs when calculating the parameters. In this case, the ROIs in the TDI examinations were placed manually by the observer, while the ROIs for the speckle tracking examination were selected almost automatically by the computer. To reduce the number of plots, an average of the endocardial and epicardial velocities were used for the TDI measures on radial velocity. This can be justified as the radial velocity gradient is assumed to be even between the endocardium and the epicardium, and that the speckle tracking measure is derived roughly from the centre of the myocardium. As could have been expected with the discrepant ROIs the method agreement on the size of the measures was not overwhelming. It is difficult to tell, if the technical differences are indeed too big to allow a perfect agreement between the two techniques, or if observed level of agreement is mainly attributable to the great variation of the measures.

No significant differences were found between the radial velocity measures obtained by 2-D colour TDI from two different examinations and two different offline analyses, respectively. The correlation of measures from different examinations varied with the individual parameters, from a strong positive correlation to almost no correlation. In contrast, all the measures from different offline analyses showed strong positive correlations. These results give an impression of how the 2-D colour TDI technique would perform in the clinic, but should be interpreted with caution due to the low sample sizes and can not match the information that a “true” validation study would provide us with.

### PROTOCOL 2: ATHLETIC VERSUS NON-ATHLETIC

The use of the horse as an athlete combined with the knowledge that cardiac tissue adapts to physical training, lead to the hypothesis that the regional myocardial function could be different in the left ventricle of an athletic horse compared to a non-athletic horse. Therefore, the second goal of this study was to investigate if the TDI and speckle tracking techniques could be used to distinguish between an athletic and non-athletic horse. For that reason, all the radial parameters obtained by the two techniques were compared between the two groups of horses.

An extension to this hypothesis was that physical training might lead to a superior diastolic function in the athletic horse, as it has been observed that the stroke volume increases significantly with training of an athletic horse (78), and that athletic horses appear to be better than non-athletic horses at maintaining the stroke volume at high heart rates (32) (see Chapter 5). More precisely, it was suspected that the myocardium of an athletic horse have an enhanced ability to relax during diastole, thus allowing the athletic horse to generate an improved diastolic filling of the left ventricle. Such an improved ventricular filling would lead to an enhanced cardiac output and thereby increased performance capability. The active process of myocardial relaxation (lusitrophy) occurs in the early diastole, and will thereby be comprehended by the E wave. Hence, it was anticipated that the diastolic E wave radial velocities would be greater in the group of athletic horses versus the group of non-athletic horses, just like it was observed for longitudinal velocities in human athletes (70) (see Chapter 5).

Unfortunately, no significant differences in the radial parameters were found between the two groups of horses, except for the late diastolic (A wave) velocities measured by 2-D colour TDI in both the endocardium and epicardium of the left ventricular free wall – which actually were found to be greater in the non-athletic horses (p-values = 0.02 and 0.003).

However, as this was a pilot trial it was unknown what to except from the standard deviation of the individual measures. Without any knowledge of the expected standard deviation it is not possible to plan the study with regard to sample sizes. To verify the sample sizes used in this study, the required sample sizes (that should have been used) were calculated retrospectively from the standard deviations observed in the study. These calculations showed that the sample sizes used in the study were much too small compared to what they should have been (see Table 5 and 6). The minimum detectable differences in the individual parameters between the two groups of horses that could be established with the sample sizes available, were also calculated retrospectively, and were accordingly a bit larger than the differences observed in this study.

As a direct consequence of these results, the above conclusions made on the presence or absence of a significant difference in the individual parameters between the two groups of horses, are not valid on a 95% certainty level as we

wish them to be. And furthermore, there was no obvious tendency in the parameters between the two groups of horses when simply regarding the relations between the sample means. Hence, it is not possible to make any valid conclusions on whether or not the regional myocardial function is altered in an athletic horse based on this particular study.

The bottom line is, that we observed a rather large dispersion of the measures and that the used sample sizes were too small. However, this study has indeed provided us with a substantial knowledge of both the merits and pitfalls of the TDI and speckle tracking techniques, as well as the tools for planning future studies. And due to the limited amount of veterinary literature on the subject and lack of solid conclusions in this study, future studies ought to be conducted. For instance, the two techniques could be applied to other cardiac chambers or other parameters could be included. The parameters in this study were chosen primarily out of convenience as to whether or not they showed consistently readable profiles in all the horses. As pointed out in the theory in Part I of this thesis, true apical projections are not available in the horse and longitudinal parameters are therefore not available with TDI due to the angle dependency of this technique. However, speckle tracking is angle independent and could therefore be used to study the longitudinal motion of the equine heart. Furthermore, the techniques should be validated for use in the horse, before their applicability in equine sport medicine can be truly assessed. And besides that, studies that will establish reference values of a healthy equine population would also be needed before the two techniques can be used for equine patients with cardiac disease. Despite the constrained results of this study, the possibilities could still be abundant, though a lot of work lies ahead before these two advanced echocardiographic methods can be decently implemented in equine cardiology.

# CONCLUSION

This thesis has reviewed the methods of tissue Doppler imaging and speckle tracking and discussed the possibilities for implementing these advanced echocardiographic techniques in equine cardiology. The thesis included a study in which the two techniques were applied to the horse. The study showed that the 2-D colour TDI and speckle tracking can indeed be used in the equine species, and that the left ventricle of the equine heart has a least two intrinsic myocardial motions – a radial and a circumferential. The study also revealed the presence of a radial velocity gradient across the ventricular wall – making the endocardium move more rapidly than the epicardium along the radial axis. The S, E and A wave gradients were 2.4 ± 1.1 cm/s, 8.1 ± 4.7 cm/s, and 1.6 ± 1.5 cm/s, respectively (p-values = 0.00001, 0.0001 and 0.003).

In general, the measurements showed a high level of dispersion, most likely due to faults concerning the used frame rates and the data handling in the conduction of the study. These errors were analysed and improvements suggested for future studies. Ideally, a comprehensive validation study should have been conducted, but the timeframe available made this impossible. To compensate for this, the agreement between 2-D colour TDI and speckle tracking, together with the correlations between TDI measurements taken from different examinations and different offline analyses, were evaluated in stead. The method agreement varied with the parameter in question, and so did the correlation of TDI measurements taken from different examinations. In contrast, the TDI measurements from different offline analyses showed a strong positive correlation.

The feasibilities of the two methods in equine sports medicine were assessed by comparing the measures of two groups of horses – 6 athletic and 5 non-athletic. However, the only two significant differences were found of the endocardial and epicardial A wave radial velocities, which were greater in the non-athletic horses (p-values = 0.02 and 0.003). Meanwhile, as this study was a pilot trial it was not possible to plan the study with regard to the required sample sizes in advance. These were then calculated retrospectively, and this demonstrated that the sample sizes used in the study were too limited. Consequently, the conclusions made on the presence of any significant differences between the athletic and non-athletic horses were not valid on a 95% confidence level. Hence, it was not possible to conclude whether or not the measures of the two groups of horses differed significantly based on the present study.

Despite the lack of solid conclusions, this thesis has still provided us with a substantial knowledge of the merits and pitfalls of the TDI and speckle tracking techniques, and should be valuable in the work that lies ahead before these two advanced echocardiographic methods can be successfully implemented in equine cardiology.

# APPENDIXES

# APPENDIX 1 – CONVENTIONAL ECHOCARDIOGRAPHIC IMAGING

## B-MODE = TWO-DIMENSIONAL ECHOCARDIOGRAPHY

"B" refers to brightness and the fact that images are presented in grey scale (5). These two-dimensional images emerge from transmission of sound waves along numerous scan lines forming a sector with the shape of a piece of pie. This sector has a width (indicated by the sector angle), a depth (cm) and a less noticeable thickness (4;31). The best image quality is achieved when the beam is orientated perpendicular to the structures being examined, as this provides increased reflection and reduces the refraction. By recording a large number of images (frames) pr second the cardiac structures on display appear to be moving in real-time (31). The 2-D echocardiogram is often used for guidance when using the other echocardiographic methods, e.g. for guidance of cursor placement in M-mode and CW Doppler.

## M-MODE

"M" refers to motion. These images display the myocardium in one dimension on the y-axis against time on the x-axis. M-mode echocardiography is suitable for examination of rapidly moving structures, e.g. cardiac valves, due to a very high sampling/frame rate compared to 2-D echocardiography (31). M-mode is also used for measuring the size of ventricular walls and internal diameters (4). For these measurements to be accurate and for optimal image quality the sound beam should be orientated perpendicular to the structures being examined (as with B-mode).

## DOPPLER

Conventional Doppler echocardiography provides information on direction, velocity, character (turbulent or laminar) and timing of blood flows (4). The Doppler shift refers to the change in frequency of the transmitted and the received sound waves that arises if either the source or the receiver of the sound moves during the propagation of a sound wave (4).

In Doppler echocardiography the Doppler shift occurs when the transducer transmits sound waves of one frequency, while the returning sound waves from reflecting structures in motion (in this case erythrocytes) has another frequency (4). If the erythrocytes are moving in the direction of the transducer, the frequency of the returning sound waves will be increased – while if the erythrocytes are moving away from the transducer, the frequency of the returning sound waves will be decreased. As the Doppler shift is calculated as $f_{recieved}$-$f_{transmitted}$ (where f = frequency) this will correspond to a positive and negative frequency shift, respectively. The velocity is then calculated form the frequency shift by the Doppler equation (4):

$$V = \frac{C \times f_d}{2(f_o) \times \cos\theta}$$

Where V is the velocity of the reflecting objects (erythrocytes), C is the speed of sound in soft tissue, $f_d$ is the frequency shift, $f_o$ is the transmitted frequency and $\theta$ is the insonation angle between the directions the sound waves and the blood flow. In contrast to B-mode and M-mode, Doppler echocardiography should be performed with the direction of the sound waves parallel to the direction

of the blood flow. Indeed the insonation angle should not exceed 20º and with angles of 90º there is no frequency shift at all (4;33).

### Continuous wave (CW) Doppler

In CW Doppler sound waves are continuously transmitted and received along a single image line. In this way, the whole range of frequency shifts and thereby velocities (including peak velocities) that occur simultaneously along the entire image line are recorded. These are then displayed against time as velocity profiles (4;31). Notice that CW Doppler lacks spatial resolution (5).

### Pulsed wave (PW) Doppler

PW Doppler records the velocities in a specific sample volume placed manually by the echocardiographer at a chosen depth on a 2-D echocardiogram. To do this, the transducer alternately transmits and receives sound waves (31). The time interval between each transmission, i.e. the pulse repetition frequency (PRF), is automatically calculated from the depth of the sample volume and the speed of sound in soft tissue (1540 m/sec) (31). The PRF must be at least twice the Doppler shift to avoid aliasing. This means that the maximum frequency shift that can be measured equals ½ PRF (Nyquist limit). Consequently, the maximum velocity measured by PW Doppler is limited and the method is not suitable for measuring peak velocities (4). It be shown that the maximum recordable velocity is inversely proportionate with the transducer frequency, and thus that low-frequency transducer are more suitable for Doppler recordings (4;31).

### Colour flow Doppler

Colour flow Doppler is a kind PW Doppler with multiple sample volumes along one or multiple image lines. The velocity data are semi-quantitative and colour coded; Blood flow towards and away from the transducer is coded red and blue, respectively. The highest velocities are coded in lighter shades and turbulent flow is coloured green (31). The colour coded information is then superimposed on either B-mode or M-mode images. The first facilitates detection of abnormal flow patterns (4), e.g. valvular regurgitation, while the latter is useful for timing of flow events (31;33).

# Appendix 2 – Abbreviations and Thesaurus

## Abbreviations

| | |
|---|---|
| 1-D | One-dimensional |
| 2-D | Two-dimensional |
| 3-D | Three-dimensional |
| A wave | Peak value in the late diastole |
| Ao | Aorta diameter |
| AV | Atrioventricular |
| B.p.m. | Beats pr minute |
| B-mode | Brightness mode = two-dimensional echocardiography |
| CV | Coefficient of variation |
| CW | Continuous wave (Doppler) |
| E wave | Peak value in the early diastole |
| ECG | Electrocardiogram |
| EF | Ejection fraction |
| Fps. | Frames pr second |
| FS% | Fractional shortening |
| IVS | Interventricular septum |
| LVFW | Left ventricular free wall |
| LVID | Left ventricular internal diameter |
| M-mode | Motion mode |
| PW | Pulsed wave (Doppler) |
| ROI | Region of interest |
| S wave | Peak value in systole |
| TDI | Tissue Doppler Imaging |

## Thesaurus

| | |
|---|---|
| Aliasing | Artefact that causes ambiguity in the sampled information – in this context: the velocity data. |
| Frame rate | Number of frames recorded pr second. |
| Image line/Scan line | "Line" along which sound waves are transmitted by the transducer. Equals the axis of the sound beam. |
| Image sector angle | Width of a 2-D echocardiographic image. |
| Insonation angle | Angle between the direction of transmitted sound waves and the direction of the target in Doppler echocardiography. |
| Off-line analysis | *(See post-processing)* |
| Post-processing | Processing of echocardiographic recordings in software systems after these have been obtained. |
| Spatial resolution | Refers to the ability to differentiate between different structures in an echocardiographic image. The spatial resolution can be divided into an axial and a lateral component. The axial resolution refers to the resolution along the sound beam axis, while the lateral resolution refers to the resolution perpendicular to the sound beam axis (4). |
| Temporal resolution | Refers to the ability to place structures in time. Depends on the frame rate – high frame rates yield better temporal resolution (4). |
| Tethering | In this context: The pull of neighbouring myocardial segments. |
| Tissue tracking | Method of displaying the displacement data achieved by the colour TDI modes. |

# Appendix 3 – Examples of synonymous terms

### In general for both techniques (TDI and speckle tracking)

Strain and strain rate imaging (54)
Strain echocardiography (7)
Tissue deformation imaging (6)

### Synonymous terms for tissue Doppler imaging

Doppler Myocardial Imaging (5;28;37)
Gewebe-Doppler-Echokardiographie (21)
Tissue Doppler Echocardiography (28;37;80)
Tissue Velocity Imaging (80)
Ultrasound Myocardial Velocity Imaging (5)

### Synonymous terms for speckle tracking

Feature tracking (computer technical language) (55)
Non-Doppler 2-D strain imaging (54)
Tissue Motion Quantification (12)
Two-dimensional strain imaging (6;57)
Two-dimensional tracking (55)
Velocity vector imaging (a specific way displaying speckle tracing derived velocities) (12;60)

# APPENDIX 4 – LAGRANGIAN VERSUS NATURAL STRAIN

Overall, strain is defined as the deformation of an object that subsequently returns to its original shape. A relative shortening produces a negative strain value, while a relative lengthening produces a positive strain value (5).

However, there is two possible ways to calculate the strain value; ***Lagrangian strain*** is the change in length relative to the initial length, while ***natural strain*** is the change in length relative to the instantaneous length (5). As there exist Lagrangian and natural strain, both Lagrangian and natural strain rates can also be calculated.

There is virtually no difference in values of the two versions of strain when dealing small strain values (5-10%). For greater strain values however, it should be both stated and noted which of the two types of strain that are being use. In practice the Lagrangian strain is predominantly used (5).

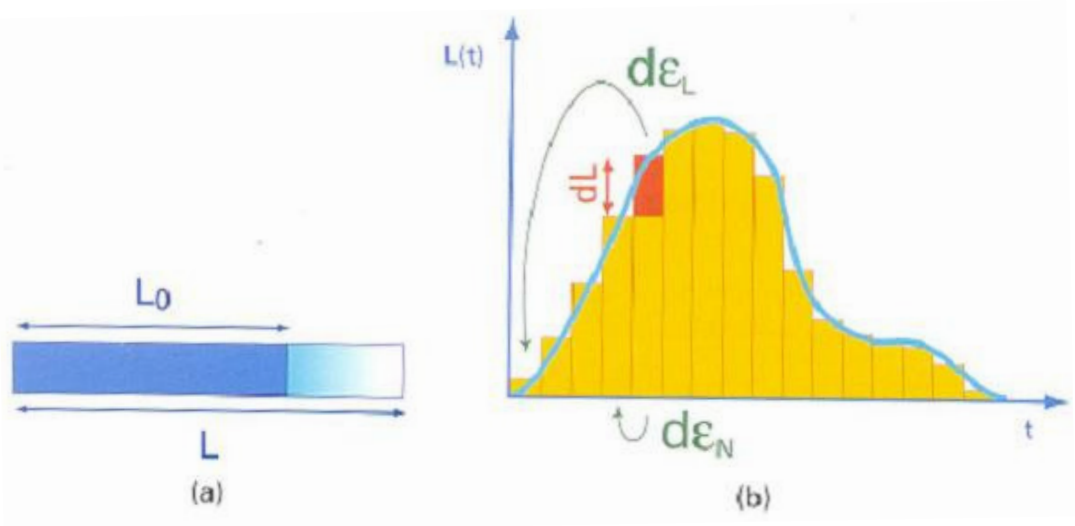


**Figure 30** Lagranian versus natural strain. a) The basic principle of Lagrangian strain. b) Comparison on the principles of Lagrangian strain $d\varepsilon_L$ and natural strain $d\varepsilon_N$. The x-axis represents the time, and the y-axis represents the length at the time t. dL is the change in length.

# APPENDIX 5 – CALCULATIONS

In the PhD thesis of Spieker (21) results on velocities are given as the median. This makes direct comparisons of results difficult. The means and standard deviation of radial velocities obtained by 2-D colour TDI in healthy controls are therefore calculated here from relevant data in the appendixes of Spieker.

Tabelle 9.2. Arithmetischer Mittelwert aus drei Einzelmessungen der einzelnen Pferde der Gruppen 1-6

Messungen mit dem farbkodierten Gewebe-Doppler an der linksventrikulären Hinterwand ($V_{IC}$ =isovolumetrische Spitzengeschwindigkeit, $V_S$ =systolische Spitzengeschwindigkeit, $V_E$ frühdiastolische Spitzengeschwindigkeit, $V_A$ =spätdiastolische Spitzengeschwindigkeit)

| Farb-GDE LVW | Pferd | Messwert in cm/s | | | |
|---|---|---|---|---|---|
| | | $V_{IC}$ | $V_S$ | $V_E$ | $V_A$ |
| Gruppe 1 | 12 | 3,97 | 8,93 | -8,87 | -8,6 |
| | 2 | 4 | 4,97 | -13,67 | -6,7 |
| | 6 | 4,67 | 5,7 | -9,33 | -8,8 |
| | 1 | 1,23 | 5,53 | -11,63 | -9,13 |
| | 13 | 3,47 | 6,17 | -10,33 | -3,77 |
| | 4 | 5,27 | 8,1 | -11,17 | -7,63 |
| | 7 | 1,7 | 3,67 | -8,33 | -7,93 |
| | 4 | 3 | 6,2 | -13,07 | -10 |
| | 10 | 3,47 | 4,17 | -8,83 | -6,57 |
| | 8 | 5,3 | 5,27 | -8,03 | -5,5 |

**Figure 31** Clip from the appendixes of Spieker.

| Peak velocities | Mean (cm/s) | Standard deviation (cm/s) |
|---|---|---|
| Systole (S wave) = $V_s$ | 5.9 | 1.6 |
| Early diastole (E wave) = $V_E$ | -10.3 | 2.0 |
| Late diastole (A wave) = $V_A$ | -7.5 | 1.9 |

# APPENDIX 6 – LAW OF LA PLACE

The law of La Place states that the *"wall tension is proportional to the radius of the chamber and the pressure within it, and inversely proportional to the wall thickness"* (32). This relationship can be summarized as:

$$wall\ tension = \frac{chamber\ radius \cdot ventricular\ pressure}{2 \cdot wall\ thickness}$$

The heart will seek to balance these factors in order to ensure a sufficient cardiac output. Pressure overload involves an increase in wall tension and the ventricles therefore respond by increasing the wall thickness – leading to concentric hypertrophy (rare in horses) (32). Volume overload also increases wall tension but in this circumstance the ventricles will try to equalize the increased tension by increasing the radius of the chamber without changing the wall thickness – leading to eccentric hypertrophy (32). Of course these compensating acts are within some limits.

# APPENDIX 7 – RESULTS

## Table 1. Animal data

| Horse | Age/years | Sex[1] | Weight/kg | Condition | Kilometre time |
|---|---|---|---|---|---|
| Ghibellino | 5 | S | 438 | athletic | 1 min 11.9 sec |
| Nerac du Bougy | 7 | G | 396 | athletic | 1 min 11.5 sec |
| Wings Summerland | 5 | M | 438 | athletic | 1 min 16.4 sec |
| Expatriate[2] | 6 | G | 458 | athletic | 1 min 15 sec |
| Mobil F.H. | 4 | G | 451 | athletic | 1 min 20 sec |
| Nectarine F.H. | 3 | M | 432 | athletic | 1 min 18 sec |
| Naomi | * | M | 532 | non-athletic | - |
| Bella | * | M | 518 | non-athletic | - |
| Mary | * | M | 589 | non-athletic | - |
| Bianca | * | M | 589 | non-athletic | - |
| Alba | * | M | 490 | non-athletic | - |

[1] G = gelding, M = mare, S = stallion

[2] Had not been trained in the preceeding 3 months due lameness

* The individual ages of the non-athletic horses belonging to the university were not known, but where overall between 4-9 years

## Table 2. Clinical examination

| Horse | Temperature/°C | Heart rate/b.p.m. | Respiration/number/min. |
|---|---|---|---|
| Ghibellino | missing data | missing data | missing data |
| Nerac du Bougy | 37.7 | 26 | 12 |
| Wings Summerland | 37.8 | 32 | 18 |
| Expatriate | 37.8 | 40 | 10 |
| Mobil F.H. | 37.5 | 36 | 18 |
| Nectarine F.H. | 38.1 | 32 | 20 |
| Naomi | 38.0 | 40 | missing data |
| Bella | 37.4 | 44 | missing data |
| Mary | 37.9 | 36 | 12 |
| Bianca | 37.7 | 44 | 16 |
| Alba | 37.9 | 40 | 16 |

## Table 3. Valvular insufficiencies - evaluation by colour flow Doppler

| Horse | Tricuspid | Pulmonary | Mitral | Aorta |
|---|---|---|---|---|
| Ghibellino | - | mild | - | - |
| Nerac du Bougy | trivial | degree 1 | trivial | - |
| Wings Summerland | trivial | - | - | - |
| Expatriate | - | degree 1 | trivial | - |
| Mobil F.H. | degree 1 | trivial | - | trivial |
| Nectarine F.H. | degree 1 | - | - | - |
| Naomi | * | * | * | * |
| Bella | * | * | * | * |
| Mary | * | * | * | * |
| Bianca | * | * | * | * |
| Alba | * | * | * | * |

* Was not examined with colour flow Doppler on the day of the examinations,
but had been evaluated on previous occasions where no significant insufficiencies were found.

## Table 4a. Preliminary echocardiographic examination - M-mode and 2-D

| Horse | IVSd/cm | IVSs/cm | LVIDd/cm | LVIDs/cm | LVFWd/cm | LVFWs/cm |
|---|---|---|---|---|---|---|
| Ghibellino | 3.2 | 5.0 | 12.7 | 8.7 | 2.6 | 3.5 |
| Nerac du Bougy | 3.2 | 4.1 | 11.8 | 7.6 | 2.6 | 3.7 |
| Wings Summerland | 3.2 | 5.4 | 11.9 | 7.3 | 2.3 | 4.3 |
| Expatriate | 3.1 | 2.3 | 12.0 | 8.5 | 2.3 | 3.6 |
| Mobil F.H. | 3.6 | 5.5 | 11.5 | 6.8 | 3.1 | 4.7 |
| Nectarine F.H. | 3.3 | 4.6 | 12.2 | 7.9 | 2.8 | 4.5 |
| Naomi | 3.3 | 4.7 | 10.6 | 6.4 | 2.6 | 4.4 |
| Bella | 2.2 | 3.9 | 8.7 | 5.4 | 1.8 | 3.0 |
| Mary | 2.9 | 4.4 | 11.4 | 7.3 | 2.7 | 4.2 |
| Bianca | 2.2 | 3.5 | 10.4 | 6.8 | 2.6 | 3.7 |
| Alba | 2.5 | 4.7 | 10.4 | 6.9 | 2.4 | 3.8 |
| **$Mean_{common}$** | 3.0 | 4.4 | 11.2 | 7.2 | 2.5 | 3.9 |
| **$Mean_{athletic}$** | 3.3 | 4.5 | 12.0 | 7.8 | 2.6 | 4.1 |
| **$Mean_{non\text{-}athletic}$** | 2.6 | 4.2 | 10.3 | 6.6 | 2.4 | 3.8 |
| **$SD_{common}$** | 0.5 | 0.9 | 1.1 | 0.9 | 0.3 | 0.5 |
| **$SD_{athletic}$** | 0.2 | 1.2 | 0.4 | 0.7 | 0.3 | 0.5 |
| **$SD_{non\text{-}athletic}$** | 0.5 | 0.5 | 1.0 | 0.7 | 0.4 | 0.5 |

## Table 4b. Preliminary echocardiographic examination - continued..

| Horse | FS/% | Heart rate | Ao/cm |
|---|---|---|---|
| Ghibellino | 32.0 | 32 | 6.7 |
| Nerac du Bougy | 35.3 | 34 | 6.7 |
| Wings Summerland | 38.8 | 39 | 6.5 |
| Expatriate | 28.8 | 38 | 6.6 |
| Mobil F.H. | 40.0 | 32 | 6.1 |
| Nectarine F.H. | 35.5 | 35 | 6.2 |
| Naomi | 39.0 | 47 | 5.5 |
| Bella | 37.5 | 41 | 6.1 |
| Mary | 36.0 | 39 | 6.4 |
| Bianca | 33.0 | 55 | 5.7 |
| Alba | 34.0 | 39 | 6.3 |

## Tissue Doppler examination - by use of 2-D colour TDI

### Table 5a. Radial velocities in the left ventricular free wall - 1st examination

| | Radial velocities/cm/s | | | | | |
|---|---|---|---|---|---|---|
| | S wave | | E wave | | A wave | |
| **Horse** | **endo[a]** | **epi[b]** | **endo[a]** | **epi[b]** | **endo[a]** | **epi[b]** |
| Ghibellino | 10.0 | 6.1 | -27.0 | -12.3 | -5.1 | -0.9 |
| Nerac du Bougy | 7.0 | 5.4 | -16.6 | -9.4 | -6.4 | -5.6 |
| Wings Summerland | 9.3 | 5.0 | -29.1 | -16.3 | -7.8 | -3.0 |
| Expatriate | 6.9 | 4.8 | -20.5 | -14.0 | -2.2 | -1.4 |
| Mobil F.H. | 9.7 | 6.0 | -34.4 | -17.6 | -2.7 | -2.0 |
| Nectarine F.H. | 6.9 | 5.3 | -17.4 | -12.5 | -5.0 | -4.4 |
| Naomi | 10.5 | 8.0 | -21.5 | -15.7 | -10.8 | -9.9 |
| Bella | 6.7 | 5.4 | -28.0 | -19.2 | -6.0 | -6.0 |
| Mary | 7.3 | 5.5 | -20.3 | -15.5 | -8.5 | -6.8 |
| Bianca | 8.2 | 6.1 | -14.3 | -12.0 | -7.5 | -6.2 |
| Alba | 8.6 | 7.3 | -16.4 | -12.3 | -13.1 | -11.4 |
| **$Mean_{common}$** | 8.3 | 5.9 | -22.3 | -14.3 | -6.8 | -5.2 |
| **$Mean_{athletic}$** | 8.3 | 5.4 | -24.2 | -13.7 | -4.9 | -2.9 |
| **$Mean_{non\text{-}athletic}$** | 8.3 | 6.5 | -20.1 | -14.9 | -9.2 | -8.1 |
| **$SD_{common}$** | 1.4 | 1.0 | 6.4 | 2.9 | 3.2 | 3.4 |
| **$SD_{athletic}$** | 1.5 | 0.5 | 7.1 | 3.0 | 2.1 | 1.8 |
| **$SD_{non\text{-}athletic}$** | 1.5 | 1.1 | 5.3 | 2.9 | 2.8 | 2.5 |
| **$CV\%_{common}$** | 17.0 | 16.6 | 28.7 | 20.1 | 47.5 | 64.4 |

[a] Measurement obtained in the endocardium

[b] Measurement obtained in the epicardium

### Table 5b. Radial velocities in the left ventricular free wall - 2nd examination

| | Radial velocities/cm/s | | | | | |
|---|---|---|---|---|---|---|
| | S wave | | E wave | | A wave | |
| **Horse** | **endo[a]** | **epi[b]** | **endo[a]** | **epi[b]** | **endo[a]** | **epi[b]** |
| Ghibellino | 9.9 | 5.1 | -28.1 | -12.8 | -6.4 | -1.9 |
| Nerac du Bougy | 9.2 | 6.7 | -23.2 | -12.3 | -7.9 | -6.3 |
| Wings Summerland | 9.4 | 4.6 | -26.7 | -12.9 | -7.1 | -2.2 |
| Expatriate | 7.3 | 4.6 | -25.0 | -13.0 | -3.6 | -1.5 |
| Mobil F.H. | 9.6 | 6.2 | -24.4 | -9.3 | -3.9 | -2.1 |
| Nectarine F.H. | 7.8 | 5.8 | -29.0 | -16.0 | -5.5 | -4.0 |
| Naomi | 10.4 | 7.4 | -20.8 | -16.0 | -11.0 | -9.9 |
| Bella | 7.7 | 6.0 | -25.4 | -18.1 | -6.7 | -6.2 |
| Mary | 7.7 | 5.8 | -21.7 | -14.8 | -6.9 | -5.5 |
| Bianca | | | | | | |
| Alba | 8.6 | 6.8 | -16.5 | -11.9 | -13.4 | -11.2 |
| **$Mean_{common}$** | 8.8 | 5.9 | -24.1 | -13.7 | -7.2 | -5.1 |
| **$Mean_{athletic}$** | 8.9 | 5.5 | -26.1 | -12.7 | -5.7 | -3.0 |
| **$Mean_{non\text{-}athletic}$** | 8.6 | 6.5 | -21.1 | -15.2 | -9.5 | -8.2 |
| **$SD_{common}$** | 1.1 | 0.9 | 3.7 | 2.5 | 3.0 | 3.4 |
| **$SD_{athletic}$** | 1.1 | 0.9 | 2.2 | 2.1 | 1.7 | 1.8 |
| **$SD_{non\text{-}athletic}$** | 1.3 | 0.8 | 3.7 | 2.6 | 3.3 | 2.8 |
| **$CV\%_{common}$** | 12.4 | 15.8 | 15.5 | 18.5 | 41.5 | 67.2 |

[a] Measurement obtained in the endocardium

[b] Measurement obtained in the epicardium

## Table 6. Radial velocity gradients in the left ventricular free wall

| Horse | Radial velocity gradient/cm/s S wave | E wave | A wave |
|---|---|---|---|
| Ghibellino | 3.9 | 14.7 | 4.2 |
| Nerac du Bougy | 1.6 | 7.2 | 0.8 |
| Wings Summerland | 4.3 | 12.8 | 4.8 |
| Expatriate | 2.1 | 6.5 | 0.8 |
| Mobil F.H. | 3.7 | 16.8 | 0.7 |
| Nectarine F.H. | 1.7 | 4.9 | 0.6 |
| Naomi | 2.5 | 5.8 | 0.9 |
| Bella | 1.3 | 8.8 | 0.0 |
| Mary | 1.8 | 4.8 | 1.7 |
| Bianca | 2.1 | 2.3 | 1.3 |
| Alba | 1.3 | 4.1 | 1.7 |
| **$Mean_{common}$** | 2.4 | 8.1 | 1.6 |
| **$Mean_{athletic}$** | 2.9 | 10.5 | 2.0 |
| **$Mean_{non-athletic}$** | 1.8 | 5.2 | 1.1 |
| **$SD_{common}$** | 1.1 | 4.7 | 1.5 |
| **$SD_{athletic}$** | 1.2 | 4.9 | 1.9 |
| **$SD_{non-athletic}$** | 0.5 | 2.4 | 0.7 |
| **$CV\%_{common}$** | 44.6 | 58.3 | 96.2 |

## Table 7. Radial strain and strain rate in the left ventricular free wall

| Horse | Strain/% | Strain/%* | Strain rate/$s^{-1}$ S wave | E wave | A wave |
|---|---|---|---|---|---|
| Ghibellino | 86.0 | 86.0 | 2.2 | -8.3 | -2.8 |
| Nerac du Bougy | 44.3 | 44.3 | 1.5 | -4.0 | -1.6 |
| Wings Summerland | 122.0 | | 1.9 | -5.3 | -2.0 |
| Expatriate | 35.6 | 35.6 | 1.3 | -5.3 | -0.5 |
| Mobil F.H. | 55.0 | 55.0 | 2.0 | -5.9 | -1.5 |
| Nectarine F.H. | 49.0 | 49.0 | 1.4 | -4.1 | -1.8 |
| Naomi | 0.4 | | 1.7 | -5.6 | -1.2 |
| Bella | 27.7 | 27.7 | 1.1 | -4.3 | -0.6 |
| Mary | 42.9 | 42.9 | 1.2 | -4.0 | -0.9 |
| Bianca | 61.1 | 61.1 | 2.0 | -4.6 | -2.8 |
| Alba | 44.3 | 44.3 | 1.5 | -4.0 | -1.6 |
| **$Mean_{common}$** | 51.7 | 49.6 | 1.6 | -5.0 | -1.6 |
| **$Mean_{athletic}$** | 65.3 | 54.0 | 1.7 | -5.5 | -1.7 |
| **$Mean_{non-athletic}$** | 35.3 | 44.0 | 1.5 | -4.5 | -1.4 |
| **$SD_{common}$** | 31.4 | 16.8 | 0.4 | 1.3 | 0.8 |
| **$SD_{athletic}$** | 32.7 | 19.2 | 0.4 | 1.6 | 0.7 |
| **$SD_{non-athletic}$** | 22.8 | 13.7 | 0.4 | 0.7 | 0.8 |
| **$CV\%_{common}$** | 60.8 | 33.9 | 22.4 | 25.6 | 48.7 |

Red numbers are suspected to be outliers

*Strain values without suspected outliers

## Speckle tracking examination - on 2-D echocardiograms

### Table 8. Radial velocities in the left ventricular free wall

| Horse | Peak systolic velocity/cm/s S wave | E wave | A wave |
|---|---|---|---|
| Ghibellino | 6.4 | -7.6 | -2.9 |
| Nerac du Bougy | 4.2 | -3.7 | -3.2 |
| Wings Summerland | 5.2 | -7.0 | -3.0 |
| Expatriate | 3.5 | -3.9 | -1.8 |
| Mobil F.H. | 4.7 | -5.9 | -2.6 |
| Nectarine F.H. | 4.0 | -3.7 | -3.0 |
| Naomi | 6.4 | -10.0 | -2.5 |
| Bella | 6.2 | -2.7 | -0.5 |
| Mary | 4.5 | -4.2 | -1.6 |
| Bianca | 6.9 | -4.1 | -2.8 |
| Alba | 5.6 | -3.7 | -5.2 |
| **$Mean_{common}$** | 5.2 | -5.1 | -2.6 |
| **$Mean_{athletic}$** | 4.7 | -5.3 | -2.7 |
| **$Mean_{non-athletic}$** | 5.9 | -4.9 | -2.5 |
| **$SD_{common}$** | 1.1 | 2.2 | 1.2 |
| **$SD_{athletic}$** | 1.0 | 1.8 | 0.5 |
| **$SD_{non-athletic}$** | 0.9 | 2.9 | 1.7 |
| **$CV\%_{common}$** | 21.8 | 43.3 | 44.3 |

### Table 9. Radial strain and strain rates in the left ventricular freewall

| Horse | Strain/% | Strain rates/$s^{-1}$ S wave | E wave | A wave |
|---|---|---|---|---|
| Ghibellino | 61.0 | 1.7 | -1.4 | -0.4 |
| Nerac du Bougy | 66.0 | 1.1 | -1.7 | -0.5 |
| Wings Summerland | 61.5 | 1.6 | -1.8 | -0.5 |
| Expatriate | 98.7 | 1.4 | -1.1 | -0.6 |
| Mobil F.H. | 72.0 | 1.0 | -0.8 | -0.5 |
| Nectarine F.H. | 48.9 | 1.8 | -1.7 | -0.7 |
| Naomi | 78.0 | 2.2 | -2.3 | -1.7 |
| Bella | 92.0 | 1.3 | -2.7 | -0.5 |
| Mary | 99.0 | 1.6 | -1.2 | -0.9 |
| Bianca | 68.6 | 1.8 | -0.4 | -0.2 |
| Alba | 37.0 | 1.8 | -1.4 | -1.6 |
| **$Mean_{common}$** | 71.2 | 1.6 | -1.5 | -0.7 |
| **$Mean_{athletic}$** | 68.0 | 1.4 | -1.4 | -0.5 |
| **$Mean_{non-athletic}$** | 74.9 | 1.7 | -1.6 | -1.0 |
| **$SD_{common}$** | 19.8 | 0.3 | 0.6 | 0.5 |
| **$SD_{athletic}$** | 16.8 | 0.3 | 0.4 | 0.1 |
| **$SD_{non-athletic}$** | 24.3 | 0.3 | 0.9 | 0.7 |
| **$CV\%_{common}$** | 27.8 | 22.3 | 43.3 | 65.8 |

## Table 10. Global rotation and rotation rate

| Horse | Rotation/° | | Rotation rate/°/s | |
|---|---|---|---|---|
| | apex[c] | base[e] | apex[c] | base[e] |
| Ghibellino | 14.3 | 1.6 | 57.8 | 10.9 |
| Nerac du Bougy | -1.8 | 6.4 | -24.0 | 19.5 |
| Wings Summerland | 10.6 | 5.0 | 36.7 | 18.0 |
| Expatriate | 10.7 | 1.3 | 45.4 | 11.7 |
| Mobil F.H. | 3.8 | 3.9 | 23.0 | 18.8 |
| Nectarine F.H. | 2.9 | -1.7 | 41.4 | 15.6 |
| Naomi | 8.9 | 2.3 | 44.5 | 27.0 |
| Bella | 13.7 | 0.8 | 58.6 | 7.0 |
| Mary | 4.6 | 3.7 | 42.2 | 37.5 |
| Bianca | 13.8 | -7.0 | 56.0 | -30.5 |
| Alba | -1.6 | 7.6 | -21.0 | 27.0 |
| **$Mean_{common}$** | 7.3 | 2.2 | 32.8 | 14.8 |
| **$Mean_{athletic}$** | 6.7 | 2.7 | 30.1 | 15.7 |
| **$Mean_{non\text{-}athletic}$** | 7.9 | 1.5 | 36.1 | 13.6 |
| **$SD_{common}$** | 6.0 | 4.0 | 29.2 | 17.3 |
| **$SD_{athletic}$** | 6.1 | 2.9 | 28.8 | 3.7 |
| **$SD_{non\text{-}athletic}$** | 6.5 | 5.4 | 32.7 | 27.0 |

[c] Short-axis view at the apical level

[e] Short-axis view at the level of the mitral valve

# APPENDIX 8 – CALCULATIONS FOR PROTOCOL 1

## Bland-Altman plot

Assume that:
$Y_{TDI,i}$ is the TDI measurement of a given parameter in horse *i, i* = 1,…,n, n=11
$Y_{speck.i}$ is the speckle tracking measurement of a given parameter in horse *i, i* = 1,…,n, n=11

Mean $m_i$ is the mean measurement of the two methods, calculated as: $m_i = (Y_{TDIi} + Y_{speck.i}) / 2$

Difference $d_i$ is the measurement difference between the two methods, calculated as: $d_i = Y_{TDIi} - Y_{speck.i}$

Mean difference between the two methods is an estimate of the bias of the methods relativ each other:

$$\overline{d} = \frac{\sum_{i=1}^{n} d_i}{n}$$

Standard deviation $s_d$:

$$s_d = \sqrt{\frac{\sum_{i=1}^{n} (d_i - \overline{d})^2}{n-1}}$$

Limits of agreement calculated as a 95% cofidence interval of the mean difference:

$$\overline{d} \pm 1.96 \times s_d$$

## Parameter: Radial velocity (S wave) in the left ventricular free wall

| Horse *i* | Condition | $TDI_{endo}$ | $TDI_{epi}$ | $Y_{TDI}$ | $Y_{speck.\ tracking}$ | Mean $m_i$ | Difference $d_i$ |
|---|---|---|---|---|---|---|---|
| 1 | Athletic | 10.0 | 6.1 | 8.1 | 6.4 | 7.2 | 1.7 |
| 2 | Athletic | 7.0 | 5.4 | 6.2 | 4.2 | 5.2 | 2.0 |
| 3 | Athletic | 9.3 | 5.0 | 7.1 | 5.2 | 6.2 | 1.9 |
| 4 | Athletic | 6.9 | 4.8 | 5.8 | 3.5 | 4.7 | 2.3 |
| 5 | Athletic | 9.7 | 6.0 | 7.8 | 4.7 | 6.3 | 3.1 |
| 6 | Athletic | 6.9 | 5.3 | 6.1 | 4.0 | 5.1 | 2.1 |
| 7 | Non-athletic | 10.5 | 8.0 | 9.2 | 6.4 | 7.8 | 2.8 |
| 8 | Non-athletic | 6.7 | 5.4 | 6.1 | 6.2 | 6.1 | -0.1 |
| 9 | Non-athletic | 7.3 | 5.5 | 6.4 | 4.5 | 5.4 | 1.9 |
| 10 | Non-athletic | 8.2 | 6.1 | 7.2 | 6.9 | 7.0 | 0.2 |
| 11 | Non-athletic | 8.6 | 7.3 | 8.0 | 5.6 | 6.8 | 2.4 |

Notice: $Y_{TDI}$ is the average of the endocardial and epicardial velocities obtained by TDI

| | |
|---|---|
| Mean difference: | 1.8 |
| Standard deviation $s_d$: | 1.0 |
| Upper limit of agreement: | 3.8 |
| Lower limit of agreement: | -0.1 |

Bland-Altman plot in which individual observartions is plottet with the coordinates ($m_i$,$d_i$), the solid line indicates the bias, and the dashed lines indicate the limits of agreement:

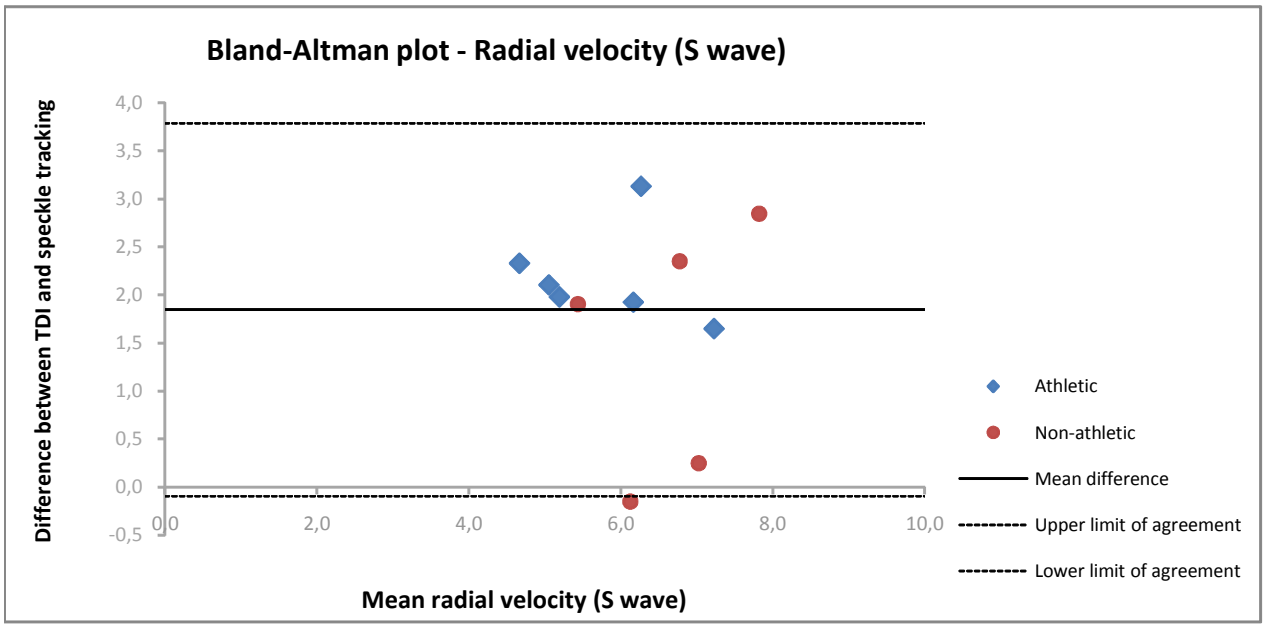


The Bland-Altman analysis indicates a questionable agreement between the 2-D colour TDI and speckle tracking techniques for measurement of radial velocity (S wave) with one horse lying outside the limits of agreement.
The mean difference (bias) of the two methods was 1.8 cm/s - indicating that the S wave velocity measured by TDI were 1.8 cm/s higher on average than those measured by speckle tracking.
The 95% limits of agreement between the two methods range from -0.1 cm/s to 3.8 cm/s

## Parameter: Radial velocity (E wave) in the left ventricular free wall

| Horse *i* | Condition | $TDI_{endo}$ | $TDI_{epi}$ | $Y_{TDI}$ | $Y_{speck.\ tracking}$ | Mean $m_i$ | Difference $d_i$ |
|---|---|---|---|---|---|---|---|
| 1 | Athletic | -27.0 | -12.3 | -19.7 | -7.6 | -13.6 | -12.1 |
| 2 | Athletic | -16.6 | -9.4 | -13.0 | -3.7 | -8.4 | -9.3 |
| 3 | Athletic | -29.1 | -16.3 | -22.7 | -7.0 | -14.9 | -15.7 |
| 4 | Athletic | -20.5 | -14.0 | -17.3 | -3.9 | -10.6 | -13.4 |
| 5 | Athletic | -34.4 | -17.6 | -26.0 | -5.9 | -16.0 | -20.1 |
| 6 | Athletic | -17.4 | -12.5 | -15.0 | -3.7 | -9.3 | -11.3 |
| 7 | Non-athletic | -21.5 | -15.7 | -18.6 | -10.0 | -14.3 | -8.6 |
| 8 | Non-athletic | -28.0 | -19.2 | -23.6 | -2.7 | -13.1 | -20.9 |
| 9 | Non-athletic | -20.3 | -15.5 | -17.9 | -4.2 | -11.1 | -13.7 |
| 10 | Non-athletic | -14.3 | -12.0 | -13.2 | -4.1 | -8.6 | -9.1 |
| 11 | Non-athletic | -16.4 | -12.3 | -14.4 | -3.7 | -9.0 | -10.7 |

Notice: $Y_{TDI}$ is the average of the endocardial and epicardial velocities obtained by TDI

| | |
|---|---|
| Mean difference: | -13.2 |
| Standard deviation $s_d$: | 4.2 |
| Upper limit of agreement: | -4.9 |
| Lower limit of agreement: | -21.4 |

Bland-Altman plot in which individual observartions is plottet with the coordinates ($m_i$,$d_i$), the solid line indicates the bias, and the dashed lines indicate the limits of agreement:

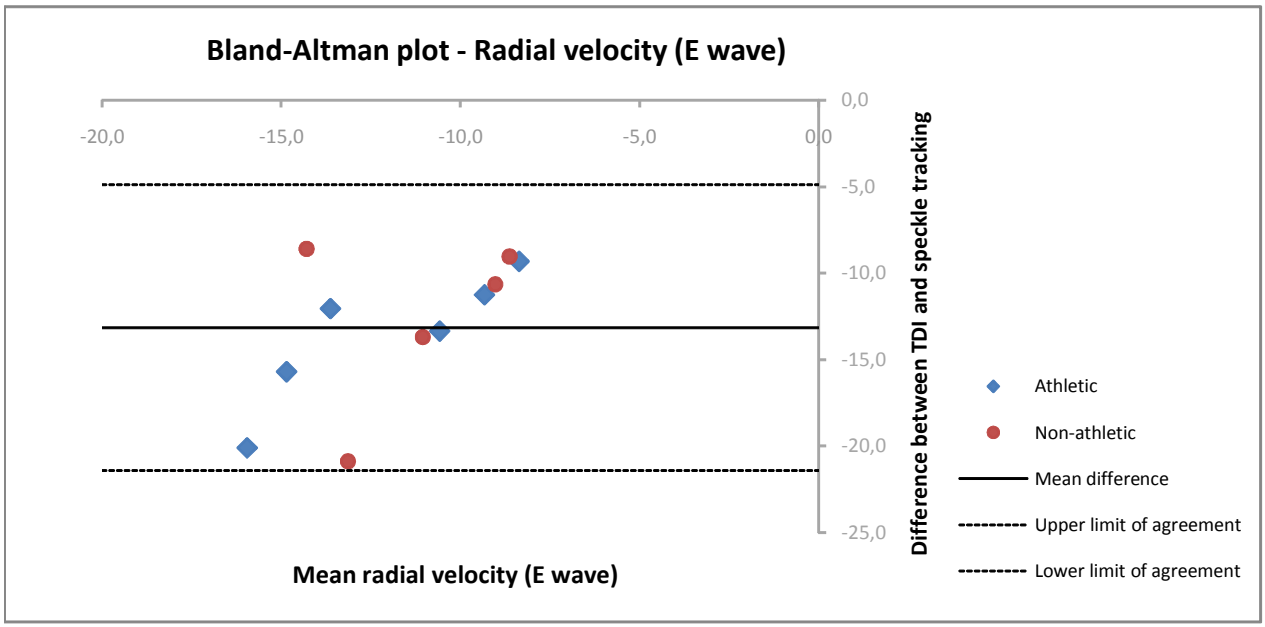


The Bland-Altman analysis indicates a poor agreement between the 2-D colour TDI and speckle tracking techniques for measurement of radial velocity (E wave) as zero is **not** within the limits of agreement.
The mean difference (bias) of the two methods was -13.2 cm/s - indicating that the E wave velocities measured by TDI were 13.2 cm/s higher on average than those measured by speckle tracking.
The 95% limits of agreement between the two methods range from -21.4 cm/s to -4.9 cm/s

## Parameter: Radial velocity (A wave) in the left ventricular free wall

| Horse *i* | Condition | $TDI_{endo}$ | $TDI_{epi}$ | $Y_{TDI}$ | $Y_{speck.\ tracking}$ | Mean $m_i$ | Difference $d_i$ |
|---|---|---|---|---|---|---|---|
| 1 | Athletic | -5.1 | -0.9 | -3.0 | -2.9 | -3.0 | -0.1 |
| 2 | Athletic | -6.4 | -5.6 | -6.0 | -3.2 | -4.6 | -2.8 |
| 3 | Athletic | -7.8 | -3.0 | -5.4 | -3.0 | -4.2 | -2.4 |
| 4 | Athletic | -2.2 | -1.4 | -1.8 | -1.8 | -1.8 | -0.1 |
| 5 | Athletic | -2.7 | -2.0 | -2.4 | -2.6 | -2.5 | 0.3 |
| 6 | Athletic | -5.0 | -4.4 | -4.7 | -3.0 | -3.9 | -1.7 |
| 7 | Non-athletic | -10.8 | -9.9 | -10.4 | -2.5 | -6.4 | -7.9 |
| 8 | Non-athletic | -6.0 | -6.0 | -6.0 | -0.5 | -3.2 | -5.5 |
| 9 | Non-athletic | -8.5 | -6.8 | -7.6 | -1.6 | -4.6 | -6.0 |
| 10 | Non-athletic | -7.5 | -6.2 | -6.8 | -2.8 | -4.8 | -4.0 |
| 11 | Non-athletic | -13.1 | -11.4 | -12.3 | -5.2 | -8.7 | -7.1 |

Notice: $Y_{TDI}$ is the average of the endocardial and epicardial velocities obtained by TDI

| | |
|---|---|
| Mean difference: | -3.4 |
| Standard deviation $s_d$: | 2.9 |
| Upper limit of agreement: | 2.3 |
| Lower limit of agreement: | -9.1 |

Bland-Altman plot in which individual observartions is plottet with the coordinates ($m_i$,$d_i$), the solid line indicates the bias, and the dashed lines indicate the limits of agreement:

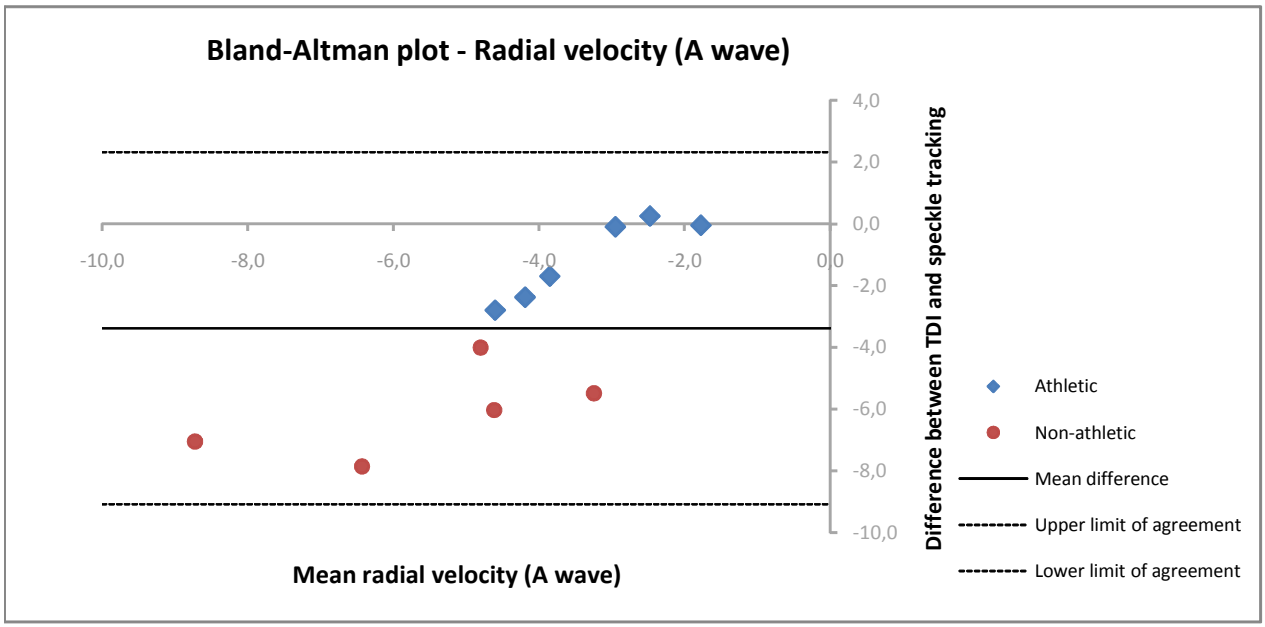


The Bland-Altman analysis indicates a questionable agreement between the 2-D colour TDI and speckle tracking techniques for measurement of radial velocity (A wave). There appeared to be a tendency in the plot; with the difference between the measures being smaller than average in the athletic horses and larger than average in the non-athletic horses.
The mean difference (bias) of the two methods was -3.4 cm/s - indicating that the A wave velocities measured by TDI were 3.4 cm/s higher on average than those measured by speckle tracking.
The 95% limits of agreement between the two methods range from -9.1 cm/s to 2.3 cm/s

## Parameter: Radial peak systolic strain in the left ventricular free wall

| Horse *i* | Condition | $Y_{TDI}$ | $Y_{speck.\ tracking}$ | Mean $m_i$ | Difference $d_i$ |
|---|---|---|---|---|---|
| 1 | Athletic | 86.0 | 61.0 | 73.5 | 25.0 |
| 2 | Athletic | 44.3 | 66.0 | 55.2 | -21.7 |
| 3 | Athletic | 122.0 | 61.5 | 91.8 | 60.5 |
| 4 | Athletic | 35.6 | 98.7 | 67.2 | -63.1 |
| 5 | Athletic | 55.0 | 72.0 | 63.5 | -17.0 |
| 6 | Athletic | 49.0 | 48.9 | 49.0 | 0.1 |
| 7 | Non-athletic | 0.4 | 78.0 | 39.2 | -77.6 |
| 8 | Non-athletic | 27.7 | 92.0 | 59.9 | -64.3 |
| 9 | Non-athletic | 42.9 | 99.0 | 71.0 | -56.1 |
| 10 | Non-athletic | 61.1 | 68.6 | 64.8 | -7.5 |
| 11 | Non-athletic | 44.3 | 37.0 | 40.7 | 7.3 |

| | |
|---|---|
| Mean difference: | -19.5 |
| Standard deviation $s_d$: | 42.7 |
| Upper limit of agreement: | 64.3 |
| Lower limit of agreement: | -103.2 |

Bland-Altman plot in which individual observartions is plottet with the coordinates ($m_i$,$d_i$), the solid line indicates the bias, and the dashed lines indicate the limits of agreement:

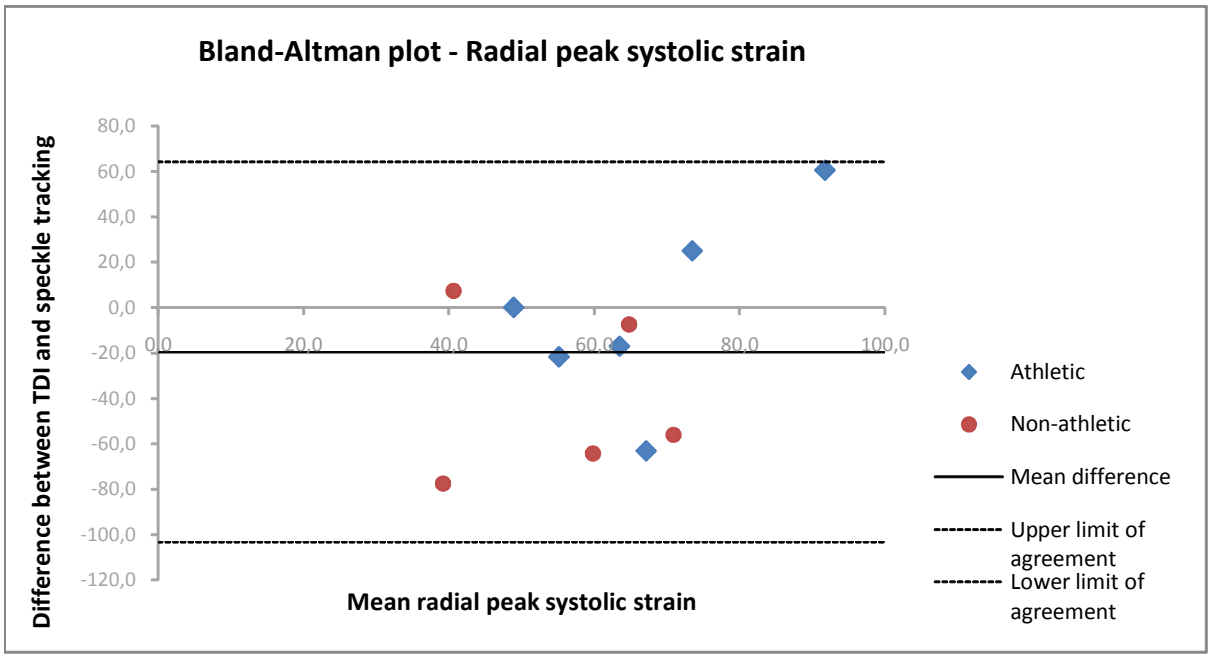


The Bland-Altman analysis indicates a questionable agreement between the 2-D colour TDI and speckle tracking techniques for measurement of radial peak systolic strain.
The mean difference (bias) of the two methods was -20% - indicating that strain values measured by speckle tracking were 20% higher on average than those measured by TDI.
The 95% limits of agreement between the two methods range from -103% to 64%.

## Parameter: Radial strain rate (S wave) in the left ventricular free wall

| Horse *i* | Condition | $Y_{TDI}$ | $Y_{speck.\ tracking}$ | Mean $m_i$ | Difference $d_i$ |
|---|---|---|---|---|---|
| 1 | Athletic | 2.2 | 1.7 | 1.9 | 0.5 |
| 2 | Athletic | 1.5 | 1.1 | 1.3 | 0.4 |
| 3 | Athletic | 1.9 | 1.6 | 1.8 | 0.3 |
| 4 | Athletic | 1.3 | 1.4 | 1.3 | -0.1 |
| 5 | Athletic | 2.0 | 1.0 | 1.5 | 1.0 |
| 6 | Athletic | 1.4 | 1.8 | 1.6 | -0.4 |
| 7 | Non-athletic | 1.7 | 2.2 | 2.0 | -0.5 |
| 8 | Non-athletic | 1.1 | 1.3 | 1.2 | -0.2 |
| 9 | Non-athletic | 1.2 | 1.6 | 1.4 | -0.4 |
| 10 | Non-athletic | 2.0 | 1.8 | 1.9 | 0.2 |
| 11 | Non-athletic | 1.5 | 1.8 | 1.6 | -0.3 |

| | |
|---|---|
| Mean difference: | 0.0 |
| Standard deviation $s_d$: | 0.5 |
| Upper limit of agreement: | 0.9 |
| Lower limit of agreement: | -0.9 |

Bland-Altman plot in which individual observartions is plottet with the coordinates ($m_i$,$d_i$), the solid line indicates the bias, and the dashed lines indicate the limits of agreement:

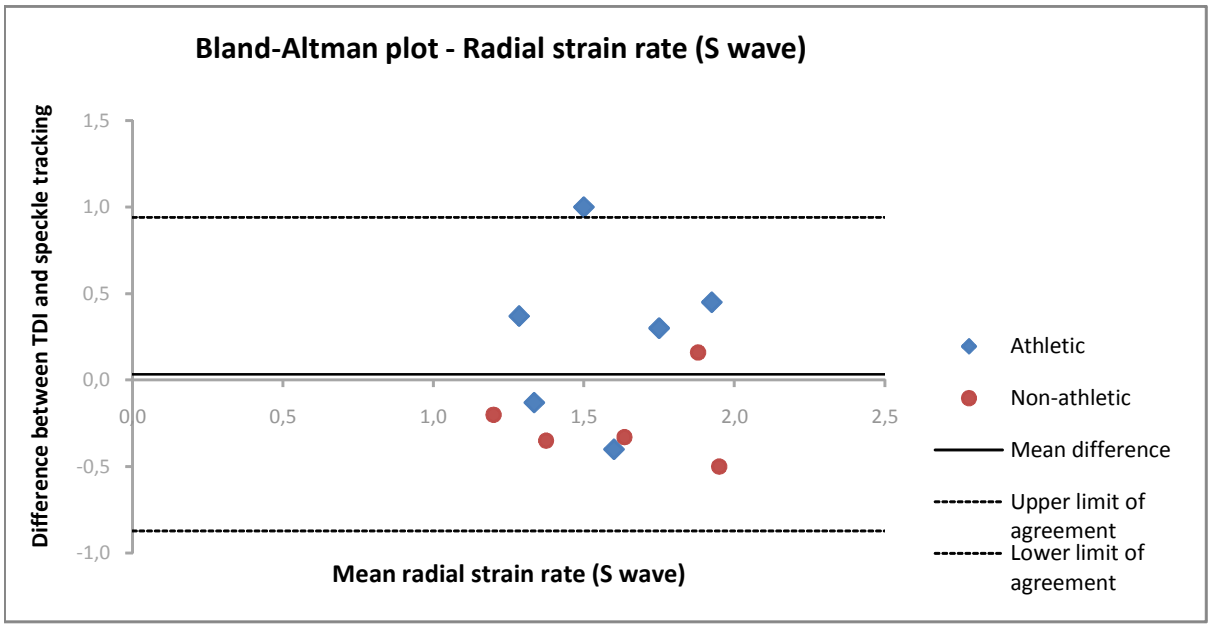


The Bland-Altman analysis indicates a good agreement between the 2-D colour TDI and speckle tracking techniques for measurement of radial strain rate (S wave) (with exception of one horse) as the mean difference (bias) of the two methods was ~ 0.0 $s^{-1}$. The 95% limits of agreement between the two methods range from -0.9$s^{-1}$ to 0.9$s^{-1}$.

## Parameter: Radial strain rate (E wave) in the left ventricular free wall

| Horse *i* | Condition | $Y_{TDI}$ | $Y_{speck.\ tracking}$ | Mean $m_i$ | Difference $d_i$ |
|---|---|---|---|---|---|
| 1 | Athletic | -8.3 | -1.4 | -4.9 | -6.9 |
| 2 | Athletic | -4.0 | -1.7 | -2.9 | -2.3 |
| 3 | Athletic | -5.3 | -1.8 | -3.6 | -3.5 |
| 4 | Athletic | -5.3 | -1.1 | -3.2 | -4.2 |
| 5 | Athletic | -5.9 | -0.8 | -3.4 | -5.1 |
| 6 | Athletic | -4.1 | -1.7 | -2.9 | -2.4 |
| 7 | Non-athletic | -5.6 | -2.3 | -4.0 | -3.3 |
| 8 | Non-athletic | -4.3 | -2.7 | -3.5 | -1.6 |
| 9 | Non-athletic | -4.0 | -1.2 | -2.6 | -2.8 |
| 10 | Non-athletic | -4.6 | -0.4 | -2.5 | -4.2 |
| 11 | Non-athletic | -4.0 | -1.4 | -2.7 | -2.6 |

| | |
|---|---|
| Mean difference: | -3.5 |
| Standard deviation $s_d$: | 1.5 |
| Upper limit of agreement: | -0.6 |
| Lower limit of agreement: | -6.5 |

Bland-Altman plot in which individual observartions is plottet with the coordinates ($m_i$,$d_i$), the solid line indicates the bias, and the dashed lines indicate the limits of agreement:

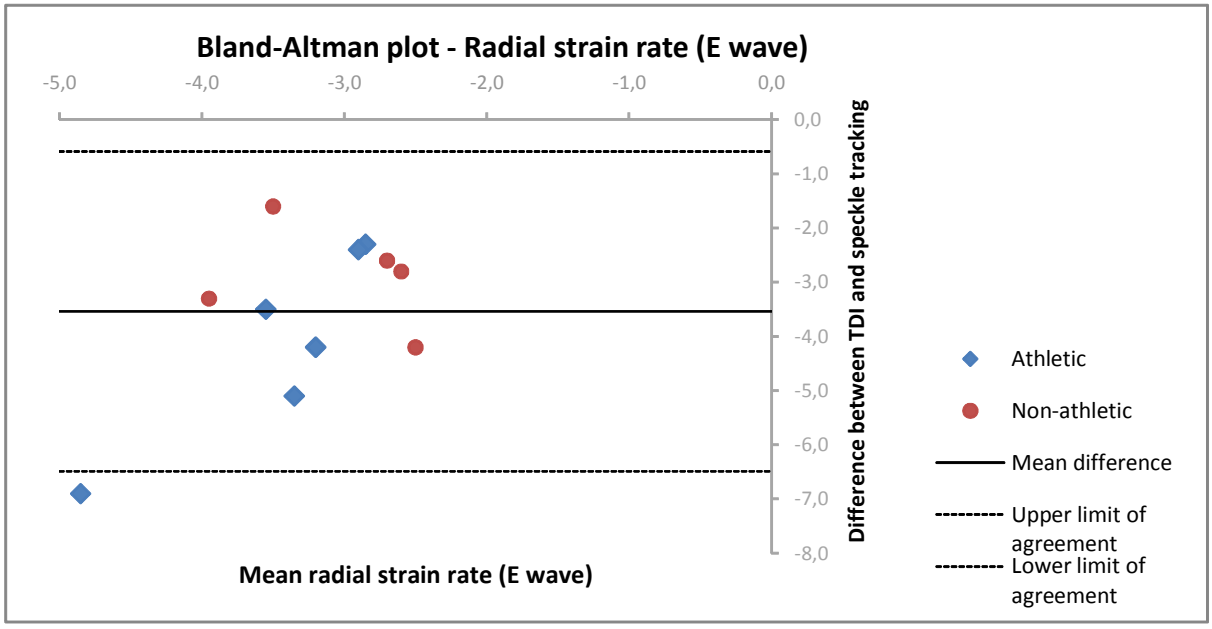


The Bland-Altman analysis indicates a poor agreement between the 2-D colour TDI and speckle tracking techniques for measurement of radial strain rate (E wave) as zero is not even within the 95% limits of agreement and one horse lies completely outside the limits.
The mean difference (bias) of the two methods was -3.5$s^{-1}$ - indicating that E wave strain rates measured by TDI were 3.5$s^{-1}$ higher on average than those measured by speckle tracking.
The 95% limits of agreement between the two methods range from -6.5$s^{-1}$ to -0.6$s^{-1}$.

## Parameter: Radial strain rate (A wave) in the left ventricular free wall

| Horse *i* | Condition | $Y_{TDI}$ | $Y_{speck.\ tracking}$ | Mean $m_i$ | Difference $d_i$ |
|---|---|---|---|---|---|
| 1 | Athletic | -2.8 | -0.4 | -1.6 | -2.4 |
| 2 | Athletic | -1.6 | -0.5 | -1.1 | -1.1 |
| 3 | Athletic | -2.0 | -0.5 | -1.3 | -1.5 |
| 4 | Athletic | -0.5 | -0.6 | -0.6 | 0.1 |
| 5 | Athletic | -1.5 | -0.5 | -1.0 | -1.0 |
| 6 | Athletic | -1.8 | -0.7 | -1.3 | -1.1 |
| 7 | Non-athletic | -1.2 | -1.7 | -1.5 | 0.5 |
| 8 | Non-athletic | -0.6 | -0.5 | -0.6 | -0.1 |
| 9 | Non-athletic | -0.9 | -0.9 | -0.9 | 0.0 |
| 10 | Non-athletic | -2.8 | -0.2 | -1.5 | -2.6 |
| 11 | Non-athletic | -1.6 | -1.6 | -1.6 | 0.0 |

| | |
|---|---|
| Mean difference: | -0.8 |
| Standard deviation $s_d$: | 1.0 |
| Upper limit of agreement: | 1.2 |
| Lower limit of agreement: | -2.8 |

Bland-Altman plot in which individual observartions is plottet with the coordinates ($m_i$,$d_i$), the solid line indicates the bias, and the dashed lines indicate the limits of agreement:

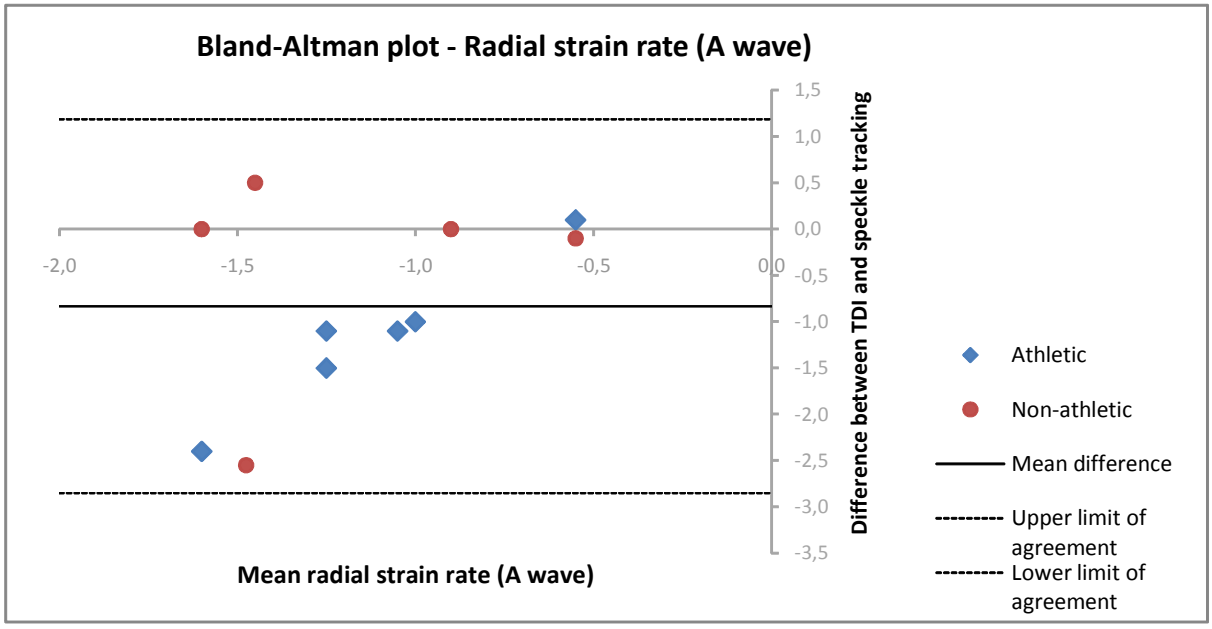


The Bland-Altman analysis indicates a questionable agreement between the 2-D colour TDI and speckle tracking techniques for measurement of radial strain rate (A wave).
The mean difference (bias) of the two methods was -0.8$s^{-1}$ - indicating that the A wave strain rates measured by TDI were 0.8$s^{-1}$ higher than those measured by speckle tracking.
The 95% limits of agreement between the two methods range from -2.9$s^{-1}$ to 1.2$s^{-1}$.

## Paired Students t-test (two-sided) of 1st versus 2nd examination

A paired t-test was used to test for a significant difference between the 1st and 2nd examination of the radial velocities by 2-D colour TDI in the left ventricular free wall of the athletic horses.
Level of significans = 0.05
$H_0$ hypothesis: There is no significant difference between the 1st and 2nd examination of the radial velocities by 2-D colour TDI.

The Pearson correlation coefficient was calculated as a measure of the correlation between examination 1 and 2. This statistical measure obtains values from -1 to 1.
0 indicates no correlation a all, while a value close to -1 or 1 indicates a strong negative or positive correlation, respectively. The Pearson correlation coefficient should be interpreted with caution at small sample sizes. The critical value for n = 6, α = 0.05, two-sided test is ±0.8114

## 1st versus 2nd examination - S wave endocardium

| Horse | 1st exam. | 2nd exam. |
|---|---|---|
| Ghibellino | 10.0 | 9.9 |
| Nerac du Bougy | 7.0 | 9.2 |
| Wings Summerland | 9.3 | 9.4 |
| Expatriate | 6.9 | 7.3 |
| Mobil F.H. | 9.7 | 9.6 |
| Nectarine F.H. | 6.9 | 7.8 |

**t-Test: Paired Two Sample for Means (two sided)**

| | *1st exam.* | *2nd exam.* |
|---|---|---|
| Mean | 8.3 | 8.9 |
| Variance | 2.2 | 1.1 |
| Observations | 6 | 6 |
| Pearson Correlation | **0.8203** | |
| Hypothesized Mean Difference | 0 | |
| df | 5 | |
| t Stat | -1.625855836 | |
| P(T<=t) two-tail | **0.164908666** | |
| t Critical two-tail | 2.570581835 | |

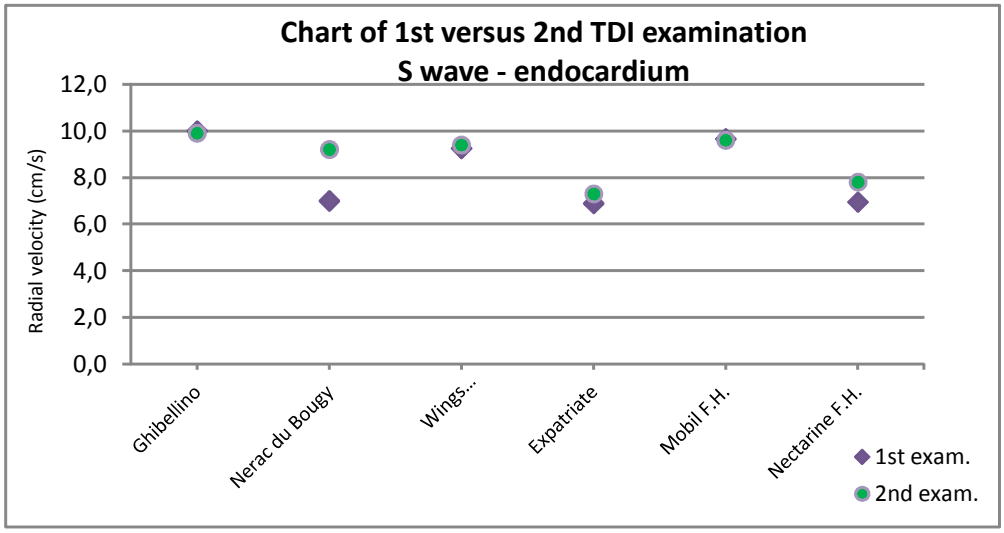


Conclusion: As the p-value > α = 0.05 the null-hypothesis was accepted.
There is with 95% certainty no significant difference between examination 1 and 2.
The Pearson correlation coefficient was 0.8203 indicating a significant positive correlation between examination 1 and 2.

## 1st versus 2nd examination - S wave epicardium

| Horse | 1st exam. | 2nd exam. |
|---|---|---|
| Ghibellino | 6.1 | 5.1 |
| Nerac du Bougy | 5.4 | 6.7 |
| Wings Summerland | 5.0 | 4.6 |
| Expatriate | 4.8 | 4.6 |
| Mobil F.H. | 6.0 | 6.2 |
| Nectarine F.H. | 5.3 | 5.8 |

**t-Test: Paired Two Sample for Means (two sided)**

| | *1st exam.* | *2nd exam.* |
|---|---|---|
| Mean | 5.4 | 5.5 |
| Variance | 0.3 | 0.8 |
| Observations | 6 | 6 |
| Pearson Correlation | **0.4247** | |
| Hypothesized Mean Difference | 0 | |
| df | 5 | |
| t Stat | -0.24328962 | |
| P(T<=t) two-tail | **0.817447212** | |
| t Critical two-tail | 2.570581835 | |

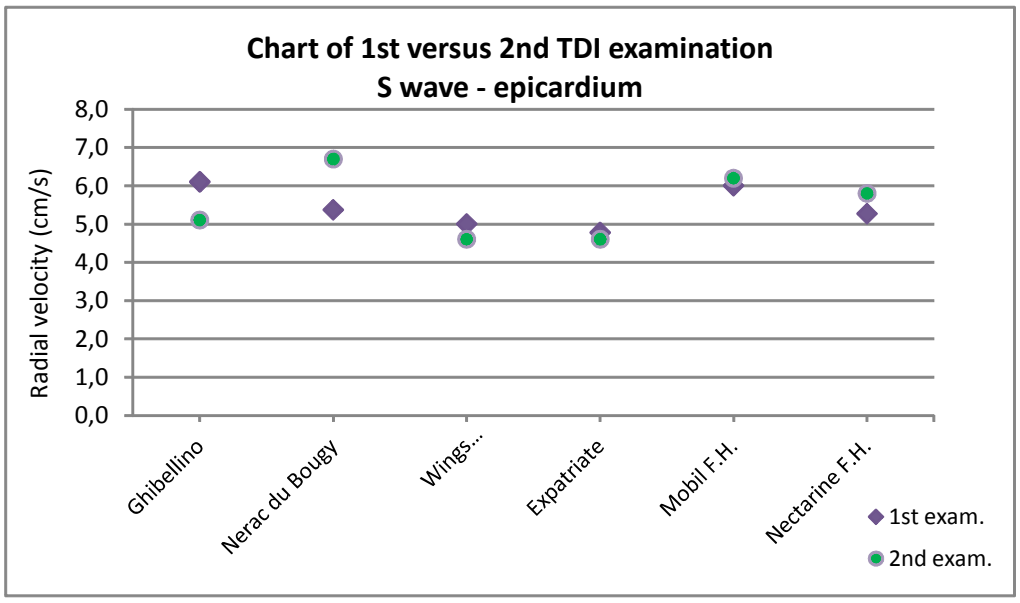


Conclusion: As the p-value >> α = 0.05 the null-hypothesis was accepted.
There is with 95% certainty no significant difference between examination 1 and 2.
The Pearson correlation coefficient was 0.4247 and thereby not enough to indicate a significant positive correlation between examination 1 and 2.

## 1st versus 2nd examination - E wave endocardium

| Horse | 1st exam. | 2nd exam. |
|---|---|---|
| Ghibellino | -27.0 | -28.1 |
| Nerac du Bougy | -16.6 | -23.2 |
| Wings Summerland | -29.1 | -26.7 |
| Expatriate | -20.5 | -25.0 |
| Mobil F.H. | -34.4 | -24.4 |
| Nectarine F.H. | -17.4 | -29.0 |

**t-Test: Paired Two Sample for Means (two sided)**

| | *1st exam.* | *2nd exam.* |
|---|---|---|
| Mean | -24.2 | -26.1 |
| Variance | 50.7 | 5.1 |
| Observations | 6 | 6 |
| Pearson Correlation | **-0.0302** | |
| Hypothesized Mean Difference | 0 | |
| df | 5 | |
| t Stat | 0.617873927 | |
| P(T<=t) two-tail | **0.563711324** | |
| t Critical two-tail | 2.570581835 | |

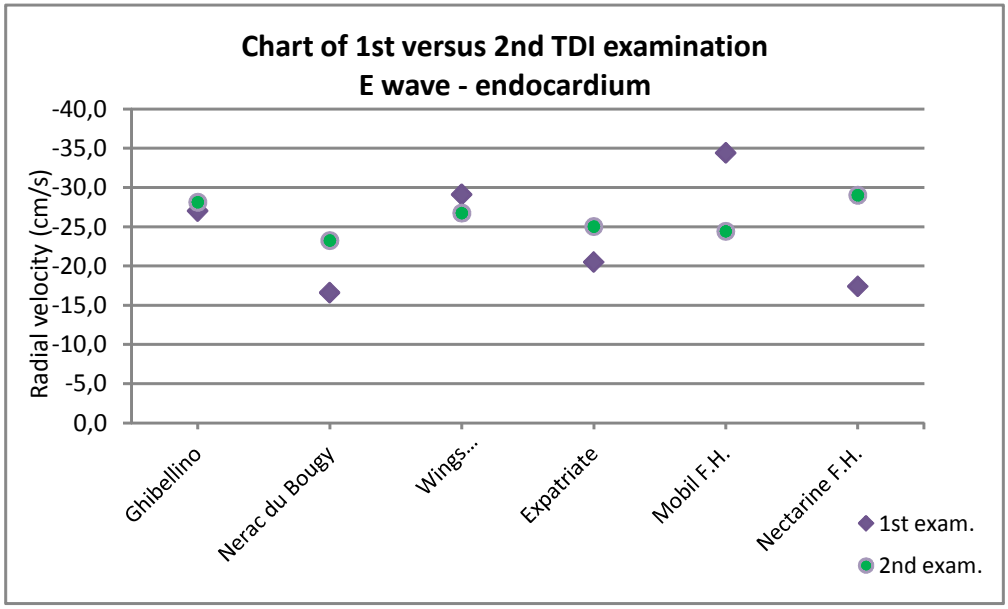


Conclusion: As the p-value >> α = 0.05 the null-hypothesis was accepted.
There is with 95% certainty no significant difference between examination 1 and 2.
The Pearson correlation coefficient was -0.0302 and thereby indicate almost no correlation between examination 1 and 2.

## 1st versus 2nd examination - E wave epicardium

| Horse | 1st exam. | 2nd exam. |
|---|---|---|
| Ghibellino | -12.3 | -12.8 |
| Nerac du Bougy | -9.4 | -12.3 |
| Wings Summerland | -16.3 | -12.9 |
| Expatriate | -14.0 | -13.0 |
| Mobil F.H. | -17.6 | -9.3 |
| Nectarine F.H. | -12.5 | -16.0 |

**t-Test: Paired Two Sample for Means (two sided)**

| | *1st exam.* | *2nd exam.* |
|---|---|---|
| Mean | -13.7 | -12.7 |
| Variance | 8.7 | 4.5 |
| Observations | 6 | 6 |
| Pearson Correlation | **-0.4777** | |
| Hypothesized Mean Difference | 0 | |
| df | 5 | |
| t Stat | -0.542852216 | |
| P(T<=t) two-tail | **0.610544775** | |
| t Critical two-tail | 2.570581835 | |

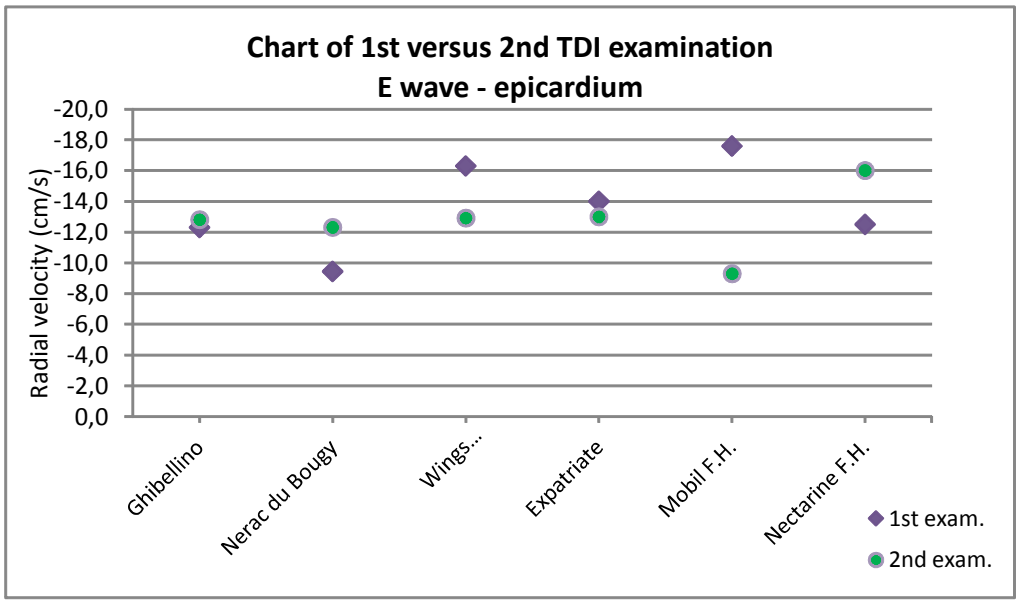


Conclusion: As the p-value >> α = 0.05 the null-hypothesis was accepted.
There is with 95% certainty no significant difference between examination 1 and 2.
The Pearson correlation coefficient was -0.4777 and thereby **not** enough to indicate a significant negative correlation between examination 1 and 2.

## 1st versus 2nd examination - A wave endocardium

| Horse | 1st exam. | 2nd exam. |
|---|---|---|
| Ghibellino | -5.1 | -6.4 |
| Nerac du Bougy | -6.4 | -7.9 |
| Wings Summerland | -7.8 | -7.1 |
| Expatriate | -2.2 | -3.6 |
| Mobil F.H. | -2.7 | -3.9 |
| Nectarine F.H. | -5.0 | -5.5 |

**t-Test: Paired Two Sample for Means (two sided)**

| | *1st exam.* | *2nd exam.* |
|---|---|---|
| Mean | -4.9 | -5.7 |
| Variance | 4.5 | 3.0 |
| Observations | 6 | 6 |
| Pearson Correlation | **0.9275** | |
| Hypothesized Mean Difference | 0 | |
| df | 5 | |
| t Stat | 2.57556836 | |
| P(T<=t) two-tail | **0.04969844** | |
| t Critical two-tail | 2.570581835 | |

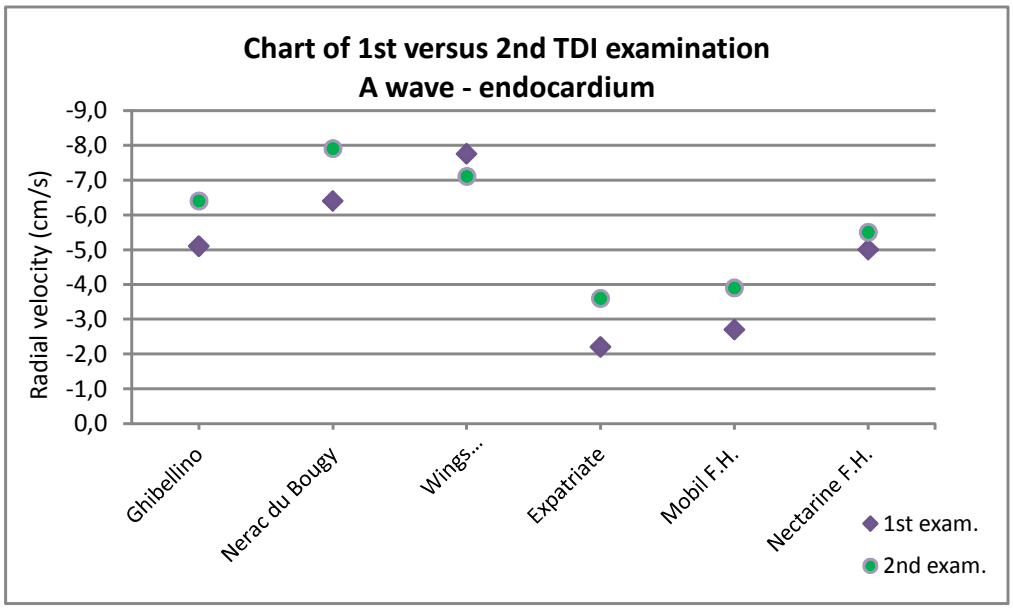


Conclusion: As the p-value >> α = 0.05 the null-hypothesis was accepted.
There is with 95% certainty no significant difference between examination 1 and 2.
The Pearson correlation coefficient was 0.9275 indicating a significant and strong positive correlation between examination 1 and 2.

## 1st versus 2nd examination - A wave epicardium

| Horse | 1st exam. | 2nd exam. |
|---|---|---|
| Ghibellino | -0.9 | -1.9 |
| Nerac du Bougy | -5.6 | -6.3 |
| Wings Summerland | -3.0 | -2.2 |
| Expatriate | -1.4 | -1.5 |
| Mobil F.H. | -2.0 | -2.1 |
| Nectarine F.H. | -4.4 | -4.0 |

**t-Test: Paired Two Sample for Means (two sided)**

| | *1st exam.* | *2nd exam.* |
|---|---|---|
| Mean | -2.9 | -3.0 |
| Variance | 3.3 | 3.4 |
| Observations | 6 | 6 |
| Pearson Correlation | **0.9333** | |
| Hypothesized Mean Difference | 0 | |
| df | 5 | |
| t Stat | 0.428072509 | |
| P(T<=t) two-tail | **0.686410644** | |
| t Critical two-tail | 2.570581835 | |

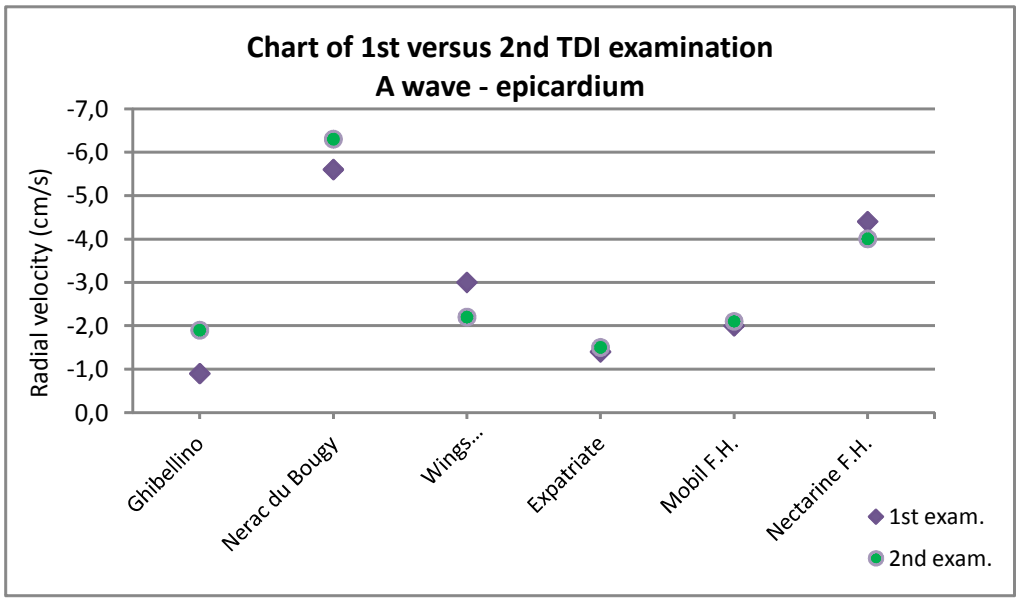


Conclusion: As the p-value >> α = 0.05 the null-hypothesis was accepted.
There is with 95% certainty no significant difference between examination 1 and 2.
The Pearson correlation coefficient was 0.9333 indicating a significant and strong positive correlation between examination 1 and 2.

## Paired Students t-test (two-sided) of 1st versus 2nd off-line analysis

A paired t-test was used to test for a significant difference between the 1st and 2nd off-line analysis of the radial velocities by 2-D colour TDI in the left ventricular free wall of the non-athletic horses.
Level of significans = 0.05
$H_0$ hypothesis: There is no significant difference between the 1st and 2nd off-line analysis of the radial velocities by 2-D colour TDI.
Notice: that data are missing for the 2nd analysis of one horse. Therefore, this horse was not included in the paired t-test. The sample size was consequently reduced to n = 4.

The Pearson correlation coefficient was calculated as a measure of the correlation between off-line analysis 1 and 2. This statistical measure obtains values from -1 to 1.
0 indicates no correlation a all, while a value close to -1 or 1 indicates a strong negative or positive correlation, respectively. The Pearson correlation coefficient should be interpreted with cauton at small sample sizes. The critical value for n = 4, α = 0.05, two-sided test is ±0.9500

## 1st versus 2nd off-line analysis - S wave endocardium

| Horse | 1st analysis | 2nd analysis |
|---|---|---|
| Naomi | 10.5 | 10.4 |
| Bella | 6.7 | 7.7 |
| Mary | 7.3 | 7.7 |
| Bianca | 8.2 | |
| Alba | 8.6 | 8.6 |

**t-Test: Paired Two Sample for Means (two sided)**

| | *1st analysis* | *2nd analysis* |
|---|---|---|
| Mean | 8.3 | 8.6 |
| Variance | 2.8 | 1.6 |
| Observations | 4 | 4 |
| Pearson Correlation | **0.9809** | |
| Hypothesized Mean Difference | 0 | |
| df | 3 | |
| t Stat | -1.302172098 | |
| P(T<=t) two-tail | **0.283814975** | |
| t Critical two-tail | 3.182446305 | |

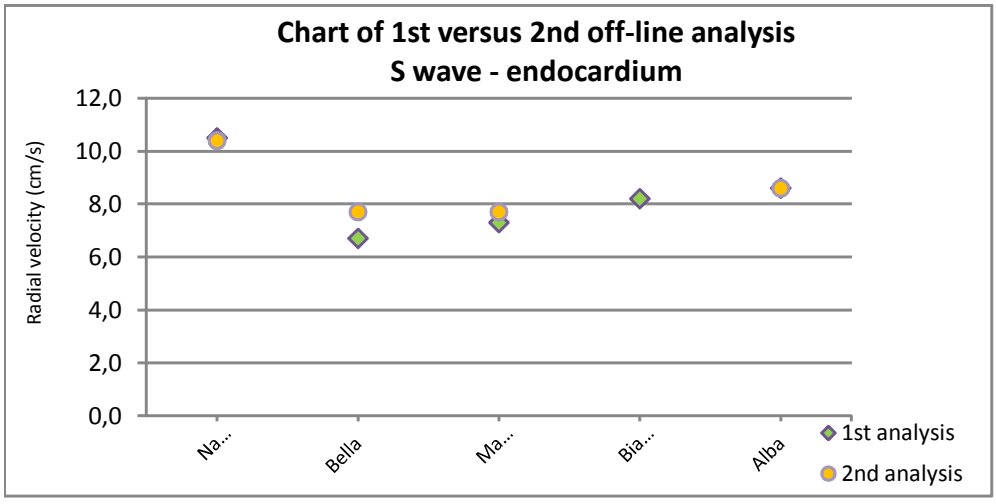


Conclusion: As the p-value > α = 0.05 the null-hypothesis was accepted.
There is with 95% certainty no significant difference between off-line analysis 1 and 2.
The Pearson correlation coefficient was 0.9809 indicating a significant and strong positive correlation between off-line analysis 1 and 2.

## 1st versus 2nd off-line analysis - S wave epicardium

| Horse | 1st analysis | 2nd analysis |
|---|---|---|
| Naomi | 8.0 | 7.4 |
| Bella | 5.4 | 6.0 |
| Mary | 5.5 | 5.8 |
| Bianca | 6.1 | |
| Alba | 7.3 | 6.8 |

**t-Test: Paired Two Sample for Means (two sided)**

| | *1st analysis* | *2nd analysis* |
|---|---|---|
| Mean | 6.5 | 6.5 |
| Variance | 1.7 | 0.6 |
| Observations | 4 | 4 |
| Pearson Correlation | **0.9810** | |
| Hypothesized Mean Difference | 0 | |
| df | 3 | |
| t Stat | 0.179592166 | |
| P(T<=t) two-tail | **0.868918038** | |
| t Critical two-tail | 3.182446305 | |

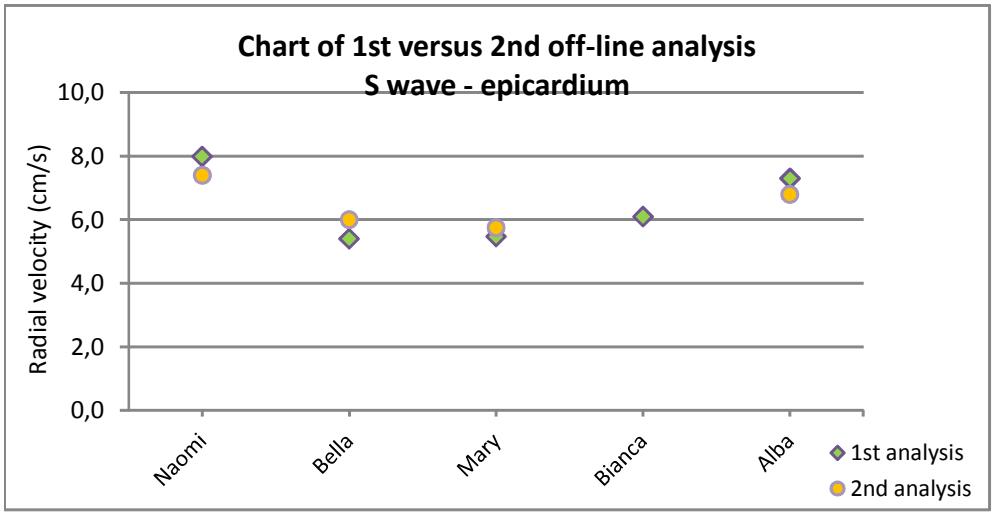


Conclusion: As the p-value >> α = 0.05 the null-hypothesis was accepted.
There is with 95% certainty no significant difference between off-line analysis 1 and 2.
The Pearson correlation coefficient was 0.9810 indicating a significant and strong positive correlation between off-line analysis 1 and 2.

## 1st versus 2nd off-line analysis - E wave endocardium

| Horse | 1st analysis | 2nd analysis |
|---|---|---|
| Naomi | -21.5 | -20.8 |
| Bella | -28.0 | -25.4 |
| Mary | -20.3 | -21.7 |
| Bianca | -14.3 | |
| Alba | -16.4 | -16.5 |

**t-Test: Paired Two Sample for Means (two sided)**

| | *1st analysis* | *2nd analysis* |
|---|---|---|
| Mean | -21.6 | -21.1 |
| Variance | 23.2 | 13.4 |
| Observations | 4 | 4 |
| Pearson Correlation | **0.9589** | |
| Hypothesized Mean Difference | 0 | |
| df | 3 | |
| t Stat | -0.537533009 | |
| P(T<=t) two-tail | **0.628213738** | |
| t Critical two-tail | 3.182446305 | |

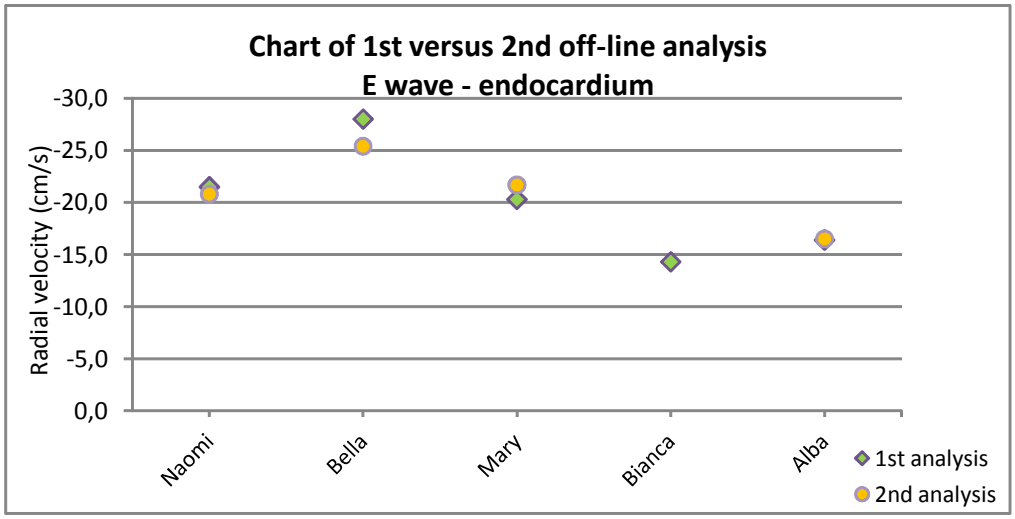


Conclusion: As the p-value >> α = 0.05 the null-hypothesis was accepted.
There is with 95% certainty no significant difference between off-line analysis 1 and 2.
The Pearson correlation coefficient was 0.9589 indicating a significant and strong positive correlation between off-line analysis 1 and 2.

## 1st versus 2nd off-line analysis - E wave epicardium

| Horse | 1st analysis | 2nd analysis |
|---|---|---|
| Naomi | -15.7 | -16.0 |
| Bella | -19.2 | -18.1 |
| Mary | -15.5 | -14.8 |
| Bianca | -12.0 | |
| Alba | -12.3 | -11.9 |

**t-Test: Paired Two Sample for Means (two sided)**

| | *1st analysis* | *2nd analysis* |
|---|---|---|
| Mean | -15.7 | -15.2 |
| Variance | 7.9 | 6.7 |
| Observations | 4 | 4 |
| Pearson Correlation | **0.9802** | |
| Hypothesized Mean Difference | 0 | |
| df | 3 | |
| t Stat | -1.611855298 | |
| P(T<=t) two-tail | **0.205384799** | |
| t Critical two-tail | 3.182446305 | |

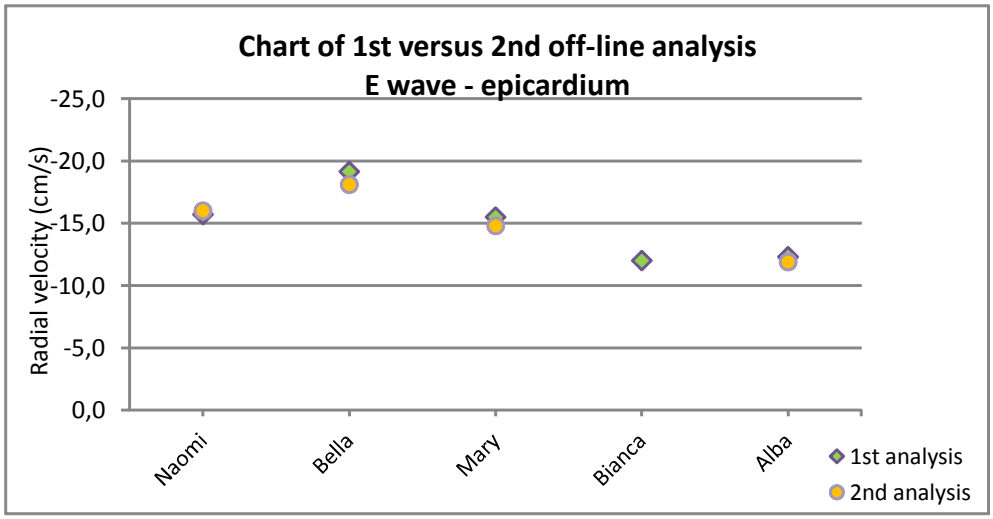


Conclusion: As the p-value > α = 0.05 the null-hypothesis was accepted.
There is with 95% certainty no significant difference between off-line analysis 1 and 2.
The Pearson correlation coefficient was 0.9802 indicating a significant and strong positive correlation between off-line analysis 1 and 2.

## 1st versus 2nd off-line analysis - A wave endocardium

| Horse | 1st analysis | 2nd analysis |
|---|---|---|
| Naomi | -10.8 | -11.0 |
| Bella | -6.0 | -6.7 |
| Mary | -8.5 | -6.9 |
| Bianca | -7.5 | |
| Alba | -13.1 | -13.4 |

**t-Test: Paired Two Sample for Means (two sided)**

| | *1st analysis* | *2nd analysis* |
|---|---|---|
| Mean | -9.6 | -9.5 |
| Variance | 9.4 | 10.7 |
| Observations | 4 | 4 |
| Pearson Correlation | **0.9513** | |
| Hypothesized Mean Difference | 0 | |
| df | 3 | |
| t Stat | -0.168515182 | |
| P(T<=t) two-tail | **0.876898739** | |
| t Critical two-tail | 3.182446305 | |

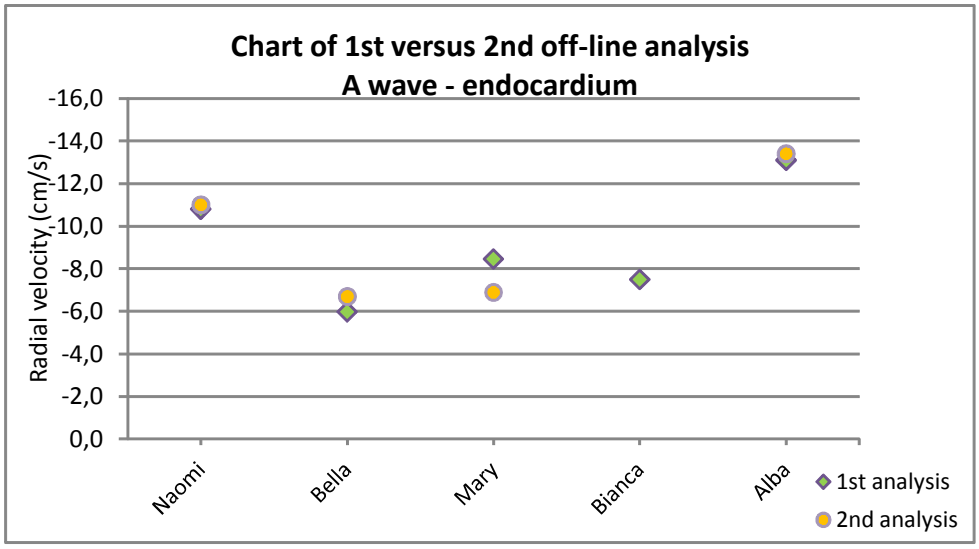


Conclusion: As the p-value >> α = 0.05 the null-hypothesis was accepted.
There is with 95% certainty no significant difference between off-line analysis 1 and 2.
The Pearson correlation coefficient was 0.9513 indicating a significant and strong positive correlation between off-line analysis 1 and 2.

## 1st versus 2nd off-line analysis - A wave epicardium

| Horse | 1st analysis | 2nd analysis |
|---|---|---|
| Naomi | -9.9 | -9.9 |
| Bella | -6.0 | -6.2 |
| Mary | -6.8 | -5.5 |
| Bianca | -6.2 | |
| Alba | -11.4 | -11.2 |

**t-Test: Paired Two Sample for Means (two sided)**

| | *1st analysis* | *2nd analysis* |
|---|---|---|
| Mean | -8.5 | -8.2 |
| Variance | 6.5 | 7.7 |
| Observations | 4 | 4 |
| Pearson Correlation | **0.9723** | |
| Hypothesized Mean Difference | 0 | |
| df | 3 | |
| t Stat | -0.989455949 | |
| P(T<=t) two-tail | **0.395385174** | |
| t Critical two-tail | 3.182446305 | |

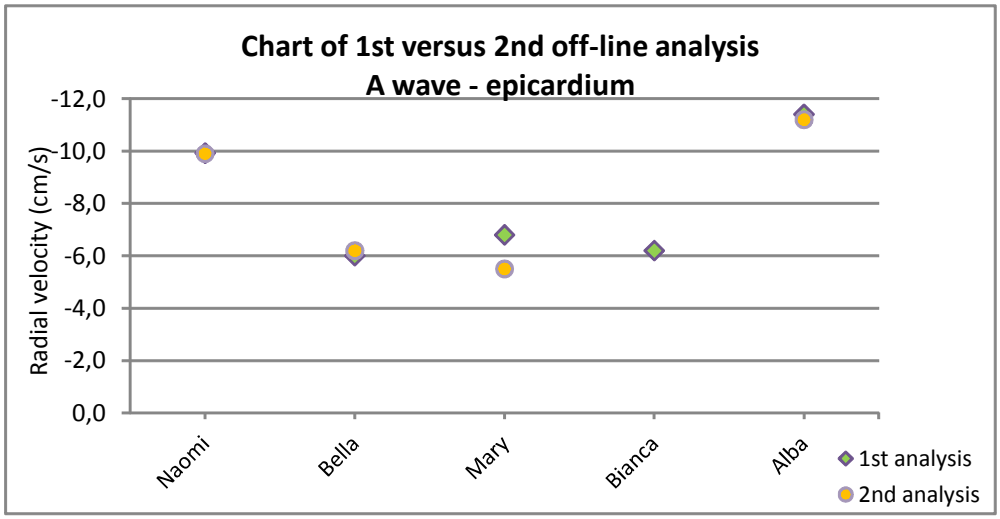


Conclusion: As the p-value >> α = 0.05 the null-hypothesis was accepted.
There is with 95% certainty no significant difference between off-line analysis 1 and 2.
The Pearson correlation coefficient was 0.9723 indicating a significant and strong positive correlation between off-line analysis 1 and 2.

# APPENDIX 9 – CALCULATIONS FOR PROTOCOL 2

## Paired Students t-test (one-sided) to detect radial velocity gradient

A paired t-test was used to test for a significant difference between the endocardial and epicardial radial velocities obtained by 2-D colour TDI in the left ventricular free wall.
The difference d was defined as the endocardial minus the epicardial velocities.
A level of significance of 0.05 was used.

$H_0$ hypothesis: There is no significant difference between the endocardial and epicardial radial velocities in the left ventricular free wall. $\bar{d} = 0$

$H_A$ hypothesis: The radial velocities are greater in the endocardium than in the epicardium. $\bar{d} > 0$

**Parameter:** **Peak systolic radial velocity (S wave)**

| Endocardium | Epicardium | Difference |
|---|---|---|
| 10.0 | 6.1 | 3.9 |
| 7.0 | 5.4 | 1.6 |
| 9.3 | 5.0 | 4.3 |
| 6.9 | 4.8 | 2.1 |
| 9.7 | 6.0 | 3.7 |
| 6.9 | 5.3 | 1.7 |
| 10.5 | 8.0 | 2.5 |
| 6.7 | 5.4 | 1.3 |
| 7.3 | 5.5 | 1.8 |
| 8.2 | 6.1 | 2.1 |
| 8.6 | 7.3 | 1.3 |

**t-Test: Paired Two Sample for Means**

| | *Endocardium* | *Epicardium* |
|---|---|---|
| Mean | 8.3 | 5.9 |
| Variance | 2.0 | 1.0 |
| Observations | 11 | 11 |
| Pearson Correlation | 0.6535 | |
| Hypothesized Mean Difference | 0 | |
| df | 10 | |
| t Stat | 7.430810334 | |
| P(T<=t) one-tail | **1.117E-05** | |
| t Critical one-tail | 1.812461102 | |

Conclusion: As the p-value << $\alpha = 0.05$ the null-hypothesis is rejected.
The peak systolic radial velocity is significantly greater in the endocardium than the epicardium proving the presence of a radial velocity gradient.

## Parameter: Early diastolic radial velocity (E wave)

| Endocardium | Epicardium | Difference |
|---|---|---|
| -27.0 | -12.3 | -14.7 |
| -16.6 | -9.4 | -7.2 |
| -29.1 | -16.3 | -12.8 |
| -20.5 | -14.0 | -6.5 |
| -34.4 | -17.6 | -16.8 |
| -17.4 | -12.5 | -4.9 |
| -21.5 | -15.7 | -5.8 |
| -28.0 | -19.2 | -8.8 |
| -20.3 | -15.5 | -4.8 |
| -14.3 | -12.0 | -2.3 |
| -16.4 | -12.3 | -4.1 |

**t-Test: Paired Two Sample for Means**

| | *Endocardium* | *Epicardium* |
|---|---|---|
| Mean | -22.3 | -14.3 |
| Variance | 41.0 | 8.2 |
| Observations | 11 | 11 |
| Pearson Correlation | 0.7385 | |
| Hypothesized Mean Difference | 0 | |
| df | 10 | |
| t Stat | -5.684095516 | |
| P(T<=t) one-tail | **0.000101347** | |
| t Critical one-tail | 1.812461102 | |

Conclusion: As the p-value << α = 0.05 the null-hypothesis is rejected.
The early diastolic radial velocity is significantly greater in the endocardium than the epicardium proving the presence of a radial velocity gradient.

## Parameter: Late diastolic radial velocity (A wave)

| Endocardium | Epicardium | Difference |
|---|---|---|
| -5.1 | -0.9 | -4.2 |
| -6.4 | -5.6 | -0.8 |
| -7.8 | -3.0 | -4.8 |
| -2.2 | -1.4 | -0.8 |
| -2.7 | -2.0 | -0.7 |
| -5.0 | -4.4 | -0.6 |
| -10.8 | -9.9 | -0.9 |
| -6.0 | -6.0 | 0.0 |
| -8.5 | -6.8 | -1.7 |
| -7.5 | -6.2 | -1.3 |
| -13.1 | -11.4 | -1.7 |

**t-Test: Paired Two Sample for Means**

| | *Endocardium* | *Epicardium* |
|---|---|---|
| Mean | -6.8 | -5.2 |
| Variance | 10.5 | 11.4 |
| Observations | 11 | 11 |
| Pearson Correlation | 0.8950 | |
| Hypothesized Mean Difference | 0 | |
| df | 10 | |
| t Stat | -3.447105802 | |
| P(T<=t) one-tail | **0.003128224** | |
| t Critical one-tail | 1.812461102 | |

Conclusion: As the p-value << α = 0.05 the null-hypothesis is rejected.
The late diastolic radial velocity is significantly greater in the endocardium than the epicardium proving the presence of a radial velocity gradient.

# T-test for differnces between the athletic and non-athletic horses

**t-test: Two samples assuming equal variances (two sided):**

A two-sided t-test was used to test for a significant difference between the means of the echocardiographic parameters obtained by 2-D colour TDI and speckle tracking in the two groups of athletic and non-athletic horses under the assumption that there is the same variance in both groups. A level of significance of 0.05 was used.

$H_0$ hypothesis: There is no significant difference between the means of the individual parameters measured in the athletic group of horses and in the non-athletic group of horses.

**Sample size to estimate a difference between means (two sided):**

The required sample size (pr. group) (n) in order to detect a significant difference in the echocardiographic parameters obtained by 2-D coulor TDI and speckle tracking in the athletic and the non-athletic horses, can be calculated still under the assumption that the standard deviation is identical in the two groups. To perform the calculations an estimate of both the difference in the means and the common standard deviation for the two groups is needed. (The group means and common variance is given with the t-test output).
A significance level of $\alpha = 0.05$ and power of 80% will be used.

The equation for a two-sided test:

$$n = \frac{2(Z_\beta + Z_{1-\alpha/2})^2 \times \sigma^2}{d^2}$$

**Minimum detectable difference**

When a limited sample size is available - like in this thesis - the minimum detectable difference ($\delta$) for the echocardiographic parameters obtained by 2-D colour TDI and speckle tracking can be derived from the equations for the required sample sizes.

The equation for a two-sided test:

$$\delta = \sqrt{\frac{2}{n}} \cdot (Z_\beta + Z_{1-\alpha/2}) \cdot \sigma$$

## Parameter: Peak systolic radial velocity (S wave) in the endocardium

| Athletic | Non-athletic |
|---|---|
| 10.0 | 10.5 |
| 7.0 | 6.7 |
| 9.3 | 7.3 |
| 6.9 | 8.2 |
| 9.7 | 8.6 |
| 6.9 | |

**t-test: Two samples assuming equal variances (two sided)**

| | *Athletic* | *Non-athletic* |
|---|---|---|
| Mean | 8.29 | 8.26 |
| Variance | 2.24 | 2.12 |
| Observations | 6 | 5 |
| Pooled Variance | 2.19 | |
| Hypothesized Mean Difference | 0 | |
| df | 9 | |
| t Stat | 0.02975462 | |
| P(T<=t) one-tail | 0.488456061 | |
| t Critical one-tail | 1.833112923 | |
| P(T<=t) two-tail | **0.976912122** | |
| t Critical two-tail | 2.262157158 | |

Conclusion: As the p-value > α = 0.05 the null-hypothesis is accepted.
There is with 95% certainty no significant difference between the two groups.

**Sample size to estimate a difference between means (two-sided test)**

| | |
|---|---|
| Mean in group 1 | 8.29 |
| Mean in group 2 | 8.26 |
| Difference | 0.03 |
| Common Standard deviation (SD) | 1.4 |
| Confidence level (1-alpha/2) | 0.95 |
| Z(1-alpha/2) | 1.96 |
| Power (1-beta) | 0.8 |
| Z(beta) | 0.84 |
| Required Sample size (per group) (n) | 34186.23 |
| Rounded Sample size (per group) (n) | **34187** |

**Minimum detectable difference (two-sided test)**

| | |
|---|---|
| Sample size (n) | 5 |
| Common Standard deviation (SD) | 1.4 |
| Confidence level (1-alpha/2) | 0.95 |
| Z(1-alpha/2) | 1.96 |
| Power (1-beta) | 0.8 |
| Z(beta) | 0.84 |
| Minimum detectable difference (d) | **2.5** |

## Parameter: Peak systolic radial velocity (S wave) in the epicardium

| Athletic | Non-athletic |
|---|---|
| 6.1 | 8.0 |
| 5.4 | 5.4 |
| 5.0 | 5.5 |
| 4.8 | 6.1 |
| 6.0 | 7.3 |
| 5.3 | |

**t-test: Two samples assuming equal variances (two sided)**

| | *Athletic* | *Non-athletic* |
|---|---|---|
| Mean | 5.4 | 6.5 |
| Variance | 0.3 | 1.3 |
| Observations | 6 | 5 |
| Pooled Variance | 0.7 | |
| Hypothesized Mean Difference | 0 | |
| df | 9 | |
| t Stat | -1.97685834 | |
| P(T<=t) one-tail | 0.039730207 | |
| t Critical one-tail | 1.833112923 | |
| P(T<=t) two-tail | **0.079460415** | |
| t Critical two-tail | 2.262157158 | |

Conclusion: As the p-value > α = 0.05 the null-hypothesis is accepted.
There is with 95% certainty no significant difference between the two groups.

**Sample size to estimate a difference between means (two-sided test)**

| | |
|---|---|
| Mean in group 1 | 5.4 |
| Mean in group 2 | 6.5 |
| Difference | 1.1 |
| Common Standard deviation (SD) | 1.0 |
| Confidence level (1-alpha/2) | 0.95 |
| Z(1-alpha/2) | 1.96 |
| Power (1-beta) | 0.8 |
| Z(beta) | 0.84 |
| Required Sample size (per group) (n) | 12.97 |
| Rounded Sample size (per group) (n) | **13** |

**Minimum detectable difference (two-sided test)**

| | |
|---|---|
| Sample size (n) | 5 |
| Common Standard deviation (SD) | 1.0 |
| Confidence level (1-alpha/2) | 0.95 |
| Z(1-alpha/2) | 1.96 |
| Power (1-beta) | 0.8 |
| Z(beta) | 0.84 |
| Minimum detectable difference (d) | **1.8** |

## Parameter: Early diastolic radial velocity (E wave) in the endocardium

| Athletic | Non-athletic |
|---|---|
| -27.0 | -21.5 |
| -16.6 | -28.0 |
| -29.1 | -20.3 |
| -20.5 | -14.3 |
| -34.4 | -16.4 |
| -17.4 | |

**t-test: Two samples assuming equal variances (two sided)**

| | *Athletic* | *Non-athletic* |
|---|---|---|
| Mean | -24.2 | -20.1 |
| Variance | 50.7 | 27.9 |
| Observations | 6 | 5 |
| Pooled Variance | 40.6 | |
| Hypothesized Mean Difference | 0 | |
| df | 9 | |
| t Stat | -1.054123156 | |
| P(T<=t) one-tail | 0.159651153 | |
| t Critical one-tail | 1.833112923 | |
| P(T<=t) two-tail | **0.319302306** | |
| t Critical two-tail | 2.262157158 | |

Conclusion: As the p-value > α = 0.05 the null-hypothesis is accepted.
There is with 95% certainty no significant difference between the two groups.

**Sample size to estimate a difference between means (two-sided test)**

| | |
|---|---|
| Mean in group 1 | -24.2 |
| Mean in group 2 | -20.1 |
| Difference | 4.1 |
| Common Standard deviation (SD) | 6.4 |
| Confidence level (1-alpha/2) | 0.95 |
| Z(1-alpha/2) | 1.96 |
| Power (1-beta) | 0.8 |
| Z(beta) | 0.84 |
| Required Sample size (per group) (n) | 38.25 |
| Rounded Sample size (per group) (n) | **39** |

**Minimum detectable difference (two-sided test)**

| | |
|---|---|
| Sample size (n) | 5 |
| Common Standard deviation (SD) | 6.4 |
| Confidence level (1-alpha/2) | 0.95 |
| Z(1-alpha/2) | 1.96 |
| Power (1-beta) | 0.8 |
| Z(beta) | 0.84 |
| Minimum detectable difference (d) | **11.3** |

## Parameter: Early diastolic radial velocity (E wave) in the epicardium

| Athletic | Non-athletic |
|---|---|
| -12.3 | -15.7 |
| -9.4 | -19.2 |
| -16.3 | -15.5 |
| -14.0 | -12.0 |
| -17.6 | -12.3 |
| -12.5 | |

**t-test: Two samples assuming equal variances (two sided)**

| | *Athletic* | *Non-athletic* |
|---|---|---|
| Mean | -13.7 | -14.9 |
| Variance | 8.7 | 8.6 |
| Observations | 6 | 5 |
| Pooled Variance | 8.7 | |
| Hypothesized Mean Difference | 0 | |
| df | 9 | |
| t Stat | 0.697082392 | |
| P(T<=t) one-tail | 0.251678973 | |
| t Critical one-tail | 1.833112923 | |
| P(T<=t) two-tail | **0.503357945** | |
| t Critical two-tail | 2.262157158 | |

Conclusion: As the p-value > α = 0.05 the null-hypothesis is accepted.
There is with 95% certainty no significant difference between the two groups.

**Sample size to estimate a difference between means (two-sided test)**

| | |
|---|---|
| Mean in group 1 | -13.7 |
| Mean in group 2 | -14.9 |
| Difference | 1.2 |
| Common Standard deviation (SD) | 2.9 |
| Confidence level (1-alpha/2) | 0.95 |
| Z(1-alpha/2) | 1.96 |
| Power (1-beta) | 0.8 |
| Z(beta) | 0.84 |
| Required Sample size (per group) (n) | 91.68 |
| Rounded Sample size (per group) (n) | **92** |

**Minimum detectable difference (two-sided test)**

| | |
|---|---|
| Sample size (n) | 5 |
| Common Standard deviation (SD) | 2.9 |
| Confidence level (1-alpha/2) | 0.95 |
| Z(1-alpha/2) | 1.96 |
| Power (1-beta) | 0.8 |
| Z(beta) | 0.84 |
| Minimum detectable difference (d) | **5.1** |

## Parameter: Late diastolic radial velocity (A wave) in the endocardium

| Athletic | Non-athletic |
|---|---|
| -5.1 | -10.8 |
| -6.4 | -6.0 |
| -7.8 | -8.5 |
| -2.2 | -7.5 |
| -2.7 | -13.1 |
| -5.0 | |

**t-test: Two samples assuming equal variances (two sided)**

| | *Athletic* | *Non-athletic* |
|---|---|---|
| Mean | -4.9 | -9.2 |
| Variance | 4.5 | 7.9 |
| Observations | 6 | 5 |
| Pooled Variance | 6.0 | |
| Hypothesized Mean Difference | 0 | |
| df | 9 | |
| t Stat | 2.888639944 | |
| P(T<=t) one-tail | 0.008961967 | |
| t Critical one-tail | 1.833112923 | |
| P(T<=t) two-tail | **0.017923934** | |
| t Critical two-tail | 2.262157158 | |

Conclusion: As the p-value < α = 0.05 the null-hypothesis is rejected.
The endocardial A wave is with 95% certainty significantly greater in the non-athletic group.

**Sample size to estimate a difference between means (two-sided test)**

| | |
|---|---|
| Mean in group 1 | -4.9 |
| Mean in group 2 | -9.2 |
| Difference | 4.3 |
| Common Standard deviation (SD) | 3.2 |
| Confidence level (1-alpha/2) | 0.95 |
| Z(1-alpha/2) | 1.96 |
| Power (1-beta) | 0.8 |
| Z(beta) | 0.84 |
| Required Sample size (per group) (n) | 8.69 |
| Rounded Sample size (per group) (n) | **9** |

**Minimum detectable difference (two-sided test)**

| | |
|---|---|
| Sample size (n) | 5 |
| Common Standard deviation (SD) | 3.2 |
| Confidence level (1-alpha/2) | 0.95 |
| Z(1-alpha/2) | 1.96 |
| Power (1-beta) | 0.8 |
| Z(beta) | 0.84 |
| Minimum detectable difference (d) | **5.7** |

## Parameter: Late diastolic radial velocity (A wave) in the epicardium

| Athletic | Non-athletic |
|---|---|
| -0.9 | -9.9 |
| -5.6 | -6.0 |
| -3.0 | -6.8 |
| -1.4 | -6.2 |
| -2.0 | -11.4 |
| -4.4 | |

**t-test: Two samples assuming equal variances (two sided)**

| | *Athletic* | *Non-athletic* |
|---|---|---|
| Mean | -2.9 | -8.1 |
| Variance | 3.3 | 6.0 |
| Observations | 6 | 5 |
| Pooled Variance | 4.5 | |
| Hypothesized Mean Difference | 0 | |
| df | 9 | |
| t Stat | 4.018754672 | |
| P(T<=t) one-tail | 0.001511863 | |
| t Critical one-tail | 1.833112923 | |
| P(T<=t) two-tail | **0.003023727** | |
| t Critical two-tail | 2.262157158 | |

Conclusion: As the p-value < α = 0.05 the null-hypothesis is rejected.
The epicardial A wave is with 95% certainty significantly greater in the non-athletic group.

**Sample size to estimate a difference between means (two-sided test)**

| | |
|---|---|
| Mean in group 1 | -2.9 |
| Mean in group 2 | -8.1 |
| Difference | 5.2 |
| Common Standard deviation (SD) | 3.4 |
| Confidence level (1-alpha/2) | 0.95 |
| Z(1-alpha/2) | 1.96 |
| Power (1-beta) | 0.8 |
| Z(beta) | 0.84 |
| Required Sample size (per group) (n) | 6.71 |
| Rounded Sample size (per group) (n) | **7** |

**Minimum detectable difference (two-sided test)**

| | |
|---|---|
| Sample size (n) | 5 |
| Common Standard deviation (SD) | 3.4 |
| Confidence level (1-alpha/2) | 0.95 |
| Z(1-alpha/2) | 1.96 |
| Power (1-beta) | 0.8 |
| Z(beta) | 0.84 |
| Minimum detectable difference (d) | **6.0** |

## Parameter: Radial velocity gradient in systole (S wave)

| Athletic | Non-athletic |
|---|---|
| 3.9 | 2.5 |
| 1.6 | 1.3 |
| 4.3 | 1.8 |
| 2.1 | 2.1 |
| 3.7 | 1.3 |
| 1.7 | |

**t-test: Two samples assuming equal variances (two sided)**

| | *Athletic* | *Non-athletic* |
|---|---|---|
| Mean | 2.9 | 1.8 |
| Variance | 1.4 | 0.3 |
| Observations | 6 | 5 |
| Pooled Variance | 0.9 | |
| Hypothesized Mean Difference | 0 | |
| df | 9 | |
| t Stat | 1.822825084 | |
| P(T<=t) one-tail | 0.050823335 | |
| t Critical one-tail | 1.833112923 | |
| P(T<=t) two-tail | **0.101646669** | |
| t Critical two-tail | 2.262157158 | |

Conclusion: As the p-value > α = 0.05 the null-hypothesis is accepted.
There is with 95% certainty no significant difference between the two groups.

**Sample size to estimate a difference between means (two-sided test)**

| | |
|---|---|
| Mean in group 1 | 2.9 |
| Mean in group 2 | 1.8 |
| Difference | 1.1 |
| Common Standard deviation (SD) | 1.1 |
| Confidence level (1-alpha/2) | 0.95 |
| Z(1-alpha/2) | 1.96 |
| Power (1-beta) | 0.8 |
| Z(beta) | 0.84 |
| Required Sample size (per group) (n) | 15.70 |
| Rounded Sample size (per group) (n) | **16** |

**Minimum detectable difference (two-sided test)**

| | |
|---|---|
| Sample size (n) | 5 |
| Common Standard deviation (SD) | 1.1 |
| Confidence level (1-alpha/2) | 0.95 |
| Z(1-alpha/2) | 1.96 |
| Power (1-beta) | 0.8 |
| Z(beta) | 0.84 |
| Minimum detectable difference (d) | **1.9** |

## Parameter: Radial velocity gradient in early diastole (E wave)

| Athletic | Non-athletic |
|---|---|
| 14.7 | 5.8 |
| 7.2 | 8.8 |
| 12.8 | 4.8 |
| 6.5 | 2.3 |
| 16.8 | 4.1 |
| 4.9 | |

**t-test: Two samples assuming equal variances (two sided)**

| | *Athletic* | *Non-athletic* |
|---|---|---|
| Mean | 10.5 | 5.2 |
| Variance | 24.2 | 5.8 |
| Observations | 6 | 5 |
| Pooled Variance | 16.1 | |
| Hypothesized Mean Difference | 0 | |
| df | 9 | |
| t Stat | 2.187821107 | |
| P(T<=t) one-tail | 0.028225192 | |
| t Critical one-tail | 1.833112923 | |
| P(T<=t) two-tail | **0.056450383** | |
| t Critical two-tail | 2.262157158 | |

Conclusion: As the p-value > α = 0.05 the null-hypothesis is accepted.
There is with 95% certainty no significant difference between the two groups.

**Sample size to estimate a difference between means (two-sided test)**

| | |
|---|---|
| Mean in group 1 | 10.5 |
| Mean in group 2 | 5.2 |
| Difference | 5.3 |
| Common Standard deviation (SD) | 4.7 |
| Confidence level (1-alpha/2) | 0.95 |
| Z(1-alpha/2) | 1.96 |
| Power (1-beta) | 0.8 |
| Z(beta) | 0.84 |
| Required Sample size (per group) (n) | 12.34 |
| Rounded Sample size (per group) (n) | **13** |

**Minimum detectable difference (two-sided test)**

| | |
|---|---|
| Sample size (n) | 5 |
| Common Standard deviation (SD) | 4.7 |
| Confidence level (1-alpha/2) | 0.95 |
| Z(1-alpha/2) | 1.96 |
| Power (1-beta) | 0.8 |
| Z(beta) | 0.84 |
| Minimum detectable difference (d) | **8.3** |

## Parameter: Radial velocity gradient in late diastole (A wave)

| Athletic | Non-athletic |
|---|---|
| 4.2 | 0.9 |
| 0.8 | 0.0 |
| 4.8 | 1.7 |
| 0.8 | 1.3 |
| 0.7 | 1.7 |
| 0.6 | |

**t-test: Two samples assuming equal variances (two sided)**

| | *Athletic* | *Non-athletic* |
|---|---|---|
| Mean | 2.0 | 1.1 |
| Variance | 3.8 | 0.5 |
| Observations | 6 | 5 |
| Pooled Variance | 2.3 | |
| Hypothesized Mean Difference | 0 | |
| df | 9 | |
| t Stat | 0.945695716 | |
| P(T<=t) one-tail | 0.184499887 | |
| t Critical one-tail | 1.833112923 | |
| P(T<=t) two-tail | **0.368999774** | |
| t Critical two-tail | 2.262157158 | |

Conclusion: As the p-value > α = 0.05 the null-hypothesis is accepted.
There is with 95% certainty no significant difference between the two groups.

**Sample size to estimate a difference between means (two-sided test)**

| | |
|---|---|
| Mean in group 1 | 2 |
| Mean in group 2 | 1.10 |
| Difference | 0.9 |
| Common Standard deviation (SD) | 1.5 |
| Confidence level (1-alpha/2) | 0.95 |
| Z(1-alpha/2) | 1.96 |
| Power (1-beta) | 0.8 |
| Z(beta) | 0.84 |
| Required Sample size (per group) (n) | 43.60 |
| Rounded Sample size (per group) (n) | **44** |

**Minimum detectable difference (two-sided test)**

| | |
|---|---|
| Sample size (n) | 5 |
| Common Standard deviation (SD) | 1.5 |
| Confidence level (1-alpha/2) | 0.95 |
| Z(1-alpha/2) | 1.96 |
| Power (1-beta) | 0.8 |
| Z(beta) | 0.84 |
| Minimum detectable difference (d) | **2.7** |

## Parameter: Peak systolic radial strain by TDI

| Athletic | Non-athletic |
|---|---|
| 86.0 | 0.4 |
| 44.3 | 27.7 |
| 122.0 | 42.9 |
| 35.6 | 61.1 |
| 55.0 | 44.3 |
| 49.0 | |

**t-test: Two samples assuming equal variances (two sided)**

| | *Athletic* | *Non-athletic* |
|---|---|---|
| Mean | 65.3 | 35.3 |
| Variance | 1067.4 | 520.2 |
| Observations | 6 | 5 |
| Pooled Variance | 824.2 | |
| Hypothesized Mean Difference | 0 | |
| df | 9 | |
| t Stat | 1.7277792 | |
| P(T<=t) one-tail | 0.059047956 | |
| t Critical one-tail | 1.833112923 | |
| P(T<=t) two-tail | **0.118095912** | |
| t Critical two-tail | 2.262157158 | |

Conclusion: As the p-value > α = 0.05 the null-hypothesis is accepted.
There is with 95% certainty no significant difference between the two groups.

**Sample size to estimate a difference between means (two-sided test)**

| | |
|---|---|
| Mean in group 1 | 65.3 |
| Mean in group 2 | 35.3 |
| Difference | 30 |
| Common Standard deviation (SD) | 31.4 |
| Confidence level (1-alpha/2) | 0.95 |
| Z(1-alpha/2) | 1.96 |
| Power (1-beta) | 0.8 |
| Z(beta) | 0.84 |
| Required Sample size (per group) (n) | 17.20 |
| Rounded Sample size (per group) (n) | **18** |

**Minimum detectable difference (two-sided test)**

| | |
|---|---|
| Sample size (n) | 5 |
| Common Standard deviation (SD) | 31.4 |
| Confidence level (1-alpha/2) | 0.95 |
| Z(1-alpha/2) | 1.96 |
| Power (1-beta) | 0.8 |
| Z(beta) | 0.84 |
| Minimum detectable difference (d) | **55.6** |

## Parameter: Peak systolic radial strain by TDI (without outliers)

| Athletic | Non-athletic |
|---|---|
| 86.0 | 27.7 |
| 44.3 | 42.9 |
| 35.6 | 61.1 |
| 55.0 | 44.3 |
| 49.0 | |

**t-test: Two samples assuming equal variances (two sided)**

| | *Athletic* | *Non-athletic* |
|---|---|---|
| Mean | 54.0 | 44.0 |
| Variance | 370.5 | 186.5 |
| Observations | 5 | 4 |
| Pooled Variance | 291.6 | |
| Hypothesized Mean Difference | 0 | |
| df | 7 | |
| t Stat | 0.8710333 | |
| P(T<=t) one-tail | 0.206304653 | |
| t Critical one-tail | 1.894578604 | |
| P(T<=t) two-tail | **0.412609307** | |
| t Critical two-tail | 2.364624251 | |

Conclusion: As the p-value > α = 0.05 the null-hypothesis is accepted.
There is with 95% certainty no significant difference between the two groups.

**Sample size to estimate a difference between means (two-sided test)**

| | |
|---|---|
| Mean in group 1 | 54.0 |
| Mean in group 2 | 44.0 |
| Difference | 10 |
| Common Standard deviation (SD) | 16.8 |
| Confidence level (1-alpha/2) | 0.95 |
| Z(1-alpha/2) | 1.96 |
| Power (1-beta) | 0.8 |
| Z(beta) | 0.84 |
| Required Sample size (per group) (n) | 44.31 |
| Rounded Sample size (per group) (n) | **45** |

**Minimum detectable difference (two-sided test)**

| | |
|---|---|
| Sample size (n) | 5 |
| Common Standard deviation (SD) | 16.8 |
| Confidence level (1-alpha/2) | 0.95 |
| Z(1-alpha/2) | 1.96 |
| Power (1-beta) | 0.8 |
| Z(beta) | 0.84 |
| Minimum detectable difference (d) | **29.8** |

## Parameter: Peak systolic radial strain rate (S wave) by TDI

| Athletic | Non-athletic |
|---|---|
| 2.2 | 1.7 |
| 1.5 | 1.1 |
| 1.9 | 1.2 |
| 1.3 | 2.0 |
| 2.0 | 1.5 |
| 1.4 | |

**t-test: Two samples assuming equal variances (two sided)**

| | *Athletic* | *Non-athletic* |
|---|---|---|
| Mean | 1.7 | 1.5 |
| Variance | 0.1 | 0.1 |
| Observations | 6 | 5 |
| Pooled Variance | 0.1 | |
| Hypothesized Mean Difference | 0 | |
| df | 9 | |
| t Stat | 0.975972112 | |
| P(T<=t) one-tail | 0.177289969 | |
| t Critical one-tail | 1.833112923 | |
| P(T<=t) two-tail | **0.354579937** | |
| t Critical two-tail | 2.262157158 | |

Conclusion: As the p-value > α = 0.05 the null-hypothesis is accepted.
There is with 95% certainty no significant difference between the two groups.

**Sample size to estimate a difference between means (two-sided test)**

| | |
|---|---|
| Mean in group 1 | 1.7 |
| Mean in group 2 | 1.5 |
| Difference | 0.2 |
| Common Standard deviation (SD) | 0.4 |
| Confidence level (1-alpha/2) | 0.95 |
| Z(1-alpha/2) | 1.96 |
| Power (1-beta) | 0.8 |
| Z(beta) | 0.84 |
| Required Sample size (per group) (n) | 62.79 |
| Rounded Sample size (per group) (n) | **63** |

**Minimum detectable difference (two-sided test)**

| | |
|---|---|
| Sample size (n) | 5 |
| Common Standard deviation (SD) | 0.4 |
| Confidence level (1-alpha/2) | 0.95 |
| Z(1-alpha/2) | 1.96 |
| Power (1-beta) | 0.8 |
| Z(beta) | 0.84 |
| Minimum detectable difference (d) | **0.7** |

## Parameter: Early diastolic radial strain rate (E wave) by TDI

| Athletic | Non-athletic |
|---|---|
| -8.3 | -5.6 |
| -4.0 | -4.3 |
| -5.3 | -4.0 |
| -5.3 | -4.6 |
| -5.9 | -4.0 |
| -4.1 | |

**t-test: Two samples assuming equal variances (two sided)**

| | *Athletic* | *Non-athletic* |
|---|---|---|
| Mean | -5.5 | -4.5 |
| Variance | 2.5 | 0.4 |
| Observations | 6 | 5 |
| Pooled Variance | 1.6 | |
| Hypothesized Mean Difference | 0 | |
| df | 9 | |
| t Stat | -1.299792118 | |
| P(T<=t) one-tail | 0.112987311 | |
| t Critical one-tail | 1.833112923 | |
| P(T<=t) two-tail | **0.225974622** | |
| t Critical two-tail | 2.262157158 | |

Conclusion: As the p-value > α = 0.05 the null-hypothesis is accepted.
There is with 95% certainty no significant difference between the two groups.

**Sample size to estimate a difference between means (two-sided test)**

| | |
|---|---|
| Mean in group 1 | -5.5 |
| Mean in group 2 | -4.5 |
| Difference | 1 |
| Common Standard deviation (SD) | 1.3 |
| Confidence level (1-alpha/2) | 0.95 |
| Z(1-alpha/2) | 1.96 |
| Power (1-beta) | 0.8 |
| Z(beta) | 0.84 |
| Required Sample size (per group) (n) | 26.53 |
| Rounded Sample size (per group) (n) | **27** |

**Minimum detectable difference (two-sided test)**

| | |
|---|---|
| Sample size (n) | 5 |
| Common Standard deviation (SD) | 1.3 |
| Confidence level (1-alpha/2) | 0.95 |
| Z(1-alpha/2) | 1.96 |
| Power (1-beta) | 0.8 |
| Z(beta) | 0.84 |
| Minimum detectable difference (d) | **2.3** |

## Parameter: Late diastolic radial strain rate (A wave) by TDI

| Athletic | Non-athletic |
|---|---|
| -2.8 | -1.2 |
| -1.6 | -0.6 |
| -2.0 | -0.9 |
| -0.5 | -2.8 |
| -1.5 | -1.6 |
| -1.8 | |

**t-test: Two samples assuming equal variances (two sided)**

| | *Athletic* | *Non-athletic* |
|---|---|---|
| Mean | -1.7 | -1.4 |
| Variance | 0.6 | 0.7 |
| Observations | 6 | 5 |
| Pooled Variance | 0.6 | |
| Hypothesized Mean Difference | 0 | |
| df | 9 | |
| t Stat | -0.607575085 | |
| P(T<=t) one-tail | 0.279242945 | |
| t Critical one-tail | 1.833112923 | |
| P(T<=t) two-tail | **0.558485889** | |
| t Critical two-tail | 2.262157158 | |

Conclusion: As the p-value > α = 0.05 the null-hypothesis is accepted.
There is with 95% certainty no significant difference between the two groups.

**Sample size to estimate a difference between means (two-sided test)**

| | |
|---|---|
| Mean in group 1 | -1.7 |
| Mean in group 2 | -1.4 |
| Difference | 0.3 |
| Common Standard deviation (SD) | 0.8 |
| Confidence level (1-alpha/2) | 0.95 |
| Z(1-alpha/2) | 1.96 |
| Power (1-beta) | 0.8 |
| Z(beta) | 0.84 |
| Required Sample size (per group) (n) | 111.63 |
| Rounded Sample size (per group) (n) | **112** |

**Minimum detectable difference (two-sided test)**

| | |
|---|---|
| Sample size (n) | 5 |
| Common Standard deviation (SD) | 0.8 |
| Confidence level (1-alpha/2) | 0.95 |
| Z(1-alpha/2) | 1.96 |
| Power (1-beta) | 0.8 |
| Z(beta) | 0.84 |
| Minimum detectable difference (d) | **1.4** |

## Parameter: Peak systolic radial velocity (S wave) by speckle tracking

| Athletic | Non-athletic |
|---|---|
| 6.4 | 6.4 |
| 4.2 | 6.2 |
| 5.2 | 4.5 |
| 3.5 | 6.9 |
| 4.7 | 5.6 |
| 4.0 | |

**t-test: Two samples assuming equal variances (two sided)**

| | *Athletic* | *Non-athletic* |
|---|---|---|
| Mean | 4.7 | 5.9 |
| Variance | 1.1 | 0.9 |
| Observations | 6 | 5 |
| Pooled Variance | 1.0 | |
| Hypothesized Mean Difference | 0 | |
| df | 9 | |
| t Stat | -2.09146286 | |
| P(T<=t) one-tail | 0.033013247 | |
| t Critical one-tail | 1.833112923 | |
| P(T<=t) two-tail | **0.066026493** | |
| t Critical two-tail | 2.262157158 | |

Conclusion: As the p-value > α = 0.05 the null-hypothesis is accepted.
There is with 95% certainty no significant difference between the two groups.

**Sample size to estimate a difference between means (two-sided test)**

| | |
|---|---|
| Mean in group 1 | 4.7 |
| Mean in group 2 | 5.9 |
| Difference | 1.3 |
| Common Standard deviation (SD) | 1.1 |
| Confidence level (1-alpha/2) | 0.95 |
| Z(1-alpha/2) | 1.96 |
| Power (1-beta) | 0.8 |
| Z(beta) | 0.84 |
| Required Sample size (per group) (n) | 12.16 |
| Rounded Sample size (per group) (n) | **13** |

**Minimum detectable difference (two-sided test)**

| | |
|---|---|
| Sample size (n) | 5 |
| Common Standard deviation (SD) | 1.1 |
| Confidence level (1-alpha/2) | 0.95 |
| Z(1-alpha/2) | 1.96 |
| Power (1-beta) | 0.8 |
| Z(beta) | 0.84 |
| Minimum detectable difference (d) | **1.9** |

## Parameter: Early diastolic radial velocity (E wave) by speckle tracking

| Athletic | Non-athletic |
|---|---|
| -7.6 | -10.0 |
| -3.7 | -2.7 |
| -7.0 | -4.2 |
| -3.9 | -4.1 |
| -5.9 | -3.7 |
| -3.7 | |

**t-test: Two samples assuming equal variances (two sided)**

| | *Athletic* | *Non-athletic* |
|---|---|---|
| Mean | -5.3 | -4.9 |
| Variance | 3.1 | 8.4 |
| Observations | 6 | 5 |
| Pooled Variance | 5.4 | |
| Hypothesized Mean Difference | 0 | |
| df | 9 | |
| t Stat | -0.254711314 | |
| P(T<=t) one-tail | 0.402335361 | |
| t Critical one-tail | 1.833112923 | |
| P(T<=t) two-tail | **0.804670722** | |
| t Critical two-tail | 2.262157158 | |

Conclusion: As the p-value > α = 0.05 the null-hypothesis is accepted.
There is with 95% certainty no significant difference between the two groups.

**Sample size to estimate a difference between means (two-sided test)**

| | |
|---|---|
| Mean in group 1 | -5.3 |
| Mean in group 2 | -4.9 |
| Difference | 0.4 |
| Common Standard deviation (SD) | 2.2 |
| Confidence level (1-alpha/2) | 0.95 |
| Z(1-alpha/2) | 1.96 |
| Power (1-beta) | 0.8 |
| Z(beta) | 0.84 |
| Required Sample size (per group) (n) | 474.86 |
| Rounded Sample size (per group) (n) | **475** |

**Minimum detectable difference (two-sided test)**

| | |
|---|---|
| Sample size (n) | 5 |
| Common Standard deviation (SD) | 2.2 |
| Confidence level (1-alpha/2) | 0.95 |
| Z(1-alpha/2) | 1.96 |
| Power (1-beta) | 0.8 |
| Z(beta) | 0.84 |
| Minimum detectable difference (d) | **3.9** |

## Parameter: Late diastolic radial velocity (A wave) by speckle tracking

| Athletic | Non-athletic |
|---|---|
| -2.9 | -2.5 |
| -3.2 | -0.5 |
| -3.0 | -1.6 |
| -1.8 | -2.8 |
| -2.6 | -5.2 |
| -3.0 | |

**t-test: Two samples assuming equal variances (two sided)**

| | *Athletic* | *Non-athletic* |
|---|---|---|
| Mean | -2.7 | -2.5 |
| Variance | 0.3 | 3.0 |
| Observations | 6 | 5 |
| Pooled Variance | 1.5 | |
| Hypothesized Mean Difference | 0 | |
| df | 9 | |
| t Stat | -0.29823235 | |
| P(T<=t) one-tail | 0.386148162 | |
| t Critical one-tail | 1.833112923 | |
| P(T<=t) two-tail | **0.772296323** | |
| t Critical two-tail | 2.262157158 | |

Conclusion: As the p-value > α = 0.05 the null-hypothesis is accepted.
There is with 95% certainty no significant difference between the two groups.

**Sample size to estimate a difference between means (two-sided test)**

| | |
|---|---|
| Mean in group 1 | -2.7 |
| Mean in group 2 | -2.5 |
| Difference | 0.2 |
| Common Standard deviation (SD) | 1.2 |
| Confidence level (1-alpha/2) | 0.95 |
| Z(1-alpha/2) | 1.96 |
| Power (1-beta) | 0.8 |
| Z(beta) | 0.84 |
| Required Sample size (per group) (n) | 565.12 |
| Rounded Sample size (per group) (n) | **566** |

**Minimum detectable difference (two-sided test)**

| | |
|---|---|
| Sample size (n) | 5 |
| Common Standard deviation (SD) | 1.2 |
| Confidence level (1-alpha/2) | 0.95 |
| Z(1-alpha/2) | 1.96 |
| Power (1-beta) | 0.8 |
| Z(beta) | 0.84 |
| Minimum detectable difference (d) | **2.1** |

## Parameter: Peak systolic radial strain by speckle tracking

| Athletic | Non-athletic |
|---|---|
| 61.0 | 78.0 |
| 66.0 | 92.0 |
| 61.5 | 99.0 |
| 98.7 | 68.6 |
| 72.0 | 37.0 |
| 48.9 | |

**t-test: Two samples assuming equal variances (two sided)**

| | *Athletic* | *Non-athletic* |
|---|---|---|
| Mean | 68.0 | 74.9 |
| Variance | 283.7 | 589.9 |
| Observations | 6 | 5 |
| Pooled Variance | 419.8 | |
| Hypothesized Mean Difference | 0 | |
| df | 9 | |
| t Stat | -0.555619528 | |
| P(T<=t) one-tail | 0.296006149 | |
| t Critical one-tail | 1.833112923 | |
| P(T<=t) two-tail | **0.592012298** | |
| t Critical two-tail | 2.262157158 | |

Conclusion: As the p-value > α = 0.05 the null-hypothesis is accepted.
There is with 95% certainty no significant difference between the two groups.

**Sample size to estimate a difference between means (two-sided test)**

| | |
|---|---|
| Mean in group 1 | 68.0 |
| Mean in group 2 | 74.9 |
| Difference | 6.9 |
| Common Standard deviation (SD) | 19.8 |
| Confidence level (1-alpha/2) | 0.95 |
| Z(1-alpha/2) | 1.96 |
| Power (1-beta) | 0.8 |
| Z(beta) | 0.84 |
| Required Sample size (per group) (n) | 129.26 |
| Rounded Sample size (per group) (n) | **130** |

**Minimum detectable difference (two-sided test)**

| | |
|---|---|
| Sample size (n) | 5 |
| Common Standard deviation (SD) | 19.8 |
| Confidence level (1-alpha/2) | 0.95 |
| Z(1-alpha/2) | 1.96 |
| Power (1-beta) | 0.8 |
| Z(beta) | 0.84 |
| Minimum detectable difference (d) | **35.1** |

## Parameter: Peak systolic radial strain rate (S wave) by speckle tracking

| Athletic | Non-athletic |
|---|---|
| 1.7 | 2.2 |
| 1.1 | 1.3 |
| 1.6 | 1.6 |
| 1.4 | 1.8 |
| 1.0 | 1.8 |
| 1.8 | |

**t-test: Two samples assuming equal variances (two sided)**

| | *Athletic* | *Non-athletic* |
|---|---|---|
| Mean | 1.4 | 1.7 |
| Variance | 0.1 | 0.1 |
| Observations | 6 | 5 |
| Pooled Variance | 0.1 | |
| Hypothesized Mean Difference | 0 | |
| df | 9 | |
| t Stat | -1.483699724 | |
| P(T<=t) one-tail | 0.086020566 | |
| t Critical one-tail | 1.833112923 | |
| P(T<=t) two-tail | **0.172041131** | |
| t Critical two-tail | 2.262157158 | |

Conclusion: As the p-value > α = 0.05 the null-hypothesis is accepted.
There is with 95% certainty no significant difference between the two groups.

**Sample size to estimate a difference between means (two-sided test)**

| | |
|---|---|
| Mean in group 1 | 1.4 |
| Mean in group 2 | 1.7 |
| Difference | 0.3 |
| Common Standard deviation (SD) | 0.3 |
| Confidence level (1-alpha/2) | 0.95 |
| Z(1-alpha/2) | 1.96 |
| Power (1-beta) | 0.8 |
| Z(beta) | 0.84 |
| Required Sample size (per group) (n) | 15.70 |
| Rounded Sample size (per group) (n) | **16** |

**Minimum detectable difference (two-sided test)**

| | |
|---|---|
| Sample size (n) | 5 |
| Common Standard deviation (SD) | 0.3 |
| Confidence level (1-alpha/2) | 0.95 |
| Z(1-alpha/2) | 1.96 |
| Power (1-beta) | 0.8 |
| Z(beta) | 0.84 |
| Minimum detectable difference (d) | **0.5** |

## Parameter: Early diastolic radial strain rate (E wave) by speckle tracking

| Athletic | Non-athletic |
|---|---|
| -1.4 | -2.3 |
| -1.7 | -2.7 |
| -1.8 | -1.2 |
| -1.1 | -0.4 |
| -0.8 | -1.4 |
| -1.7 | |

**t-test: Two samples assuming equal variances (two sided)**

| | *Athletic* | *Non-athletic* |
|---|---|---|
| Mean | -1.4 | -1.6 |
| Variance | 0.2 | 0.8 |
| Observations | 6 | 5 |
| Pooled Variance | 0.5 | |
| Hypothesized Mean Difference | 0 | |
| df | 9 | |
| t Stat | 0.447033013 | |
| P(T<=t) one-tail | 0.332707614 | |
| t Critical one-tail | 1.833112923 | |
| P(T<=t) two-tail | **0.665415228** | |
| t Critical two-tail | 2.262157158 | |

Conclusion: As the p-value > α = 0.05 the null-hypothesis is accepted.
There is with 95% certainty no significant difference between the two groups.

**Sample size to estimate a difference between means (two-sided test)**

| | |
|---|---|
| Mean in group 1 | -1.4 |
| Mean in group 2 | -1.6 |
| Difference | 0.2 |
| Common Standard deviation (SD) | 0.6 |
| Confidence level (1-alpha/2) | 0.95 |
| Z(1-alpha/2) | 1.96 |
| Power (1-beta) | 0.8 |
| Z(beta) | 0.84 |
| Required Sample size (per group) (n) | 141.28 |
| Rounded Sample size (per group) (n) | **142** |

**Minimum detectable difference (two-sided test)**

| | |
|---|---|
| Sample size (n) | 5 |
| Common Standard deviation (SD) | 0.6 |
| Confidence level (1-alpha/2) | 0.95 |
| Z(1-alpha/2) | 1.96 |
| Power (1-beta) | 0.8 |
| Z(beta) | 0.84 |
| Minimum detectable difference (d) | **1.1** |

## Parameter: Late diastolic radial strain rate (A wave) by speckle tracking

| Athletic | Non-athletic |
|---|---|
| -0.4 | -1.7 |
| -0.5 | -0.5 |
| -0.5 | -0.9 |
| -0.6 | -0.2 |
| -0.5 | -1.6 |
| -0.7 | |

**t-test: Two samples assuming equal variances (two sided)**

| | *Athletic* | *Non-athletic* |
|---|---|---|
| Mean | -0.5 | -1.0 |
| Variance | 0.0 | 0.4 |
| Observations | 6 | 5 |
| Pooled Variance | 0.2 | |
| Hypothesized Mean Difference | 0 | |
| df | 9 | |
| t Stat | 1.64881542 | |
| P(T<=t) one-tail | 0.066793204 | |
| t Critical one-tail | 1.833112923 | |
| P(T<=t) two-tail | **0.133586407** | |
| t Critical two-tail | 2.262157158 | |

Conclusion: As the p-value > α = 0.05 the null-hypothesis is accepted.
There is with 95% certainty no significant difference between the two groups.

**Sample size to estimate a difference between means (two-sided test)**

| | |
|---|---|
| Mean in group 1 | -0.5 |
| Mean in group 2 | -1.0 |
| Difference | 0.5 |
| Common Standard deviation (SD) | 0.5 |
| Confidence level (1-alpha/2) | 0.95 |
| Z(1-alpha/2) | 1.96 |
| Power (1-beta) | 0.8 |
| Z(beta) | 0.84 |
| Required Sample size (per group) (n) | 15.70 |
| Rounded Sample size (per group) (n) | **16** |

**Minimum detectable difference (two-sided test)**

| | |
|---|---|
| Sample size (n) | 5 |
| Common Standard deviation (SD) | 0.5 |
| Confidence level (1-alpha/2) | 0.95 |
| Z(1-alpha/2) | 1.96 |
| Power (1-beta) | 0.8 |
| Z(beta) | 0.84 |
| Minimum detectable difference (d) | **0.9** |

# LIST OF REFERENCES FOR FIGURES

Figure 1 Own making.

Figure 2 Modified from http://en.wikipedia.org/wiki/Cardiac_cycle

Figure 3 Sutherland GR, Hatle L, Claus P, D'hooge J, Bijnens B; Doppler Myocardial Imaging - A Textbook. Hasselt: BSWK bvba; 2006. ISBN: 9081059211. p. 7

Figure 4 Young AA, Kramer CM, Ferrari VA, Axel L, Reichek N; Three-dimensional left ventricular deformation in hypertrophic cardiomyopathy. *Circulation* 1994 Aug 1;90(2):854-67.

Figure 5 Modified from http://folk.ntnu.no/stoylen/lectures/Klinisk%20bruk%20240904%20nettversjon.pdf

Figure 6 Modified from http://folk.ntnu.no/stoylen/lectures/Klinisk%20bruk%20240904%20nettversjon.pdf

Figure 7 Teske A, De Boeck B, Melman P, Sieswerda G, Doevendans P, Cramer M; Echocardiographic quantification of myocardial function using tissue deformation imaging, a guide to image acquisition and analysis using tissue Doppler and speckle tracking. *Cardiovascular Ultrasound* 2007;5(1):27.

Figure 8 Teske A, De Boeck B, Melman P, Sieswerda G, Doevendans P, Cramer M; Echocardiographic quantification of myocardial function using tissue deformation imaging, a guide to image acquisition and analysis using tissue Doppler and speckle tracking. *Cardiovascular Ultrasound* 2007;5(1):27.

Figure 9 Modified from http://folk.ntnu.no/stoylen/strainrate/

Figure 10 Modified from http://folk.ntnu.no/stoylen/strainrate/

Figure 11 Own making

Figure 12 Reef VB; Cardiovascular ultrasonography. In: Reef VB, editor; Equine Diagnostic Ultrasound. Philadelphia: WB Saunders Company; 1998. p. 215-72.

Figure 13 Spieker EP; Gewebe-Doppler-Echokardiographie beim Pferd: Eine Pilotstudie [PhD Thesis] Freie Universität Berlin; 2006.

Figure 14 Spieker EP; Gewebe-Doppler-Echokardiographie beim Pferd: Eine Pilotstudie [PhD Thesis] Freie Universität Berlin; 2006.

Figure 15 Own making

Figure 16 Own making

Figure 17 Own making

Figure 18 Own making

Figure 19 Modified from http://folk.ntnu.no/stoylen/lectures/Klinisk%20bruk%20240904%20nettversjon.pdf

Figure 20 Modified from http://folk.ntnu.no/stoylen/lectures/Vevsdoppler_Horten_04.pdf

Figure 21 Teske A, De Boeck B, Melman P, Sieswerda G, Doevendans P, Cramer M; Echocardiographic quantification of myocardial function using tissue deformation imaging, a guide to image acquisition and analysis using tissue Doppler and speckle tracking. *Cardiovascular Ultrasound* 2007;5(1):27.

Figure 22 Own making

Figure 23 Own making

Figure 24 Own making

Figure 25 Own making

Figure 26 Own making

Figure 27 Own making

Figure 28 Own making

Figure 29 Own making

Figure 30 Sutherland GR, Hatle L, Claus P, D'hooge J, Bijnens B; Doppler Myocardial Imaging - A Textbook. Hasselt: BSWK bvba; 2006. ISBN: 9081059211. p. 10.

Figure 31 Spieker EP; Gewebe-Doppler-Echokardiographie beim Pferd: Eine Pilotstudie [PhD Thesis] Freie Universität Berlin; 2006.

# LIST OF REFERENCES IN TEXT


(1) Reef VB, Whittier M, Allam LG; Echocardiography. *Clinical Techniques in Equine Practice* 2004;3(3):274-83.

(2) Buhl R; Cardiac development assessed by echocardiography in young standardbred trotters [PhD Thesis] The Royal Veterinary and Agricultural University of Denmark; 2005.

(3) Marr CM; Equine echocardiography - sound advice at the heart of the matter. *British Veterinary Journal* 1994;150(6):527-45.

(4) Boon J; Manual of Veterinary Echocardiography. 1st ed. Baltimore: Williams & Wilkins; 1998. ISBN: 0683009389. Chapter 1 and 2.

(5) Sutherland GR, Hatle L, Claus P, D'hooge J, Bijnens B; Doppler Myocardial Imaging - A Textbook. Hasselt: BSWK bvba; 2006. ISBN: 9081059211. Chapters 2, 3 and 4.

(6) Teske A, De Boeck B, Melman P, Sieswerda G, Doevendans P, Cramer M; Echocardiographic quantification of myocardial function using tissue deformation imaging, a guide to image acquisition and analysis using tissue Doppler and speckle tracking. *Cardiovascular Ultrasound* 2007;5(1):27.

(7) Korinek J, Kjaergaard J, Sengupta PP, Yoshifuku S, McMahon EM, Cha SS, et al.; High Spatial Resolution Speckle Tracking Improves Accuracy of 2-Dimensional Strain Measurements: An Update on a New Method in Functional Echocardiography. *Journal of the American Society of Echocardiography* 2007 Feb;20(2):165-70.

(8) Armstrong G, Pasquet A, Fukamachi K, Cardon L, Olstad B, Marwick T; Use of Peak Systolic Strain as an Index of Regional Left Ventricular Function: Comparison with Tissue Doppler Velocity During Dobutamine Stress and Myocardial Ischemia. *Journal of the American Society of Echocardiography* 2000 Aug;13(8):731-7.

(9) Wilkenshoff UM, Sovany A, Wigström L, Olstad B, Lindström L, Engvall J, et al.; Regional Mean Systolic Myocardial Velocity Estimation by Real-Time Color Doppler Myocardial Imaging: A New Technique for Quantifying Regional Systolic Function. *Journal of the American Society of Echocardiography* 1998 Jul;11(7):683-92.

(10) Støylen A; Regional venstre Ventrikkelfunksjon bedømt med vevsdopplerbaserte metoder: Tissue velocity, Strain Rate Imaging, Tissue Tracking og Farge M-mode. *Hjerteforum* 2002;15(2):33-43.

(11) Pasquet A, Armstrong G, Beachler L, Lauer MS, Marwick T; Use of Segmental Tissue Doppler Velocity to Quantitate Exercise Echocardiography. *Journal of the American Society of Echocardiography* 1999 Nov;12(11):901-12.

(12) Zamorano Gomez JL; New Echocardiographic Modalities in the Detection and Monitoring of Heart Failure - The Clinical Potential of Speckle-tracking Technology. *European Cardiovascular Disease 2007* 2007;(1):115-8.

(13) Chetboul V, Carlos Sampedrano C, Testault I, Pouchelon JL; Use of tissue Doppler imaging to confirm the diagnosis of dilated cardiomyopathy in a dog with equivocal echocardiographic findings. *Journal of the American Veterinary Medical Association* 2004 Dec 3;225(12):1877-80.

(14) Chetboul V, Carlos C, Blot S, Thibaud JL, Escriou C, Tissier R, et al.; Tissue Doppler assessment of diastolic and systolic alterations of radial and longitudinal left ventricular motions in Golden Retrievers during the preclinical phase of cardiomyopathy associated with muscular dystrophy. *American Journal of Veterinary Research* 2004 Oct 27;65(10):1335-41.

(15) Chetboul V, Blot S, Carlos Sampedrano C, Thibaud JL, Granger N, Tissier R, et al.; Tissue Doppler Imaging for Detection of Radial and Longitudinal Myocardial Dysfunction in a Family of Cats Affected by Dystrophin-Deficient Hypertrophic Muscular Dystrophy. *Journal of Veterinary Internal Medicine* 2006;20(3):640-7.

(16) Estrada A, Chetboul V; Tissue Doppler evaluation of ventricular synchrony. *Journal of Veterinary Cardiology* 2006 Nov;8(2):129-37.

(17) Schwarzwald CC, Schober KE, Bonagura JD; Echocardiographic Evidence of Left Atrial Mechanical Dysfunction after Conversion of Atrial Fibrillation to Sinus Rhythm in 5 Horses. *Journal of Veterinary Internal Medicine* 2007;21(4):820-7.

(18) Schwarzwald CC, Schober KE, Bonagura JD. Echocardiographic characterization of left ventricular radial wall motion in horses using tissue Doppler imaging: Methodology and reliability. *Journal of Veterinary Internal Medicine* 21[3], 590-591. Ref Type: Abstract

(19) Schwarzwald CC, Schober KE, Bonagura JD; Methods and reliability of echocardiographic assessment of left atrial size and mechanical function in horses. *American Journal of Veterinary Research* 2007 Jul 18;68(7):735-47.

(20) Sepulveda MF, Perkins JD, Bowen IM, Marr CM; Demonstration of regional differences in equine ventricular myocardial velocity in normal 2-year-old Thoroughbreds with Doppler tissue imaging. *Equine Veterinary Journal* 2005;37(3):222-6.

(21) Spieker EP; Gewebe-Doppler-Echokardiographie beim Pferd: Eine Pilotstudie [PhD Thesis] Freie Universität Berlin; 2006.

(22) Schwarzwald CC, Schober KE, Bonagura JD. Echocardiographic characterization of left ventricular radial and circumferential wall motion in horses using strain, strain rate, and displacement by 2D speckle tracking: Methodology and reliability. *Journal of Veterinary Internal Medicine* 22[3], 759-760. Ref Type: Abstract

(23) Serri K, Reant P, Lafitte M, Berhouet M, Le Bouffos V, Roudaut R, et al.; Global and Regional Myocardial Function Quantification by Two-Dimentional Strain. *Journal of the American College of Cardiology* 2006;47(6):1175-81.

(24) Delfino JG; Magnetic Resonance Phase Velocity Mapping of Cardiac Dyssynchrony [PhD Thesis] Georgia Institute of Technology/Emery University; 2007.

(25) Young AA, Kramer CM, Ferrari VA, Axel L, Reichek N; Three-dimensional left ventricular deformation in hypertrophic cardiomyopathy. *Circulation* 1994 Aug 1;90(2):854-67.

(26) Karwatowski SP, Mohiaddin RH, Yang GZ, Firmin DN, Sutton MSJ, Underwood SR, et al. Assessment of Regional Left Ventricular Motion with MR velocity Mapping in Healthy Subjects. *Journal of Magnetic Resonance Imaging* 2, 152-155. Ref Type: Abstract

(27) Støylen A, Ingul C, Torp H; Strain and strain rate parametric imaging. A new method for post processing to 3-/4-dimensional images from three standard apical planes. Preliminary data on feasibility, artefact and regional dyssynergy visualisation. *Cardiovascular Ultrasound* 2003;1(1):11.

(28) Sutherland GR, Bijnens B, McDicken N; Tissue Doppler Echocardiography - Historical Perspective and Technical Considerations. *Echocardiography* 1999;16(5):445-53.

(29) Pan C, Hoffmann R, Kühl H, Severin E, Franke A, Hanrath P; Tissue Tracking Allows Rapid and Accurate Visual Evaluation of Left Ventricular Function. *European Journal of Echocardiography* 2001;2(3):197-202.

(30) Garcia Fernandez M-A, Bermejo J, Perez David E, Lopez Fernandez T, Ledesma MJ, Caso P, et al.; New Techniques for the Assessment of Regional Left Ventricular Wall Motion. *Echocardiography* 2003;20(7):659-72.

(31) Reef VB; Cardiovascular ultrasonography. In: Reef VB, editor.; Equine Diagnostic Ultrasound. Philadelphia: WB Saunders Company; 1998. p. 215-72.

(32) Patteson M; Equine Cardiology. Blackwell Science; 1996. ISBN: 0632032995. Chapter 1 and 4.

(33) Hoffmann KL; Echocardiography. In: Ratanen N, McKinnon A, editors.; Equine Diagnostic Ultrasonography. 1st ed. Baltimore: Williams & Wilkins; 1998. p. 19-39.

(34) Miyatake K, Yamagishi M, Tanaka N, Uematsu M, Yamazaki N, Mine Y, et al.; New method for evaluating left ventricular wall motion by color-coded tissue doppler imaging: In vitro and in vivo studies. *Journal of the American College of Cardiology* 1995 Mar 1;25(3):717-24.

(35) Chetboul V; Tissue Doppler Imaging: a promising technique for quantifying regional myocardial function. *Journal of Veterinary Cardiology* 2002 Nov;4(2):7-12.

(36) Heimdal A, Støylen A, Torp H, Skjærpe T; Real-Time Strain Rate Imaging of the Left Ventricle by Ultrasound. *Journal of the American Society of Echocardiography* 1998 Nov;11(11):1013-9.

(37) Sutherland GR, Kukulski T, Voight JU, D'hooge J; Tissue Doppler Echocardiography - Future Developements. *Echocardiography* 1999;16(5):509-20.

(38) Storaa C, Åberg P, Lind B, Brodin L-Å; Effect of Angular Error on Tissue Doppler Velocities and Strain. *Echocardiography* 2003;20(7):581-7.

(39) Lind B, Nowak J, Dorph J, van der Linden J, Brodin L-Å; Analysis of Temporal Requirements for Myocardial Tissue Velocity Imaging. *European Journal of Echocardiography* 2002;3(3):214.

(40) Kukulski T, Voight JU, Wilkenshoff UM, Strotmann JM, Wranne B, Hatle L, et al.; A Comparison of Regional Myocardial Velocity Information Derived by Pulsed and Color Doppler Techniques: An In Vitro and In Vivo Study. *Echocardiography* 2000;17(7):639-51.

(41) Garcia MJ, Rodriguez L, Ares M, Griffin BP, Klein AL, Stewart WJ, et al.; Myocardial wall velocity assessment by pulsed Doppler tissue imaging: Characteristic findings in normal subjects. *American Heart Journal* 1996 Sep;132(3):648-56.

(42) Vinereanu D, Khokhar A, Fraser AG; Reproducibility of Pulsed Wave Tissue Doppler Echocardiography. *Journal of the American Society of Echocardiography* 1999 Jun;12(6):492-9.

(43) Donovan CL, Armstrong WF, Bach DS; Quantitative Doppler tissue imaging of the left ventricular myocardium: Validation in normal subjects. *American Heart Journal* 1995 Jul;130(1):100-4.

(44) Hashimoto I, Mori Y, Rusk RA, Davies CH, Li X, Mack GK, et al.; Strain Rate Imaging: An In Vitro "Validation" Study Using a Physiologic Balloon Model Mimicking the Left Ventricle. *Echocardiography* 2002;19(8):669-77.

(45) Chetboul V, Athanassiadis N, Carlos C, Nicolle A, Zilberstein L, Pouchelon JL, et al.; Assessment of repeatability, reproducibility, and effect of anesthesia on determination of radial and longitudinal left ventricular velocities via tissue Doppler imaging in dogs. *American Journal of Veterinary Research* 2004 Jul 18;65(7):909-15.

(46) Chetboul V, Carlos Sampedrano C, Concordet D, Tissier R, Lamour T, Ginesta J, et al.; Use of quantitative two-dimensional color tissue Doppler imaging for assessment of left ventricular radial and longitudinal myocardial velocities in dogs. *American Journal of Veterinary Research* 2005 Jun 15;66(6):953-61.

(47) Chetboul V, Carlos Sampedrano C, Gouni V, Nicolle A, Pouchelon JL, Tissier R; Ultrasonographic Assessment of Regional Radial and Longitudinal Systolic Function in Healthy Awake Dogs. *Journal of Veterinary Internal Medicine* 2006;20(4):885-93.

(48) Chetboul V, Carlos Sampedrano C, Gouni V, Concordet D, Lamour T, Ginesta J, et al.; Quantitative Assessment of Regional Right Ventricular Myocardial Velocities in Awake Dogs by Doppler Tissue Imaging: Repeatability, Reproducibility, Effect of Body Weight and Breed, and Comparison with Left Ventricular Myocardial Velocities. *Journal of Veterinary Internal Medicine* 2005;19(6):837-44.

(49) Chetboul V, Athanassiadis N, Carlos C, Nicolle A, Tissier R, Pouchelon JL, et al.; Quantification, repeatability, and reproducibility of feline radial and longitudinal left ventricular velocities by tissue Doppler imaging. *American Journal of Veterinary Research* 2004 May 12;65(5):566-72.

(50) Nelson RW, Couto CG; Small Animal Internal Medicine. 3rd ed. St. Louis: Mosby; 2003. ISBN: 0-323-01724-X. Chapter 2.

(51) Eriksen L; Klinisk Undersøgelsesmetodik og Journalskrivning. 1 ed. Frederiksberg: KVL-bogladen; 2002. ISBN: 9677415174.

(52) Chetboul V, Carlos Sampedrano C, Tissier R, Gouni V, Saponaro V, Nicolle A, et al.; Quantitative assessment of velocities of the annulus of the left atrioventricular valve and left ventricular free wall in healthy cats by use of two-dimensional color tissue Doppler imaging. *American Journal of Veterinary Research* 2006 Feb 3;67(2):250-8.

(53) Chetboul V, Carlos Sampedrano C, Tissier R, Gouni V, Nicolle A, Pouchelon JL; Reference range values of regional left ventricular myocardial velocities and time intervals assessed by tissue Doppler imaging in young nonsedated Maine Coon cats. *American Journal of Veterinary Research* 2005 Nov 30;66(11):1936-42.

(54) Perk G, Tunick PA, Kronzon I; Non-Doppler Two-dimensional Strain Imaging by Echocardiography-From Technical Considerations to Clinical Applications. *Journal of the American Society of Echocardiography* 2007 Mar;20(3):234-43.

(55) Stefani L, Toncelli L, Gianassi M, Manetti P, Di Tante V, Vono M, et al.; Two-dimensional tracking and TDI are consistent methods for evaluating myocardial longitudinal peak strain in left and right ventricle basal segments in athletes. *Cardiovascular Ultrasound* 2007;5(1):7.

(56) Suffoletto MS, Dohi K, Cannesson M, Saba S, Gorcsan J; Novel Speckle-Tracking Radial Strain From Routine Black-and-White Echocardiographic Images to Quantify Dyssynchrony and Predict Response to Cardiac Resynchronization Therapy. *Circulation* 2006 Feb 21;113(7):960-8.

(57) Artis NJ, Oxborough DL, Williams G, Pepper CB, Tan LB; Two-dimensional strain imaging: A new echocardiographic advance with research and clinical applications. *International Journal of Cardiology* 2008 Jan 24;123(3):240-8.

(58) Rappaport D, Adam D, Lysyansky P, Riesner S; Assessment of myocardial regional strain and strain rate by tissue tracking in B-mode echocardiograms. *Ultrasound in Medicine & Biology* 2006 Aug;32(8):1181-92.

(59) Leitman M, Lysyansky P, Sidenko S, Shir V, Peleg E, Binenbaum M, et al.; Two-dimensional strain-a novel software for real-time quantitative echocardiographic assessment of myocardial function. *Journal of the American Society of Echocardiography* 2004 Oct;17(10):1021-9.

(60) Kutty S, Deatsman SL, Nugent M, Russell D, Frommelt P; Assessment of Regional Right Ventricular Velocities, Strain, and Displacement in Normal Children Using Velocity Vector Imaging. *Echocardiography* 2008;25(3):294-307.

(61) Helle-Valle T, Crosby J, Edvardsen T, Lyseggen E, Amundsen BH, Smith HJ, et al.; New Noninvasive Method for Assessment of Left Ventricular Rotation: Speckle Tracking Echocardiography. *Circulation* 2005 Nov 15;112(20):3149-56.

(62) Chetboul V, Serres F, Gouni V, Tissier R, Pouchelon JL; Radial strain and strain rate by two-dimensional speckle tracking echocardiography and the tissue velocity based technique in the dog. *Journal of Veterinary Cardiology* 2007 Nov;9(2):69-81.

(63) Chetboul V, Serres F, Gouni V, Tissier R, Pouchelon JL; Noninvasive Assessment of Systolic Left Ventricular Torsion by 2-Dimensional Speckle Tracking Imaging in the Awake Dog: Repeatability, Reproducibility, and Comparison with Tissue Doppler Imaging Variables. *Journal of Veterinary Internal Medicine* 2008;22(2):342-50.

(64) Schwarzwald, Colin C., Dr. med. vet., PhD, Dipl. ACVIM, Section Internal Medicine, Equine Department, Vetsuisse Faculty, University of Zurich, Switzerland; Results on radial and circumferential strain and strain rates obtained by speckle tracking in horses. Personal Communication. 16-9-2008. Poster made by Dr. Schwarzwald for the ACVIM conference 2008 is in the author's possession.

(65) Ingul CB, Torp H, Aase SA, Berg S, Støylen A, Slordahl SA; Automated Analysis of Strain Rate and Strain: Feasibility and Clinical Implications. *Journal of the American Society of Echocardiography* 2005 May;18(5):411-8.

(66) Stout M; Athletes' Heart and Echocardiography: Athletes' Heart. *Echocardiography* 2008.

(67) Grossman W, Jones D, McLaurin LP; Wall Stress and Patterns of Hypertrophy in the Human Left Ventricle. *The Journal of Clinical Investigation* 1975;56:56-64.

(68) Pluim BM, Zwinderman AH, van der Laarse A, van der Wall EE; The Athlete's Heart : A Meta-Analysis of Cardiac Structure and Function. *Circulation* 2000 Jan 25;101(3):336-44.

(69) Spirito P, Pelliccia A, Proschan MA, Granata M, Spataro A, Bellone P, et al.; Morphology of the "athlete's heart" assessed by echocardiography in 947 elite athletes representing 27 sports. *The American Journal of Cardiology* 1994 Oct 15;74(8):802-6.

(70) Poulsen SH, Hjortshøj S, Korup E, Poenitz V, Espersen G, Søgaard P, et al.; Strain rate and tissue tracking imaging in quantitation of left ventricular systolic function in endurance and strength athletes. *Scandinavian Journal of Medicine & Science in Sports* 2007;17(2):148-55.

(71) Saghir M, Areces M, Makan M; Strain Rate Imaging Differentiates Hypertensive Cardiac Hypertrophy from Physiologic Cardiac Hypertrophy (Athlete's Heart). *Journal of the American Society of Echocardiography* 2007 Feb;20(2):151-7.

(72) Stefani L, Toncelli L, Di Tante V, Vono M, Cappelli B, Pedrizzetti G, et al.; Supernormal functional reserve of apical segments in elite soccer players: an ultrasound speckle tracking handgrip stress study. *Cardiovascular Ultrasound* 2008;6(1):14.

(73) Richand V, Lafitte S, Reant P, Serri K, Lafitte M, Brette S, et al.; An Ultrasound Speckle Tracking (Two-Dimensional Strain) Analysis of Myocardial Deformation in Professional Soccer Players Compared With Healthy Subjects and Hypertrophic Cardiomyopathy. *The American Journal of Cardiology* 2007 Jul 1;100(1):128-32.

(74) Young LE; Equine athletes, the equine athlete's heart and racing success. *Experimental Physiology* 2003;88(5):659-63.

(75) Young LE; Cardiac responses to training in 2-year-old Thoroughbreds: an echocardiographic study. *Equine Veterinary Journal, Supplement* 1999;30:195-8.

(76) Buhl R, Ersbøll AK, Eriksen L, Koch J; Changes over time in echocardiographic measurements in young Standardbred racehorses undergoing training and racing and association with racing performance. *Journal of the American Veterinary Medical Association* 2005 Jun 15;226(11):1881-7.

(77) Gehlen H, Marnette S, Rohn K, Ellendorff F, Stadler P; Echocardiographic comparison of left ventricular dimensions and function after standardized treadmill exercise in trained and untrained healthy warmblood horses. *Equine and Comparative Exercise Physiology* 2005;3(1):3-11.

(78) Ohmura H, Hiraga A, Matsui A, Aida H, Inoue Y, Asai Y, et al.; Physiological responses of young Thoroughbreds during their first year of race training. *Equine Veterinary Journal, Supplement* 2002;34:140-6.

(79) Buhl R, Ersbøll AK, Eriksen L, Koch J; Sources and magnitude of variation in echocardiographic measurements in normal standardbred horses. *Veterinary Radiology and Ultrasound* 2004;45(6):505-12.

(80) Thomas G; Tissue Doppler echocardiography - A case of right tool, wrong use. *Cardiovascular Ultrasound* 2004;2(1):12.

Stud. Med. Vet.

Mette Flethøj